DOE/ER/03624 - 20

North Carolina State University Nuclear Structure Research at the Triangle Universities Nuclear Laboratory

Progress Report

C. R. Gould, G. E. Mitchell, L. W. Seagondollar, D. R. Tilley
and Students

North Carolina State University at Raleigh
Raleigh, North Carolina

Contract Period 1 April 1979 - 31 March 1980

Date of last Progress Report: 12 January 1979
Date of this Progress Report: 1 February 1980

PREPARED FOR

THE UNITED STATES DEPARTMENT OF ENERGY
UNDER CONTRACT DE-AS05-76ER03624

DISCLAIMER

NCSU - TUNL PERSONNEL

Faculty

Gould, C.R. (Associate Professor)
Mitchell, G.E. (Professor)
Seagondollar, L.W. (Professor)
Tilley, D.R. (Professor)

Associated Theorists

Cotanch, S.R. (Assistant Professor)
Park, J.Y. (Professor)

Associated Experimentalists

Mowat, J.R. (Assistant Professor)
Waltner, A.W. (Professor)

Graduate Students

Beyerle, A.G.
Chou, B.H.
Jensen, M.J.
Sales, K.B.
Thambidurai, P.M.
Ward, L.B.

TABLE OF CONTENTS

APPENDICES

INTRODUCTION

The inter-universities nature of the TRIANGLE UNIVERSITIES NUCLEAR LABORATORY and the team approaches that are necessary for experiments on large accelerators make progress reports from the three universities have a large amount of overlap.

Each year TUNL prepares an annual report which is a progress report for the entire laboratory. A report coordinator asks certain physicists to write up the work that has been done in a certain area or areas and these reports are combined. The names of the personnel working in each area are listed in the report of the area.

To avoid duplication of effort and to increase accuracy, this progress report for the NCSU group (Contract DE-AS05-76ER03624) is direct Xerox copy of that portion of the TUNL Annual Report XVIII (1 January 1979 - 31 December 1979) in which NCSU contract personnel and/or NCSU associated personnel were involved. Since this portion is not all of the TUNL XVIII report, appropriate changes in indexing of categories, figures, tables and references thereto have been made so that such indices are sequential in this report.

In each area of activity, the names of all personnel involved are listed and the names of NCSU personnel are underlined for easier identification.

A. NEUTRON CROSS SECTION EXPERIMENTS

1. Neutron Time of Flight Program - General Status

(A. Beyerle, S. G. Glendinning, C. R. Gould, H. H. Hogue,* Sadiq El Kadi, C. E. Nelson, R. Pedroni, F. O. Purser, L. W. Seagondollar, P. Thambidurai, R. L. Walter)

For the last five years TUNL has been involved in an extensive program of neutron elastic and inelastic scattering cross section measurements in support of the U. S. fusion energy program. The measurements were primarily undertaken to address the high priority medium and long range differential nuclear data needs of the Office of Fusion Energy. However, the information gained is also of fundamental interest in terms of optical model parameterizations of nucleon scattering, studies of isospin dependence in nucleon scattering, nuclear level density measurements and studies of pre-equilibrium emission processes.

The early work at TUNL concentrated on measurements of elastic and discrete inelastic neutron scattering cross sections from p-shell nuclei (Li, Be, B, C, O) in the 8 to 15 MeV bombarding energy region. This work was performed with the $D(d,n)^3He$ source reaction and is now essentially completed. Results for Li, B and O scattering are summerized below.

The main thrust of the present program is toward measurements of continuum neutron emission spectra from medium and heavy mass nuclei. This work necessitated installation of a tritium gas target capability, development and calibration of two neutron detection systems operating at low neutron threshold energy (~300 keV) and development of codes for acquiring and correcting continuum neutron scattering data. Progress in these areas and our first experimental results for Fe, Cu, Ni and Pb are discussed below. In support of these continuum measurements we have also undertaken discrete scattering studies with separated ^{54}Fe, ^{56}Fe, ^{63}Cu and ^{65}Cu samples. Much of this current work was reported at the Conference on Nuclear Cross Sections for Technology held at Knoxville in Oct. 22-26 this year and will appear in the Proceedings.

The coordination meeting of representatives of the laboratories currently participating in the Office of Basic Energy Sciences nuclear data procurement program was held in March of this year at TUNL. The progress towards satisfying the nuclear data needs of the fusion energy program was discussed, and plans for future work were outlined by the participating laboratories. This was the second review meeting, the first having been held in Oak Ridge in 1976. The meeting was coordinated by F. Perey and included representatives from Brookhaven, Rockwell, Argonne, Livermore, Hanford, Oak Ridge, Los Alamos, DOE, TUNL and Ohio.

---

* Y-12 plant, Oak Ridge, Tennessee

2. Summary of Recent Facility Improvements

Neutrons for the TOF facilities are produced by bombardment of gas targets by protons or deuterons. Negative hydrogen ions are produced in a direct extraction negative ion source (DENIS II--see Cyclo-Graaff Laboratory layout). The ions are accelerated by the FN tandem electrostatic generator and then deflected 38° into the time-of-flight area. This beam leg extends 25 m and terminates in either a deuterium or tritium gas target. The beam leg contains appropriate valves, focussing lenses, beam-defining slits and vacuum systems. Almost all gaskets are indium. The vacuum systems are part of an over-all safety system that is needed when tritium gas is used in order to prevent unacceptable contamination of personnel and/or equipment.[1]

The cross-section of the tritium target is shown in Fig. A2-1. The

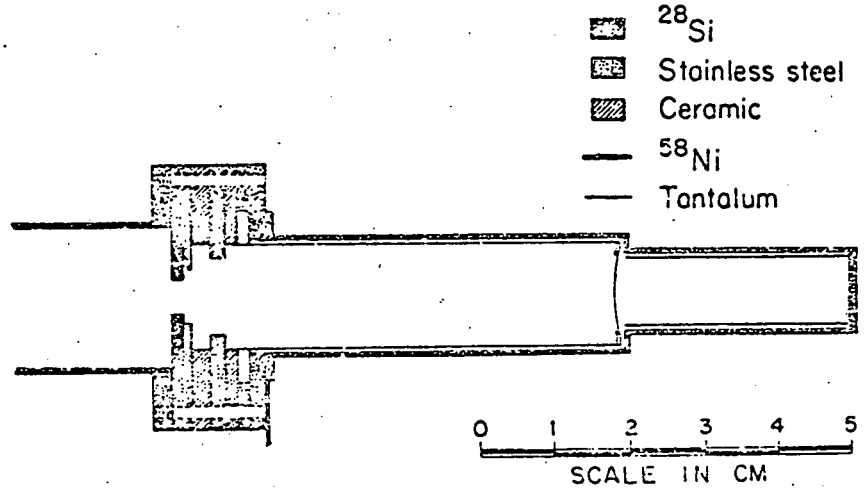

Fig. A2-1. Cross section of the TUNL gas target. The curved foil is 3.5 μm molybdenum. Gas enters cell through tube at bottom of drawing.

tritium, usually at about 2 atm absolute pressure, is separated from the vacuum in the beam leg by foils of about 3.5 μm thickness. In accord with the measurements of Drosg et al.,[2] a ^{28}Si collimator and a ^{58}Ni beam stop are used. The gas filling system for the tritium target permits evacuation of the target to fore-vacuum pressure, filling with helium gas, and filling with tritium. The tritium reservoir is a uranium furnace which can be heated electrically to furnish tritium up to 2 atm absolute pressure. A liquid-nitrogen cooled, activated charcoal trap can also be used to store additional tritium which can be released subsequently to the target if higher pressures are desired. Originally the tritium gas pressure was determined during filling by a small Bourdon gauge and the gauge was monitored by closed circuit television during runs. This gauge has been replaced by a silicon pressure transducer (National

[1] See Triangle Universities Nuclear Laboratory Progress Report for 1977 (TUNL XVI).
[2] M. Drosg and C. F. Auchambaugh, Nuc. Inst. and Meth., 140 (1977) 515

Semiconductor Device LX1704GB). The gas volume of this device is less than that of the Bourdon gauge. Also, instead of having a visual indicator, it puts out a small dc voltage proportional to the absolute pressure. Fig. A2-2 shows the linearity of the

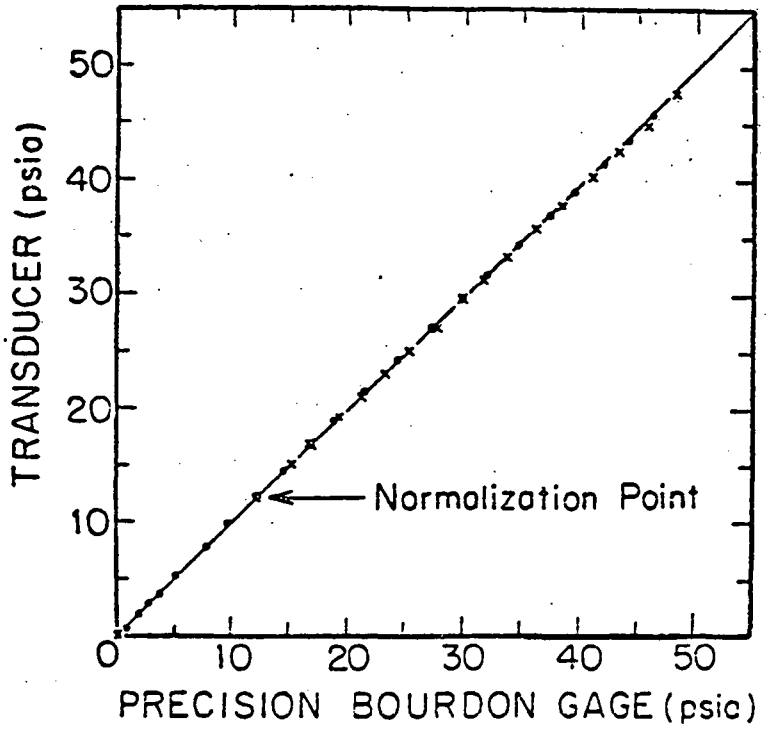

Fig. A2-2. Calibration of silicon pressure transducer against a precision Bourdon gage. The normalization point was 1 atm -- 14.4 psia on both gages.

device as determined by comparison with a precision Bourdon gauge (Wallace and Tiernan, Series 1000 Dial Instrument). The dc voltage is used as input to a digital voltmeter near the filling system, another digital voltmeter in the control room and also, in the control room, a strip chart recorder and a D'Arsonval meter containing adjustable upper and lower limit controls. The strip chart recorder gives us continuous "written" record of the target pressure during a run; a particularly informative record if a target foil begins to fail. The limit controls set off an audible alarm if the target pressure varies beyond the adjustable limits. The transducer system has only been used on one 5-day run to date and it functioned as expected. Two worries existed about the system; (a) the hot tritium gas from the furnace might raise the temperature of the transducer above its maximum design operating temperature, and (b) radiation damage might occur. Built into the transducer is a lead which gives voltage variations with temperature variations--2 to 4 mv/°C. As the target was filled, this voltage variation was observed with a separate digital voltmeter. The tritium target was filled several times during the run. In each case, the temperature rise of the transducer was less than 10°C. Also, the pressure readings of the transducer were compared over a wide range of pressures to that of a small Bourdon gauge still in the filling system before and after the run. There is no indication of radiation damage to

the transducer. However, since this run was a particularly low current run, a radiation shield will be installed between the transducer and the neutron target before the next run.

Neutrons are detected at this facility by four liquid scintillators. Two of them are used as monitors. One monitor is mounted overhead at a distance of 2 m from the target and an angle of 60° above the beam line. It is in a 350 kg copper shield with a straight aperture directed towards the neutron target. The other monitor has no shield, is portable, and is usually placed at about 4 m from the target along the 0° line. The other two detectors are in massive shields and are used to measure angular distributions of scattered neutrons. Each of them is on its own steel cart which pivots along a line directly below the axis of the scattering samples. Each detector can be located by convenient electric drive at any angle between 0° and 155° from the beam line with a precision of about 0.1°. One detector and its shield has been described[1] earlier. That unit can be moved radially for flight paths of 2.7 m to almost 4 m. The other shielded detector is similar to the first except: (a) it uses a larger scintillator (12.5 cm-diameter, 5 cm-thick), (b) the shield has about 30 cm more material in back of the detector to further reduce background neutrons scattered from the laboratory walls, and (c) the path can be changed from 2.7 m to almost 6 m. Both detectors are used simultaneously. Fig. A2-3 shows a cross-section of the second detector and its shield.

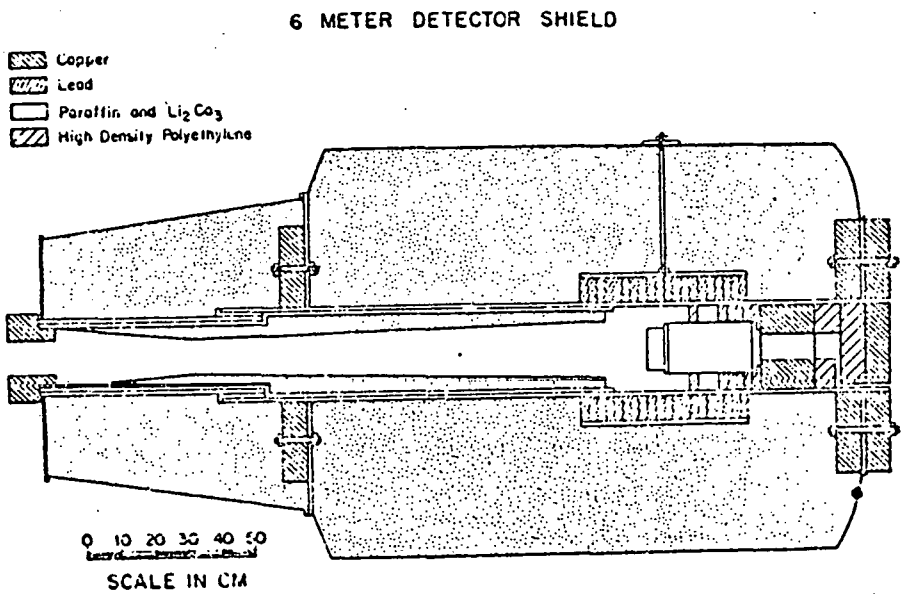

Fig. A2-3. Cross section of the new detector and shield.

[1] Glasgow et al., Nat. Bur. Stand. (U.S.) Spec. Publ. 425, 1, 99 (1975)

3. Elastic and Inelastic Scattering of 7- to 14-MeV Neutrons from ^{6}Li and ^{7}Li

This work has been published in Nucl. Sci. and Eng. 69 (1979) 22. The abstract appears below:

"Differential cross sections are reported for the elastic and discrete inelastic scattering of neutrons from ^{6}Li and ^{7}Li. Source neutrons were provided by the ^{2}H(d,n)^{3}He reaction in the energy range 7 to 14 MeV. Scattered neutrons were detected at a distance of 3.9 m at angles from 25° to 160° in 5° intervals. Total cross sections were obtained for elastic scattering from ^{6}Li and for the sum of elastic and 0.478-MeV state inelastic scattering from ^{7}Li. Inelastic scattering cross sections were obtained for the 2.18-MeV state in ^{6}Li and the 4.63-MeV state in ^{7}Li. The results are compared to ENDF/B-IV predictions and to previous measurements. Inelastic scattering to the 4.63-MeV state in ^{7}Li accounts for less than half of the total tritium production cross section for neutron interactions with ^{7}Li."

4. Elastic Scattering of 8-14 MeV Neutrons from ^{10}B, ^{11}B and ^{16}O

a. Boron Data

Boron data described in earlier reports (TUNL XVII) have been studied using a spherical optical model. Our ^{10}B(n,n)^{10}B data when combined with the ^{10}B(p,p)^{10}B data of Watson (1969) provide an opportunity to examine the isospin dependence of the model for T(target) = 0. That this dependence should take the form of a correction to the incident energy of the projectile was suggested by Rapaport (1976). An empirical value for this energy correction was calculated by the program GENOA, which fit all the angular distributions for both incident neutrons and protons simultaneously. Our results show an energy reduction of 4.6 ± 1.4 MeV for incident protons as compared with neutrons. The value for the Coulomb correction term in the real well depth would then be $0.66 * Z/(A^{1/3})$.

The ^{11}B data were also included in a search to find a set of global optical model parameters for boron data between 8 and 14 MeV. Our previously reported ^{11}B data were used. Angular distributions which were very near two sharp resonances in the ^{11}B total neutron cross section were omitted from the search. The results of these searches are presented in Table A4-1 and in Figs. A4-1, A4-2, and A4-3.

The ^{11}B data were also suitable for analysis using the coupled-channels optical model of Tamura. In this method, the inelastic data for the state at 4.44 MeV (5/2-) were predicted by assuming that ^{11}B is a permanently deformed nucleus with a quadrupole deformation parameter of 0.037 b. The values for the other

TABLE A4-1

Optical Model Parameters for ^{10}B and ^{11}B

Parameter	^{10}B Data	^{11}B Data	Both Isotopes
V_o (MeV)	48.1 - 0.3 Ecm	45.7 - 0.005 Ecm	45.8 - 0.06 Ecm
r_o (fm)	1.34	1.40	1.37
a_o (fm)	0.55	0.35	0.49
W_d (MeV)	0.16 - 0.78 Ecm	-6.27 + 1.13 Ecm	0.05 + 0.78 Ecm
r_i (fm)	1.41	1.10	1.31
a_i (fm)	0.34	0.50	0.33
V_{so} (MeV)	5.5	5.5	5.5
r_{so} (fm)	1.15	1.15	1.15
a_{so} (fm)	0.57	0.57	0.57
V_c (MeV)	0.66	-	0.66
V_s (MeV)	-	-	24.5
W_s (MeV)	-	-	11.5

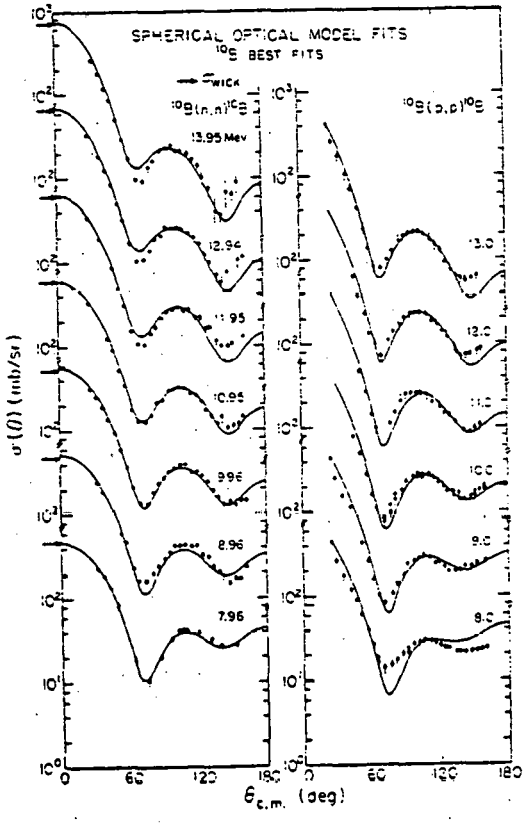

Fig. A4-1. Optical model fits to ^{10}B elastic scattering data.

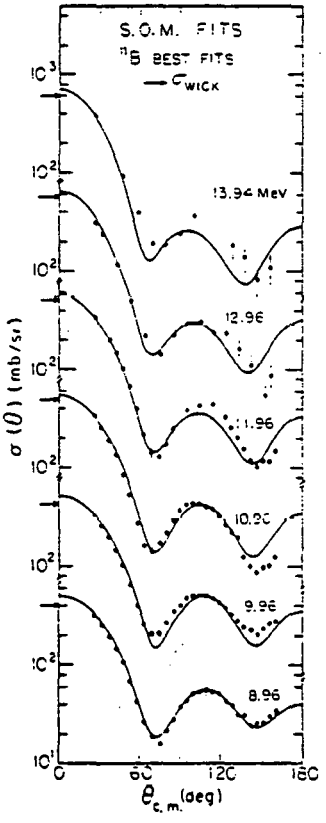

Fig. A4-2. Optical model fits to ^{11}B elastic scattering data.

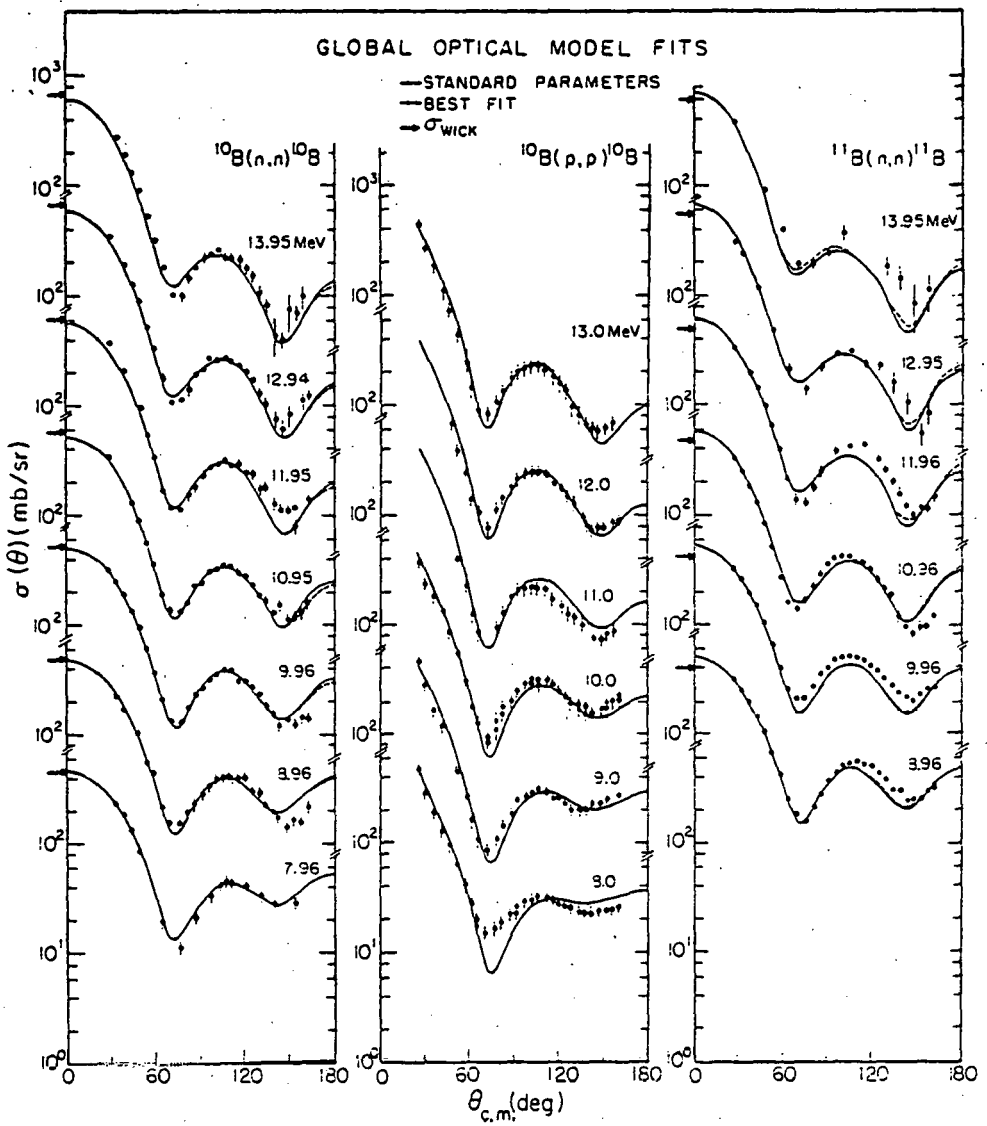

Fig. A4-3. Global optical model fits to ^{10}B and ^{11}B elastic scattering data.

optical model parameters which gave the best fits to the elastic data are shown in Table A4-2 and the fits are shown in Fig. A4-4. The program JUPITOR (Karlsruhe version) was used to perform the calculations.

TABLE A4-2

Coupled - Channels Optical Model Parameters for ^{11}B

Parameter	Coupled - channels Value	S.O.M. Value
V_o (MeV)	71.86 - 2.91 Ecm	45.7 - 0.005 Ecm
r_o (fm)	1.40	1.40
a_o (fm)	0.35	0.35
W_d (MeV)	-3.74 + 0.58 Ecm	-6.27 + 1.13 Ecm
r_i (fm)	1.22	1.11
a_i (fm)	0.35	0.50
V_{so} (MeV)	5.5	5.5
r_{so} (fm)	1.15	1.15
a_{so} (fm)	0.57	0.57
(b)	0.037	

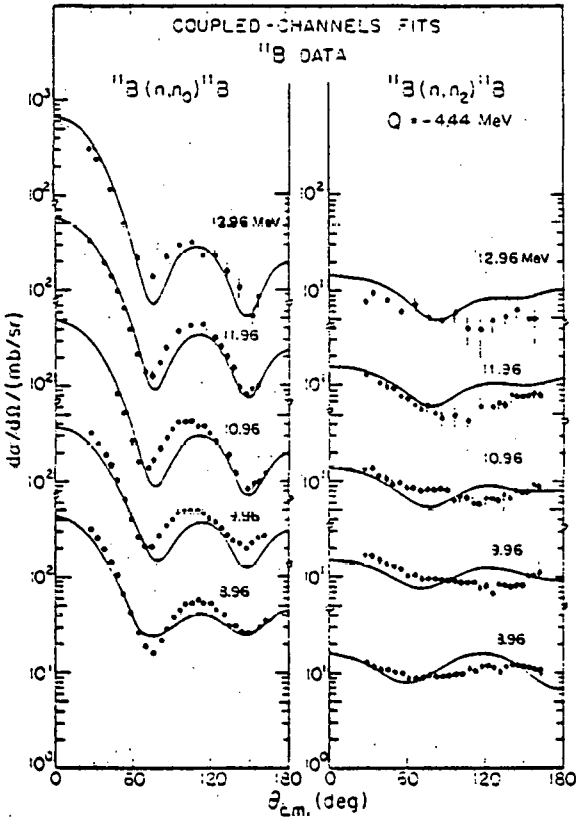

Fig. A4-4. Coupled-Channels optical model fits to ^{11}B data.

b. ^{16}O Data

The $^{16}O(n,n)^{16}O$ data reported earlier have also been studied using a spherical optical model, modified to include the presence of resonances. Background optical model parameters were obtained using the program GENOA to fit angular distributions at 9.21, 10.71, 12.94 and 13.94 MeV which were near minima in the total cross sections. Resonances at Elab = 10.13, 11.15 and 11.54 MeV were included, and tentative assignments of $J^{\pi} = 7/2^-$, $7/2^-$ and $5/2^+$ were chosen. Results of these calculations are shown in Table A4-3 and Figs. A4-5 and A4-6.

TABLE A4-3

Optical Model and Resonance Parameters for ^{16}O

Optical Model Parameter	Value
V_o (MeV)	65.8 - 1.52 Ecm
r_o (fm)	1.27
a_o (fm)	0.51
W_d (MeV)	-0.64 + 0.80 Ecm
r_i (fm)	1.45
a_i (fm)	0.24
V_{so} (MeV)	5.5
r_{so} (fm)	1.15
a_{so} (fm)	0.55

Resonance energy (com)			J
9.51	0.40	0.10	(7/2)-
10.50	0.34	0.14	(5/2)-
10.80	0.18	0.06	(5/2)+

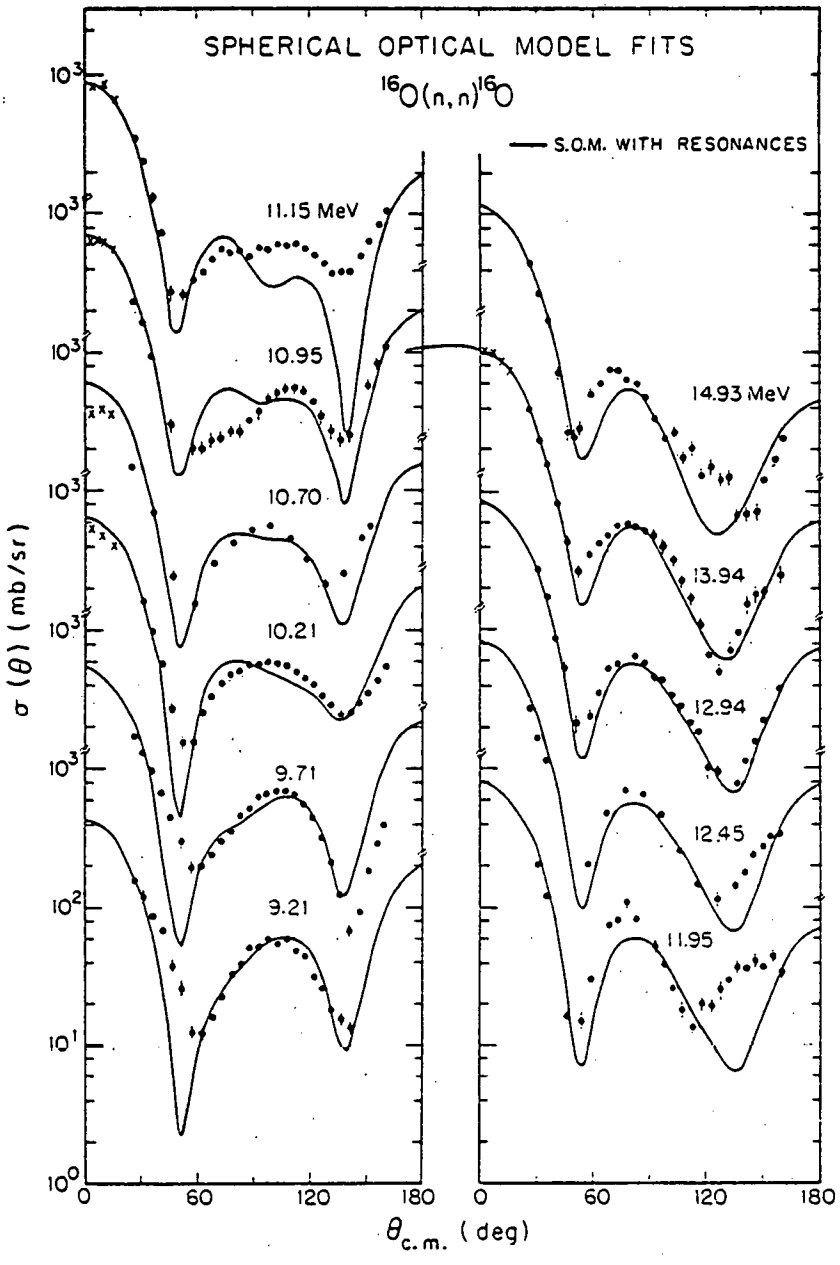

Fig. A4-5. Spherical optical model fits to $^{16}O(n,n)^{16}O$ data.

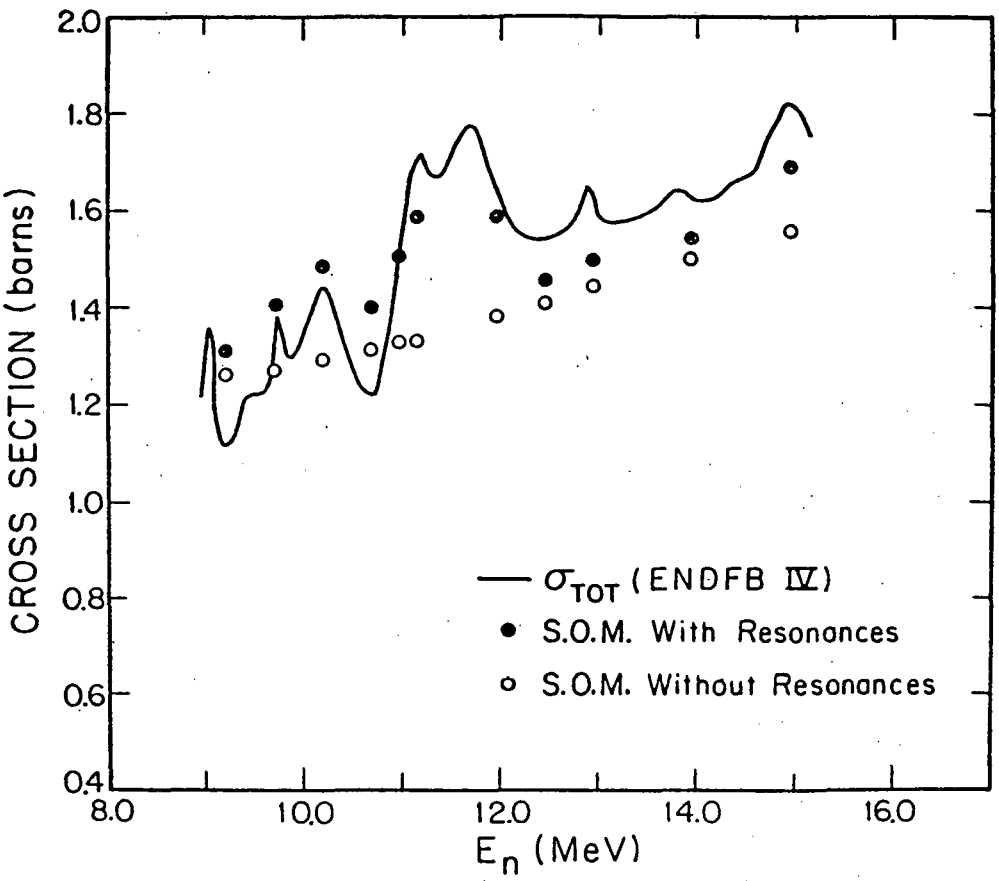

Fig. A4-6. Total cross section predictions for ^{16}O. The circles represent calculations from the S.O.M. background parameters and the dots are ANSPEC calculations.

5. Double Differential Neutron Scattering Cross Sections for Fe, Cu, Ni and Pb between 8 and 12 MeV

In order to complement theoretical predictions of neutron emission cross sections, we have undertaken a program of (n,n') measurements on medium mass to heavy nuclei, with particular emphasis on inelastic scattering to the continuum region. Our first experiments concentrated on neutron emission spectra measurements for natural iron, nickel, copper and lead following 7.5-MeV, 10- and 12-MeV neutron bombardment. Here we review our progress in converting the data to absolute double differential inelastic scattering cross sections.

The proton or deuteron beams were pulsed and bunched into about 2 ns bursts at a repetition rate of 1 MH_z with typical beam currents on target of 1.5 μA. The neutron flight paths were 2.76 and 3.73 m respectively for the two detectors, permitting detection of neutrons below 300 keV in energy without overlap from previous beam bursts. The neutron detectors were biased near the pulse height minimum between the 26- and 59-keV γ rays from our ^{241}Am source, corresponding to a threshold neutron energy of ~300 keV. The detection efficiency of the scintillators was measured in separate experiments from threshold to ~20 MeV.

The data at 7.5 MeV were taken with the $^{2}H(d,n)$ reaction. This corresponds to a deuteron energy which is below threshold for deuterium gas breakup and therefore this neutron source is strictly monoenergetic apart from ^{2}H breakup in the cell and entrance foil. At higher energies the D+d gas breakup cross section relative to the monoenergetic cross section rises more rapidly than for the $^{3}H(p,n)$ reaction. The $^{3}H(p,n)$ source is a factor of 3 better in this respect than the $^{2}H(d,n)$ reaction. Therefore, the 10- and 12-MeV data were taken with the $^{3}H(p,n)$ reaction. Background neutrons from (p,n) reactions in the cell material and beam stop are also present but, as in the case of the D+d experiment, can be taken into account by performing a gas-out measurement. These background contributions were large for the T+p experiments, even with the use of a ^{58}Ni beam dump. For the D+d experiments a tantalum beam dump was used and the backgrounds were much lower. The entrance foil in all experiments was of 3.5 μm molybdenum.

At 7.5 MeV the samples were in the form of small solid cylinders 3.0 cm high and 2.0 cm in diameter. At 10 and 12 MeV hollow cylindrical samples were used of height 4.5 cm, 3.0 cm outside diameter and 1.3 cm inside diameter.

Neutron angular distributions were typically measured at five angles from 40° to 145° at each energy. At each angle four TOF spectra were accumulated. These corresponded to (1) gas in, sample in, (2) gas out, sample in, (3) gas in, sample out, (4) gas out, sample out. Here "gas in" refers to deuterium or tritium gas in the cell. "Gas out" refers to the hydrogen isotope having been removed and replaced by an equal pressure of helium. This simulates energy loss effects. These four spectra were normalized to the integrated charged particle beam on target. Fig. A5-1 shows TOF spectra for the scattering of 10-MeV neutrons from iron at 100°. The neutron elastic scattering peak is visible in about channel 700 only in spectrum 1. The sample out backgrounds in spectra 3 and 4 are relatively flat. The contribution of the (p,n)

background in spectrum 2 is structured because of resonances in the elastic scattering cross section of iron. The background associated with (p,n) reactions in the cell material is eliminated by forming the difference (1-3)-(2-4). This is the final TOF spectrum and is shown in Fig. A5-2. Most of the structure between channels 400 and

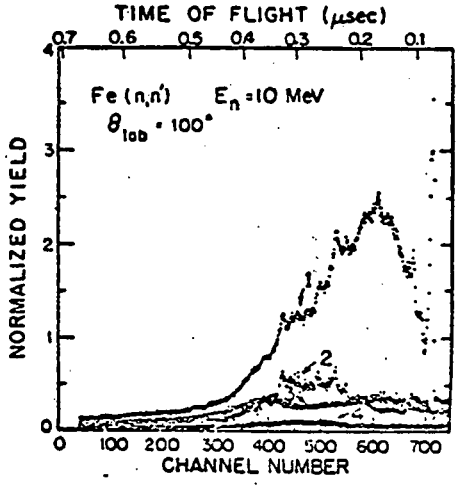

Fig. A5-1. Four neutron scattering spectra.
1) Tritium in cell, sample in place
2) Helium in cell, sample in place
3) Tritium in cell, sample removed
4) Helium in cell, sample removed

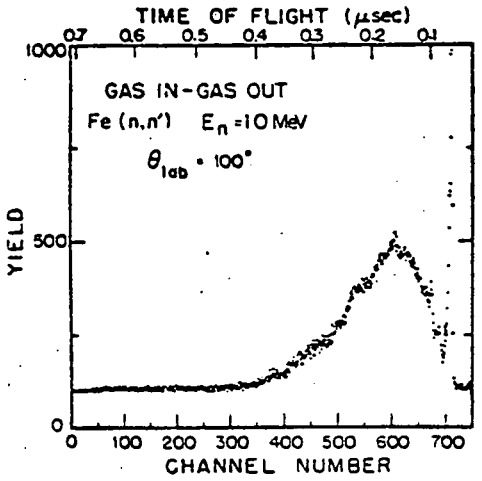

Fig. A5-2. Difference spectrum from Fig. A5-1 (1-3)-(2-4). This spectrum is biased by 100 counts.

550 is removed and the final spectrum is relatively smooth. Scattering of tritium-gas breakup neutrons is still present in this spectrum and is not removed by subtracting the "gas out" spectra. The contribution of these neutrons to the continuum yield is taken into account later in the analysis.

The final time of flight spectra are transformed to energy spectra, folding in the detector efficiency. Figure A5-3 shows energy spectra for iron, nickel, copper and lead scattering at 125° for an incident neutron energy of 12 MeV. These spectra are arbitrarily normalized and are not corrected for attenuation effects or for multiple scattering. The fluctuations below ~2 MeV for the iron and nickel data at 12 MeV are an artifact of the data due to a slight energy shift between the gas-in and gas-out runs. There is some evidence for collective enhancement in the region of the 3^- states of the even-even nuclei.

Fig. A5-4 shows the angular distributions for the scattering of 10-MeV neutrons from iron. The spectral shapes are almost identical apart from the effects of the highly anisotropic elastic scattering peak.

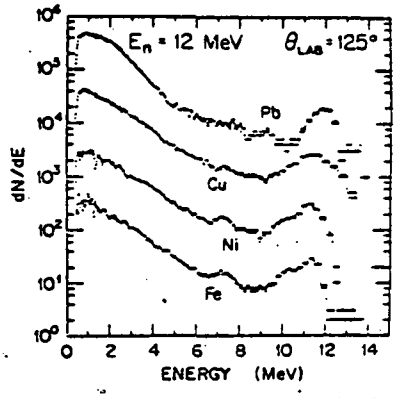

Fig. A5-3. Energy spectra for neutron scattering from Fe, Ni, Cu, Pb at 125° for an incident neutron energy of 12 MeV. The vertical scale is arbitrarily normalized and is in counts per 20 keV energy internal.

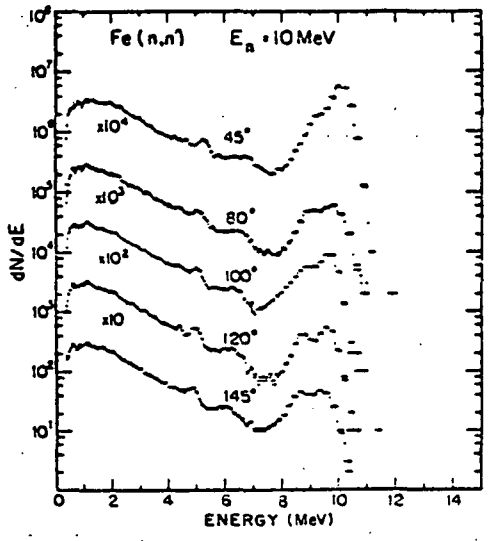

Fig. A5-4. As Fig. A5-3 except Fe scattering at 10 MeV for five different laboratory scattering angles.

6. Multiple Scattering Corrections

Work has continued on development of the Monte Carlo programs for the correction of neutron scattering data. Aimed at producing a realistic simulation of the time-of-flight experiment and data reduction conditions, EFFIGY and EFFIGYC include the effects of finite volume of the neutron production sites, the scattering sample, and the detector, as well as non-zero time and energy resolution. Multiple scattering and attenuation are also calculated. Included are capabilities for multi-element samples of hollow cylindrical shape. Kinematics are calculated to allow for energy loss in light elements and cross section searches have been speeded up. The simulation procedure is outlined in Fig. A6-1. During the past year work to make the programs nearly identical to the user and to simplify operation has neared completion. A detailed description of both codes and their operation should be ready early in 1980.

EFFIGY calculates corrections to angular distributions of up to ten discrete groups. Time-of-flight spectra are generated and windows summed to derive "experimental" angular distributions which are compared to the measured values. Cross section tables are updated and the procedure is repeated iteratively until agreement between experiment and calculation are obtained. For multi-element samples, effects of known cross sections may be removed from the calculation to obtain single element cross sections where levels overlap. An example of the results of these processes is shown in Fig. A6-2 for ^{11}B elastic scattering data. This code has had no major revision in the simulation process for the period of this report and has been used to correct the data for the discrete scattering program.

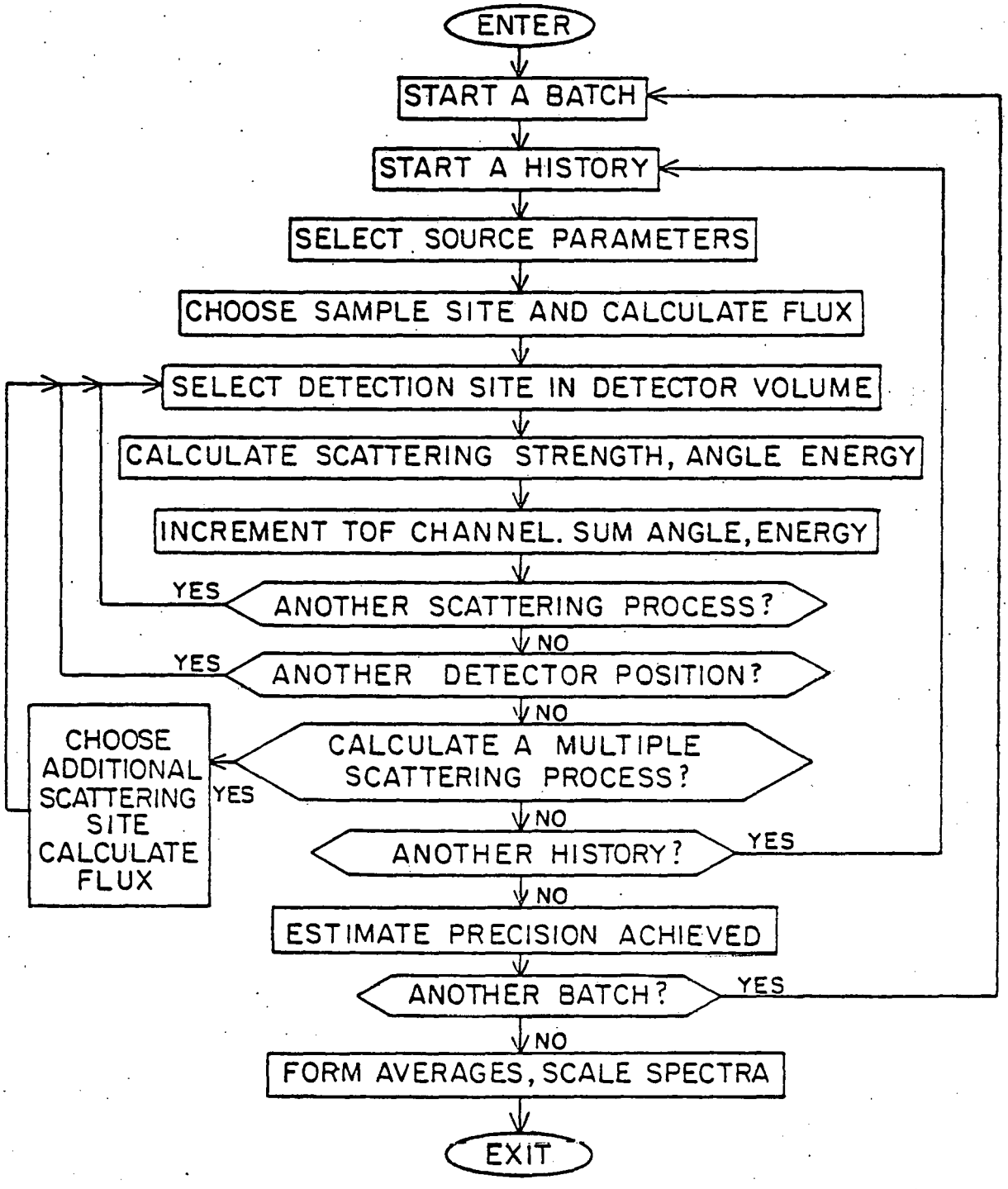

Fig. A6-1. Simulation procedure in multiple-scattering correction code.

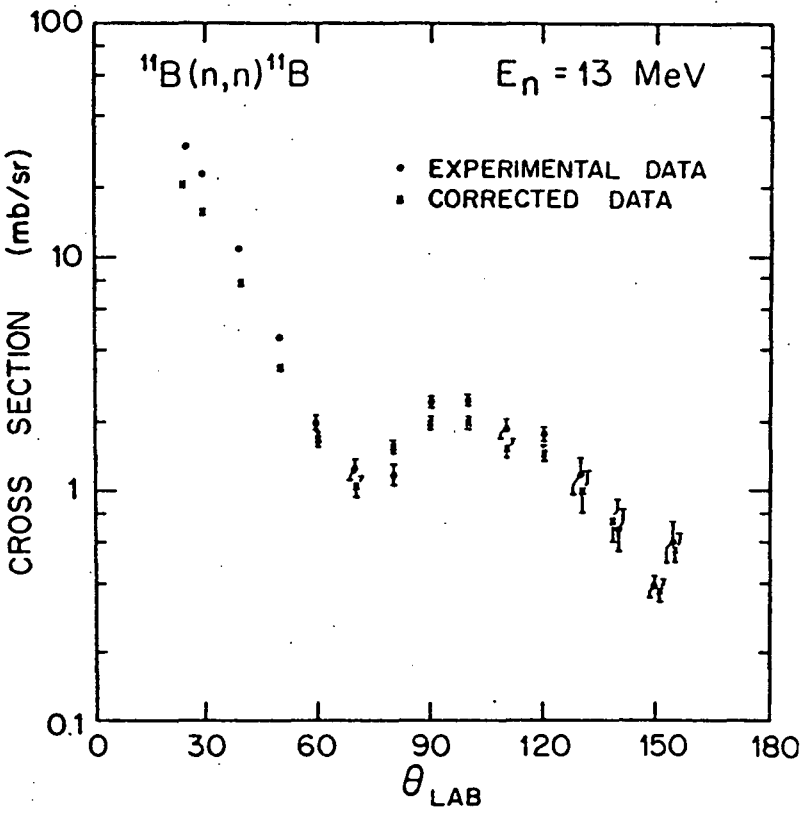

Fig. A6-2. EFFIGYC calculation of time-of-flight spectra compared to experimental spectra for E_n=12 MeV.

EFFIGYC calculates corrections to the energy distributions of continuous neutron emission spectra, including effects of up to ten continuum and discrete processes. Cross sections for 1 unknown continuum process are updated and the effects of 1 known continuum process and up to nine discrete processes may be removed. Any of these processes may overlap the continuum. For source distributions which are not monoenergetic, EFFIGYC calculates the effects of gas breakups and removes this from the cross section. Time-of-flight spectra for up to five angles are compared to experiment and the cross sections tables are updated. EFFIGYC iterates until the calculation agrees with experiment. Fig. A6-3 shows the results of such a calculation. The data are the circles and the line is the result of the calculation.

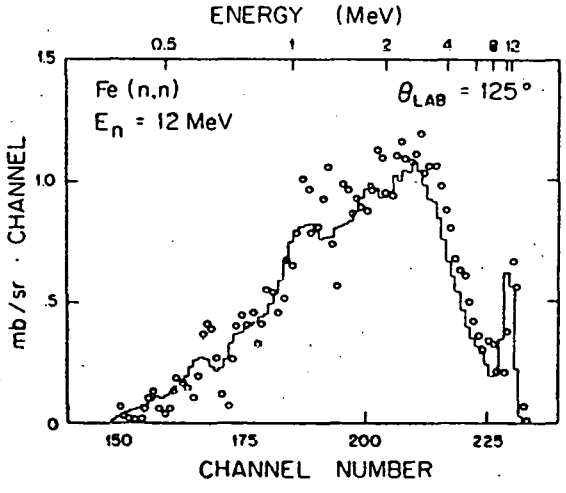

Fig. A6-3. Effect of EFFIGY correction on a typical angular distribution for ^{11}B.

7. Elastic Scattering of 8-, 10- and 12 MeV Neutrons from ^{54}Fe, ^{56}Fe, ^{63}Cu and ^{65}Cu

Angular distributions of elastically scattered neutrons have been obtained at 8.0, 10.0 and 12.0 MeV for greater than 98% pure isotopically enriched samples of ^{54}Fe, ^{56}Fe, ^{63}Cu and ^{65}Cu. Measurements were made in 5° steps from 30° to 155° to a statistical accuracy of about ±3% or better. The $^{2}H(d,n)^{3}He$ source reaction was employed, and the overall time resolution was about 3 ns. Data were also obtained at 14.0 MeV, but, because there were difficulties with the neutron monitor detector, the data may need to be remeasured.

The time resolution was not sufficient to separate the first inelastic groups from the elastic group at all angles. The spectra do permit determination of the inelastic cross sections when the elastic-to-inelastic ratio is less than 50:1 at the two lowest energies. This allows a determination of $\sigma(\theta)$ for Fe(n,n') and Cu(n,n') for angles between about 45° and 160° at 8 and 10 MeV. However, to extract the inelastic $\sigma(\theta)$, a gaussian peak fitting routine must be used. The accuracy of the data is deleteriously affected by the use of this procedure and by a tail of unknown origin which begins at the elastic peak and extends under all the inelastic peaks. The uncertainties that will be assigned to the inelastic data are in the range of 10%.

The elastic data were normalized to the yield obtained with a hydrogenous scatterer. This method, coupled to our knowledge of the detector relative efficiencies, i.e., calibrated to about ±3%, should give cross-section determination to a relative accuracy of about 5% and an absolute accuracy of under 8%.

A preliminary analysis of the data was shown at the International Nuclear Cross Section meeting at Knoxville. Fig. A7-1 illustrates the shape of the

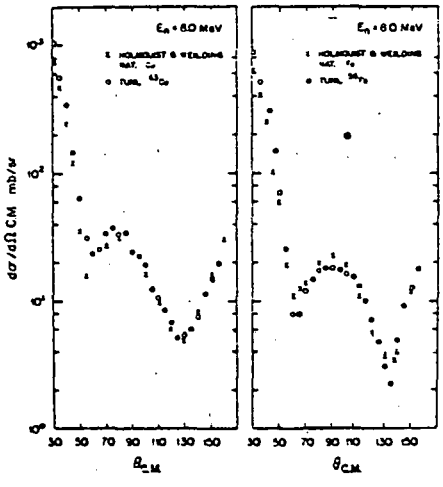

Fig. A7-1. Comparison of present results to previous work.

cross section and how the present data compare to the earlier data of Holmquist and Weilding.[1] Our data have been processed with the multiple scattering code EFFIGY

[1] B. Holmquist and T. Weilding, A. B. Atomenergi, Studsvik, Sweden, Report AE-303 (1967); BNL 400, TID-4500 (1970), EANDC(US)-138 "U".

This program also accounts for geometrical effects and the relative efficiency of the detector. Our corrected data are in good agreement with those of Holmquist and Weilding, except for the forward angles.

Optical model comparisons of the data for all four isotopes were initiated, using our preliminary cross-section values. The results for ^{63}Cu and ^{56}Fe are shown in Figs. A7-2 through A7-5. In Fig. A7-2 and A7-3 the data are compared to the predictions using the Wilmore and Hodgson[1] parameters, after adding the "standard" spin-orbit term of Ref. 2, $V_{so} = 6.2$ MeV, $r_{so} = 1.1$ fm, and $a_{so} = 0.75$ fm. The agreement is already quite good without varying any of the parameters. The neutron optical model set given by Bechetti and Greenlees describes the data poorly.

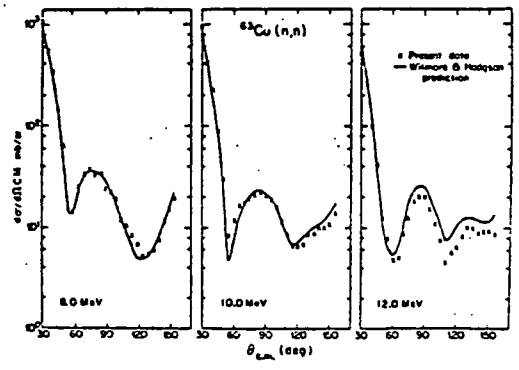

Fig. A7-2. Present results compared to optical model predictions based on Wilmore and Hodgson parameters.

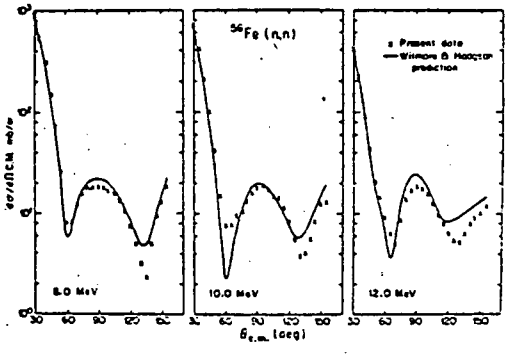

Fig. A7-3. Present results compared to optical model predictions based on Wilmore and Hodgson parameters.

A quick search on the real-well depth and the imaginary-well depth was made using the code GENOA of F. Perey. The search started with the Wilmore-Hodgson set. The results for two isotopes are shown in Figs. A7-4 and A7-5. The ^{63}Cu data are quite well described, but the ^{56}Fe calculations undershoot the data in the first minimum. Compound-nucleus contributions can fill in such minima, but we expect these effects to be small.

Before the data will be published we intend to do the following:

[1] D. Wilmore and P. E. Hodgson, Nucl. Phys. 55 (1964) 673

[2] F. D. Bechetti, Jr. and G. W. Greenlees, Polarization Phenomena in Nuclear Reactions, edited by H. H. Barschall and W. Haeberli, The University of Wisconsin Press, p. 682, Madison (1971).

(1) recheck each measurement, carefully evaluating the inelastic contribution to the elastic peak and extracting the best inelastic yield; (2) examine our procedure for assigning errors; (3) conduct compound nucleus calculations to estimate the size of this contribution; (4) carry out a careful systematic global optical model search of the data for these four isotopes.

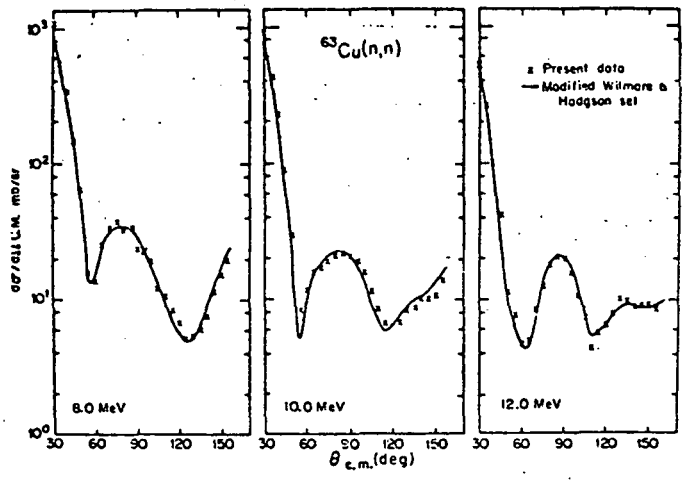

Fig. A7-4. Present results compared to optical model search on V_o and W_o.

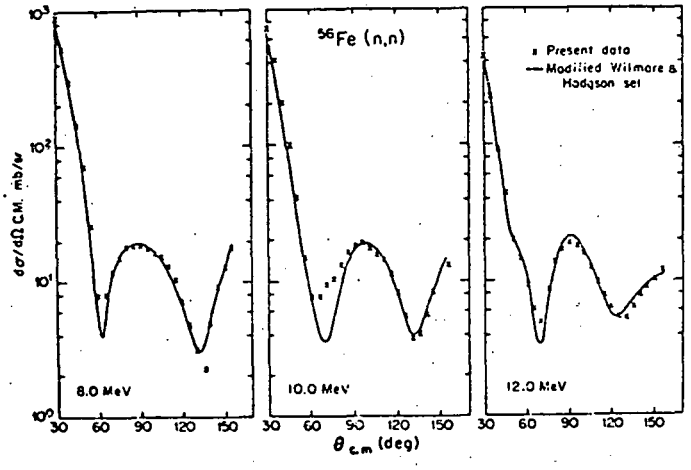

Fig. A7-5. Present results compared to optical model search on V_o and W_o.

B. HIGH RESOLUTION STUDIES

1. High Resolution Elastic Scattering (E. G. Bilpuch, G. E. Mitchell, B. Dubendorff, R. O. Nelson, K. B. Sales, W. A. Watson, C. R. Westerfeldt)

Interests in elastic scattering involve both statistical properties and analogue state properties. Study of the zinc isotopes extends our proton strength function measurements to higher A values. Measurement of elastic and inelastic scattering from ^{56}Fe is our first complete study (multichannel, broad energy range) with the tandem high resolution system. Study of ^{29}Si represents our first experiment with non-zero spin targets.

a. ^{64}Zn, ^{66}Zn

Initial efforts were hampered by difficulty in obtaining stable, uniform zinc targets. Since the level density in ^{65}Ga was rather low, we obtained satisfactory results for ^{64}Zn even with less than ideal targets. The ^{64}Zn(p,p) reaction was measured between E_p = 2.50 and 3.24 MeV with the high resolution system on the 3 MV accelerator. Thirty-nine resonances were observed, including thirty-two $1/2^+$ resonances. Analogues of the 0.867 MeV($1/2^-$), 0.910 MeV($3/2^-$) and 1.370 MeV($5/2^+$) states in ^{65}Zn were observed at E_p = 2.77, 2.82, and 3.22 MeV. Coulomb energies and spectroscopic factors were determined for these analogue states. The $s_{1/2}$ proton strength function was determined to be S = 0.050 ± 0.012, where the error is the statistical error alone. A preliminary report on this work was presented at a meeting of the Southeastern Section of the American Physical Society: K. B. Sales, G. E. Mitchell, E. G. Bilpuch, and C. R. Westerfeldt, Bull. Am. Phys. Soc. 24, 107 (1979).

For the ^{66}Zn(p,p) experiment improved targets were essential, since the level density in ^{67}Ga was several times greater than in ^{65}Ga. A different target making procedure was adopted, utilizing a glow discharge system which we designed and built. Targets were fabricated using this new glow-discharge system to clean the target backings before evaporating the zinc isotope. This new method gave targets with greater stability and uniformity than our previous methods of target preparation. In addition, improved detector and beam line collimators were designed and built.

The differential cross section for ^{66}Zn(p,p) was measured from E_p = 2.60 to 3.26 MeV at laboratory angles of 90°, 105°, 135° and 160°. The overall energy resolution varied between about 350 and 400 eV. Analyses of these data yield 102 s-wave and 46 p-wave resonances. The statistical distributions of resonance widths and spacings for the $1/2^+$ resonances were examined. The value of the s-wave strength function is s = 0.058 ± .008. This value is slightly larger than the typical value of the s-wave strength function for nuclei between A = 60 to 65. However, for nuclei with A = 55 to 65 s is between 0.04 and 0.06. There is thus no clear evidence in our data for the 35 Size resonance. Our overall strength function data are shown in Fig. B1-1. The majority of the p-wave resonances were identified

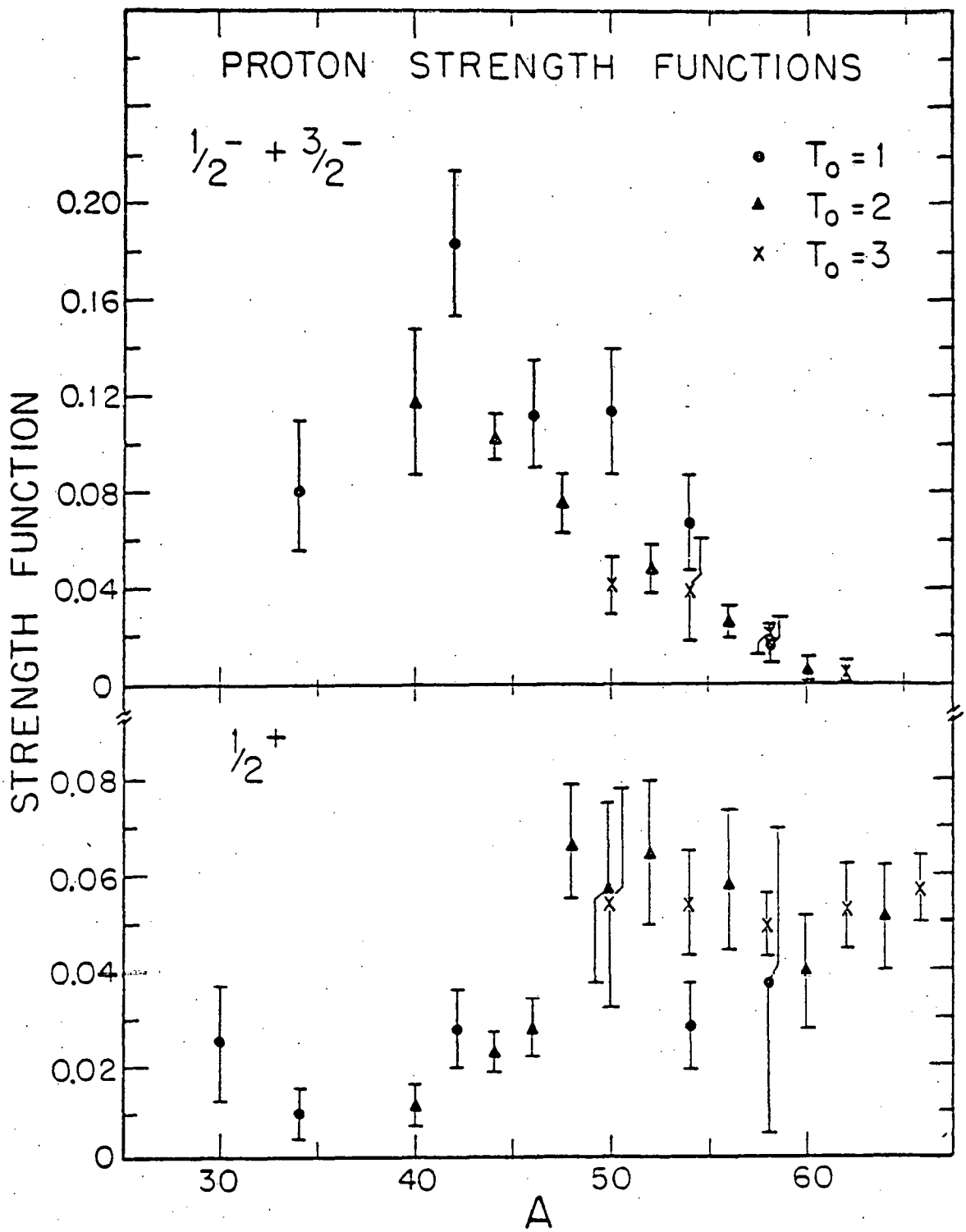

Fig. B1-1. Proton strength function for $\ell = 1$ and $\ell = 0$ resonances.

as fragmented analogues of the second ($1/2^-$) and fourth ($3/2^-$) excited states of ^{67}Zn. Spectroscopic factors and Coulomb energies were determined for these analogues. Analyses of the fine structure distribution for each analogue is in process.

b. ^{29}Si

All of our previous elastic scattering experiments have been on spin-zero targets, in order to make the analysis feasible. However, non spin-zero targets would open up a wide range of interesting experiments. We decided to explore these possibilities by studying one target with ground state spin 1/2 and with rather low level density. ^{29}Si was chosen, since it satisfies these two criteria, and stable uniform silicon targets are relatively easy to prepare. In addition, there were previous elastic scattering results available, although there were no very high-resolution data. Overall there was more information available for ^{29}Si than for any other convenient target of interest. The primary motivation was to examine the practical difficulties and ambiguities involved in such analyses, before embarking on a major study of non spin-zero targets.

The differential cross section for elastic and inelastic scattering from ^{29}Si was measured from E_p = 1.3 - 3.3 MeV (inelastic scattering is appreciable only above 2.5 MeV). The 160° cross section is shown in Fig. B1-2. These data are in qualitative agreement with earlier measurements, although we do see some additional resonances, and naturally with improved resolution the narrower resonances are more striking. Analysis of these data is now at the preliminary stage.

c. ^{56}Fe

As part of a program to extend high resolution elastic and inelastic scattering data beyond the 3.3 MeV achievable with the 3 MV Van de Graaff accelerator, excitation functions for the reactions ^{56}Fe(p,p) and ^{56}Fe(p,p') were measured from E_p = 3.1 to 4.0 MeV using the TUNL FN tandem Van de Graaff accelerator. As described in previous reports, the tandem laboratory is equipped with a three-loop energy regulating system which includes an optical feedback path permitting high voltage modulation of the terminal stripper, canceling residual energy fluctuations not removed by the corona loop. Using this system, proton beam energy resolution was typically 425 eV. The data were taken in steps of 80 to 240 eV (typically 100 eV) at center of mass angles 90°, 107°, 125°, 150°, and 160°. Because of unfavorable kinematics, the inelastic data for 150° and 160° end at about 3.75 MeV.

Analysis of this work is still in progress, but some results are available. Thus far, over 250 resonances have been fit, over half of which have $\ell = 2$. The 150 or so d-wave resonances include a fragmented analogue state at E_p = 3.75 MeV. The p-wave resonances include two fragmented analogues: a $3/2^-$ state near E_p = 3.81 MeV and a $1/2^-$ state near 3.93 MeV. The two f-wave analogues (at 3.35 and 3.45 MeV) predicted by (d,p) measurements have not been observed, probably due to their small spectroscopic factors and the high f-wave level density expected in this region. The g-wave analogue at E_p = 3.70 MeV has

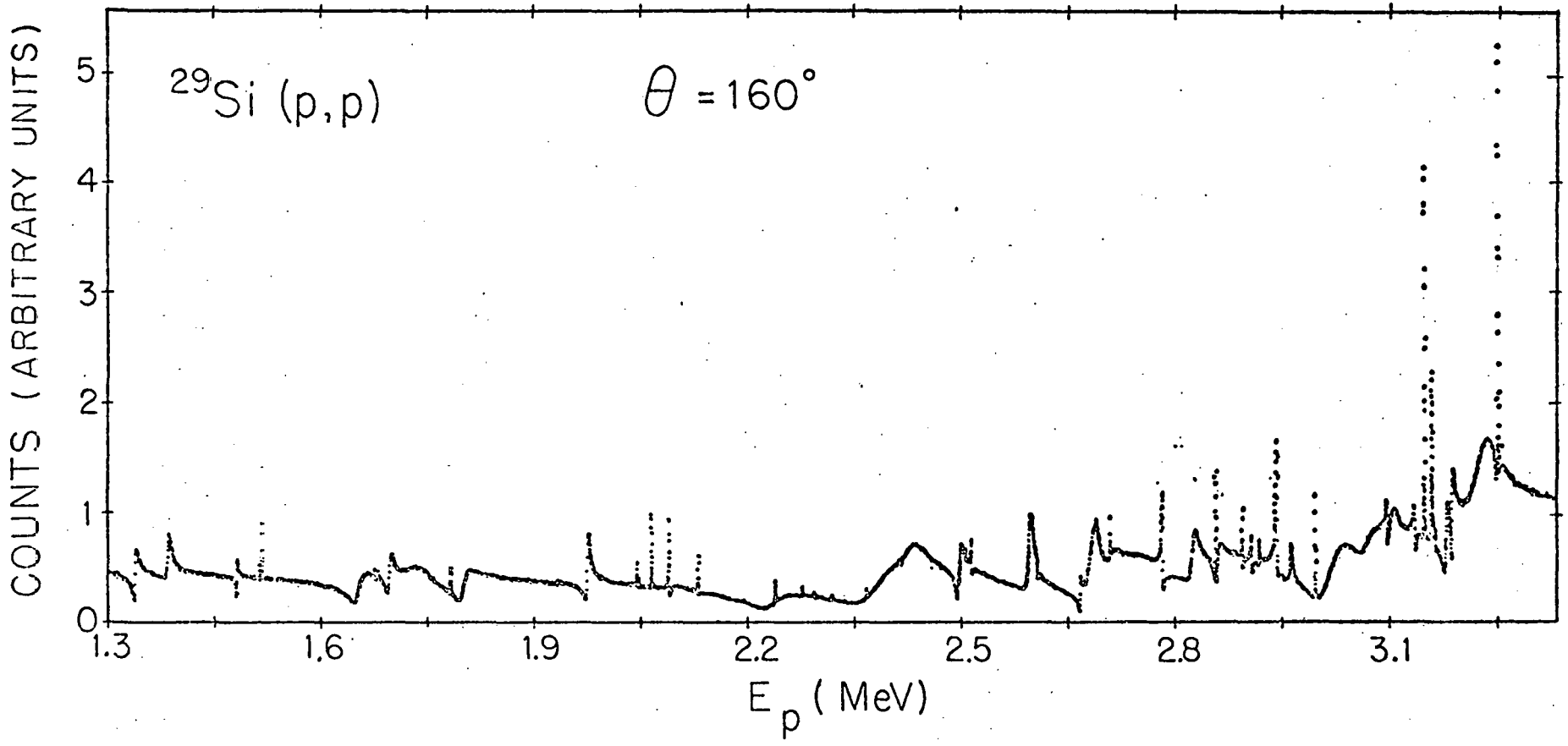

Fig. B1-2. Differential cross section for ^{29}Si(p,p) at θ= 160°.

also not been seen, but the analysis of this section of the data is still incomplete.

Some anomalous s-wave strength is observed from about 3.7 to 3.9 MeV. It is not an analogue state (not observed in (d,p) measurements) and is too localized to be part of the 3s size resonance. It is interesting to note that this same sort of phenomenon was observed in ^{54}Fe(p,p) from 3.9 to 4.2 MeV. Although in ^{56}Fe the effect is not as dramatic (the sum of elastic widths in approximately 15 keV vs 70 keV in ^{54}Fe), the occurance of this phenomenon in neighboring nuclides is interesting.

Because it is usually not possible to assign the spin of narrow d-wave resonances from proton elastic and inelastic scattering data, angular distributions of de-excitation γ-rays were measured for all d-wave resonances for which $\Gamma_p\Gamma_{p'}/(\Gamma_p + \Gamma_{p'})$ was greater than 10 eV (i.e., those resonances for which the yield would be high). This includes about 100 of the d-wave resonances. The presence of an a_4 term in these γ-ray angular distributions is used as the criterion for a spin assignment of $5/2^+$. Thus far, 20% of the d-wave spin assignments are $3/2^+$ and 80% are $5/2^+$. This is a significant deviation from a purely statistical set, for which the $5/2^+$ to $3/2^+$ ratio is 1.5. One possible explanation for this difference could be a larger $d_{5/2}$ strength function.

Further analysis will include examination of the s-wave strength function, analogue spectroscopic factors and fine structure, and the statistical distributions of resonance widths and spacings. The new terminal high voltage amplifier described in last year's report has been installed, tested, and is now in use. As previously reported, the new amplifier has a higher current capacity, and some improvements in linearity were observed. A third terminal amplifier, similar to the second, is now being fabricated. Further improvements in linearity are expected.

A microprocessor is now in use driving the stepping motor which steps the programming voltage to the magnets. This relieves the computer of the necessity of directly driving the stepping motor. In conjunction with the digitally programmed frequency synthesizer used in an NMR control system, this microprocessor allows stepping of the machine energy in precise increments in less than a second.

2. High Resolution Inelastic Scattering (G. E. Mitchell, E. G. Bilpuch, B. H. Chou, J. Shriner, W. A. Watson, C. R. Westerfeldt, K. M. Whatley)

a. General Description

Emphasis on high resolution inelastic scattering has continued during the past year. The determination of the relative signs of inelastic amplitudes provides new and more sensitive tests for both doorway state theory and for statistical theories. The central point is that these nuclear theories are formulated in terms of reduced width amplitudes γ, but almost all experiments measure only the magnitude of γ. The sign of the amplitude itself is impossible

to determine. Thus, the measurement of the magnitudes and relative regions of width amplitudes in multichannel processes are the most sensitive measurements possible.

Isolated resonances are studied with the reaction $A(p,p')B^*$ followed by $B^* \rightarrow + B + \gamma$. For all of our experiments $j^\pi_A = j^\pi_B = 0^+$ and $j^\pi_{B^*} = 2^+$. Angular distributions of the inelastically scattered protons and of the de-excitation γ-rays are measured. Since only singles measurements are involved, the study of many resonances is possible. Performing the experiments at low energies (relative to the Coulomb and angular momentum barriers) reduces the number of exit orbital angular momenta involved and make the analysis feasible. The critical point is the coherence of the decay amplitudes from the compound nuclear state to the residual state.

For notational convenience we label the compound nuclear state by $1/2^+$, $1/2^-$, $3/2^-$, $3/2^+$, etc. and the decay amplitudes by $p_{1/2}$, $p_{3/2}$, $d_{3/2}$, etc. Ratios of width amplitudes are defined as mixing ratios $\delta_{AB} = \delta_A/\delta_B$. The function $\phi = \tan^{-1}\delta$ is also very convenient.

In the following summary the term "number of equations" means the numbers of experimental coefficients in a Legendre polynomial expansion ($a_2(p')$, $a_2(\gamma)$, etc.), and the column labeled "interesting" refers to the possibility of obtaining information on interference effects.

TABLE B2-1

Resonance	No. of Equations	No. of Exit ℓ' Values		Interesting?
$1/2^+$	0	$d_{3/2}$, $d_{5/2}$	1	No
$1/2^-$	0	$p_{1/2}$, $p_{3/2}$	1[a]	No
$3/2^-$	2	$p_{1/2}$, $p_{3/2}$	1[a]	Yes!
$3/2^+$	2	$s_{1/2}$, $d_{3/2}$, $d_{5/2}$	2	Maybe
$5/2^+$	4	$s_{1/2}$, $d_{3/2}$, $d_{5/2}$	2	Yes!
$5/2^-$	4	$p_{1/2}$, $p_{3/2}$, $f_{5/2}$, $f_{7/2}$	2[b]	Yes
$7/2^-$	5	$p_{3/2}$, $f_{5/2}$, $f_{7/2}$	2[b]	Moderately
$7/2^+$	5	$d_{3/2}$, $d_{5/2}$	1[c]	Moderately
$9/2^+$	6	$d_{5/2}$	1[c]	No

a) The $\ell' = 3$ terms were neglected in the analysis of the $3/2^-$. For detailed reasons given below this is a much better approximation than one would normally expect.

b) Here the $\ell' = 3$ terms are included, even with the additional complexity of the angular distributions. The analysis is sensitive to even small $\ell' = 3$ admixtures.

c) $\ell' = 4$ is neglected.

The first crucial question is whether there are more equations than unknowns. At these low energies the ratio of penetrabilities for ℓ' and $\ell' + 2$ is typically about 100. Although one may safely list the term in the $(\ell' + 2)$ amplitude squared, the interference term is still of order 10%. However, there is an additional effect due to the Coulomb phase shift which cancels except in the interference term. The net result is an additional multiplicative factor $\cos(\sigma_{\ell'+2} - \sigma_{\ell'})$. For the $\ell' = 1$ and $\ell' = 3$ combination this factor is usually small in our mass and energy region. It is therefore a reasonable approximation to neglect the $\ell' = 3$ term for the study of $3/2^-$ resonances. For the $5/2^-$ resonances we have sufficient equations to solve the problem completely and the $\ell' = 3$ term is included. In practice it is usually rather small. However, in our experiments the cosine factor is not small for the $\ell' = 0$ and 2 mixture. The relatively large size of the interference is of great aid in the analysis of the decay of $5/2^+$ resonances. In our data we see mainly s, p, and d-wave resonances, a few f-wave resonances, and very few g-wave resonances. Since the nuclei being studied are in the region of the nuclear 1f-2p shell, the analogues are almost all p and f resonances. From Table C2-1 it is clear that $J = 1/2$ resonances are not suitable for these studies. From these general considerations, the main thrust of our program becomes clear. We study in detail $3/2^-$ and $5/2^+$ resonances, the former primarily for analogue states and the latter primarily for statistical purposes. An overview of this work has been presented recently in invited talks by G. E. Mitchell at two conferences: International Conference on Theory and Applications of Moment Methods in Many Fermion Systems, Ames, Iowa, September, 1979, and Adriatic Europhysics Study Conference on Statistical Properties of Nuclei, Hvar, Yugoslavia, October, 1979. The abstract for the latter talk is given below:

> "The several thousand proton resonances studied by our group provide a body of resonance data unmatched in charged particle spectroscopy. Since these data include both analogue and background regions, a large amount of statistical information is available in addition to analogue state properties. Statistical information is obtained for both average properties (proton strength functions, average level densities, average capture widths) and for local properties (long-and short-range correlations for level spacings, correlations between partial widths in different channels). Recent results on the relative sign of width amplitudes verify predicted properties of doorway states and establish new non-statistical effects."

b. Distribution of Mixing Ratios

The expected distribution of the mixing ratios depends upon the physical assumptions adopted. Consider two extreme cases: the fine structure distribution of a doorway state and a purely statistical collection of compound nuclear levels.

For the doorway state, a simple heuristic argument provides a useful guide. "Before" mixing, the single analogue state by definition had some mixing ratio δ_A. Then one expects that δ_A should be approximately constant for a fragmented analogue state. For a uniform background, Lane showed explicitly that for an isolated common doorway the relative phase is the same for all levels. Thus the formal result agrees with the intuitive expectation. The prediction for the fragmented analogue state is that the mixing ratio δ (or the angle ϕ) should have approximately the same magnitude and sign for all states of the analogue. The extreme alternative hypothesis is that the amplitudes for each state in each channel are random. Assume the random phase approximation, and assume that the widths of the two distributions are equal. Then the distribution for $\gamma_{\lambda c}, \gamma_{\lambda c'}$ are Gaussians of zero mean. If one samples at random from the distributions for c and c', then the distribution for the ratio $\gamma_{\lambda c}/\gamma_{\lambda c'} \equiv \delta$ is a Cauchy distribution

$$P(\delta)d\delta = \frac{1}{\pi(1+\delta^2)}\, d\delta \quad .$$

With the transformation $\delta = \tan\phi$, this distribution becomes

$$W(\phi)d\phi = \frac{1}{\pi}\, d\phi \quad .$$

The assumption that the amplitudes in the two channels are completely uncorrelated therefore leads to a uniform distribution for the variable ϕ. (If the average values for the widths in the two channels are not equal, one can renormalize to an effective ϕ'(or δ') and the same reasoning carries through. The two extreme assumptions of interest lead to distributions which are dramatically different: a constant ϕ for a common doorway state and a uniform distribution for ϕ for a statistical collection of states. This is shown schematically in Fig. B2-1.

c. ^{44}Ca - $3/2^-$ Fragmented Analogue State

Several papers have been published on the results for the $^{44}Ca(p,p'\gamma)$ reaction in the vicinity of the $3/2^-$ fragmented analogue resonance near E_p = 2.6 MeV. Two of these papers were published during the past year: "Experimental Demonstration of Phase Relation for Common Doorway States", G. E. Mitchell, T. R. Dittrich, and E. G. Bilpuch, Neutron Capture Gamma-Ray Spectroscopy, ed. R. E. Chrien and W. R. Kane (Plenum Press, New York, 1979) p. 696 and "Study of Inelastic Proton Amplitudes for a Fragmented Analogue State in ^{45}Sc", G. E. Mitchell, T. R. Dittrich, and E. G. Bilpuch, Zeitschrift für Physik A289, 211 (1979). The following is the abstract of the latter paper:

> "The relative sign of inelastic proton-channel amplitudes has been measured for 31 resonances in ^{45}Sc. These resonances include the fragmented $3/2^-$ analogue state observed at E_p = 2.62 MeV in the $^{44}Ca(p,p)$ and $^{44}Ca(p,p')$ reactions. The analogue fine structure is analyzed for the elastic and two inelastic channels; the Robson asymmetry is displayed clearly in the inelastic channels. The relative sign of the mixing ratio remains the same for the 15 fine structure

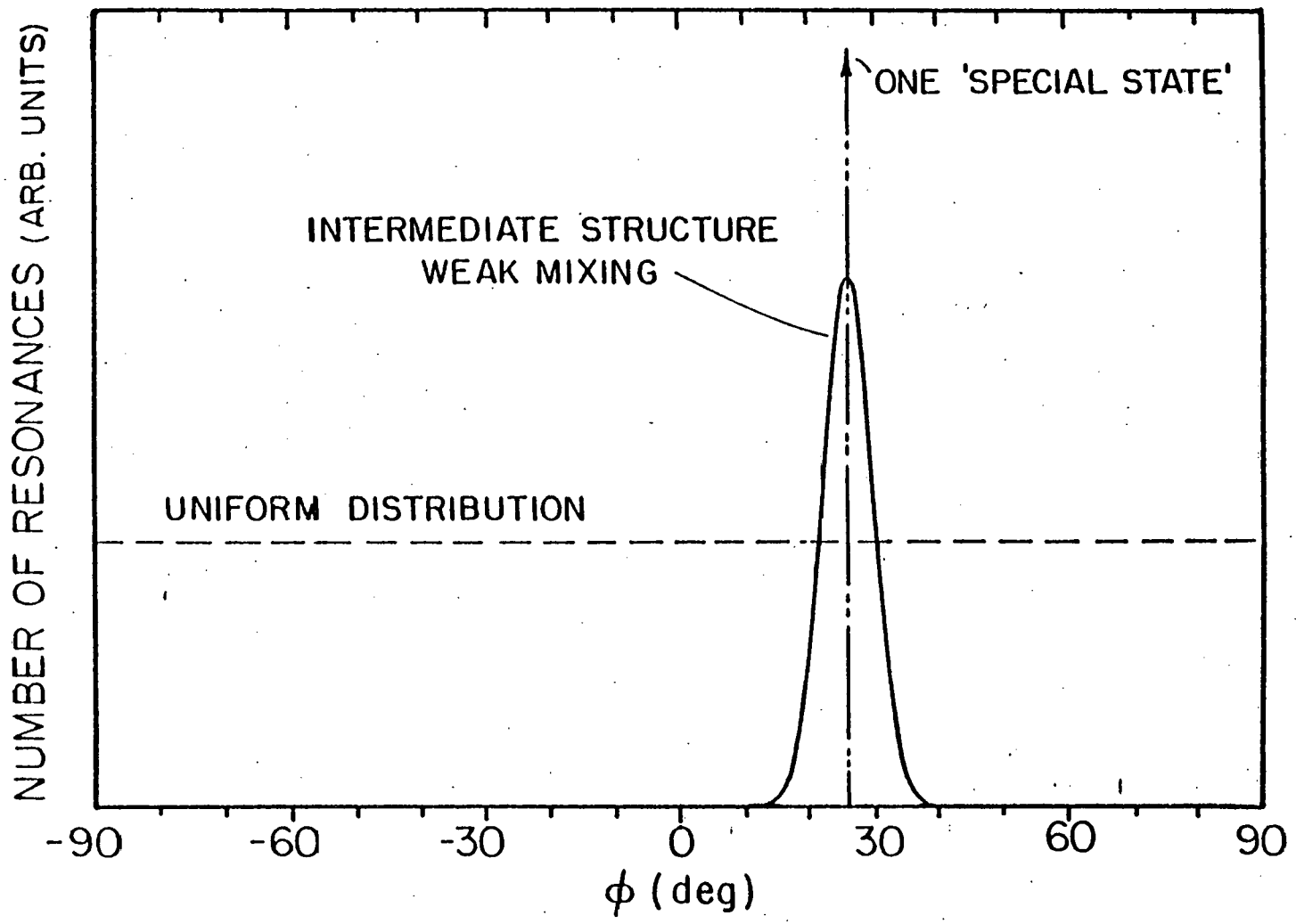

Fig. B2-1. Expected distribution for the mixing parameter $\phi = \tan^{-1}\delta$ for a common doorway state and in the extreme statistical limit.

resonances of the analogue. The mixing ratios enable the determination of the amplitude correlation of the widths in the inelastic channels. The recently introduced "off-diagonal strength function" is constructed from these data and compared with the theory of analogue state broadening."

A key feature of these data is agreement with Lane's prediction that δ(or ϕ) would be constant for a common doorway. The values of ϕ for the 15 resonances which constitute the fine structure of the $3/2^-$ analogue are shown in Fig. B2-2.

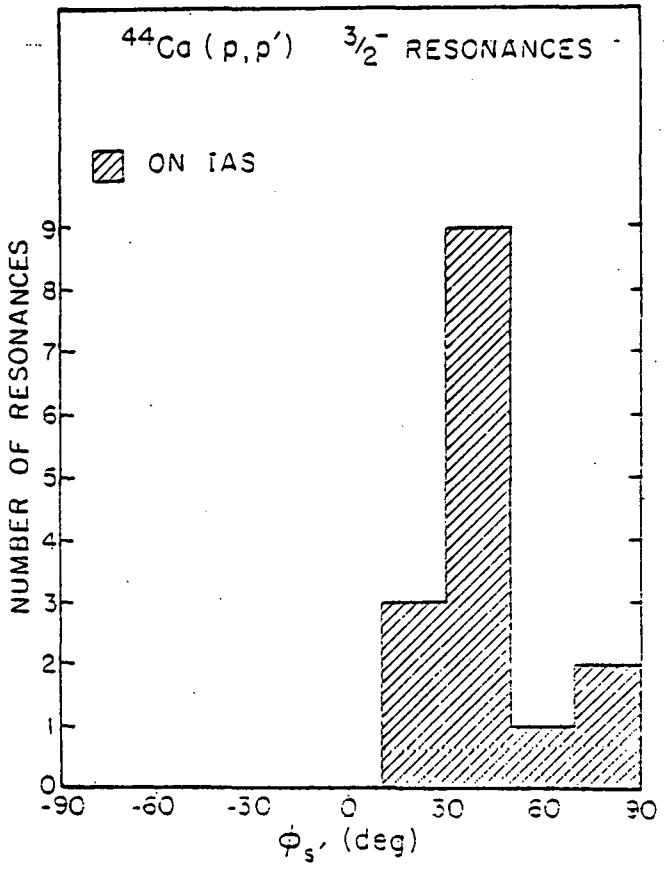

Fig. B2-2. Distribution of the mixing parameter ϕ for fragments of a $3/2^-$ analog state in ^{45}Sc.

d. ^{46}Ti - $3/2^-$ Fragmented Analogue State

Results for a fragmented analogue state in ^{47}V confirm the earlier work on ^{44}Ca described in the previous section. A paper has been published on this work: "Phase Relation for a Common Doorway State in ^{47}V", J. R. Chandler, G. E. Mitchell, and E. G. Bilpuch, Physical Review C, 20, 52 (1979). The following is the abstract of that paper:

"The $^{46}Ti(p,p\gamma)^{46}Ti$ reaction has been studied from E_p = 2.25 to 3.10 MeV with an overall energy resolution of about 350 eV. The magnitudes and relative signs of inelastic decay amplitudes were determined for the fine-structure resonances of a $3/2^-$ analog state in ^{47}V. The relative sign of the decay amplitudes is constant for the fine-structure states, in agreement with both the theoretical prediction and the one previous measurement."

e. ^{48}Ti - $3/2^-$ Resonances

This nucleus was chosen for study since 120 $\ell = 1$ resonances had been observed in our earlier elastic scattering studies, and since only one $\ell = 1$ analogue had been observed. Even this one analogue apparently was not fragmented. Thus $3/2^-$ resonances in ^{49}V seemed well suited for statistical analysis. Detailed information was obtained for seventy-two $3/2^-$ resonances. There was no anomalous variation of γ^2 with energy for either inelastic channel and the reduced width distributions agreed with the Porter-Thomas distribution. These data appeared to agree with conventional statistical tests. The results for the mixing parameter ϕ are shown in Fig. B2-3. These anomalies are statistically significant; detailed analysis indicates

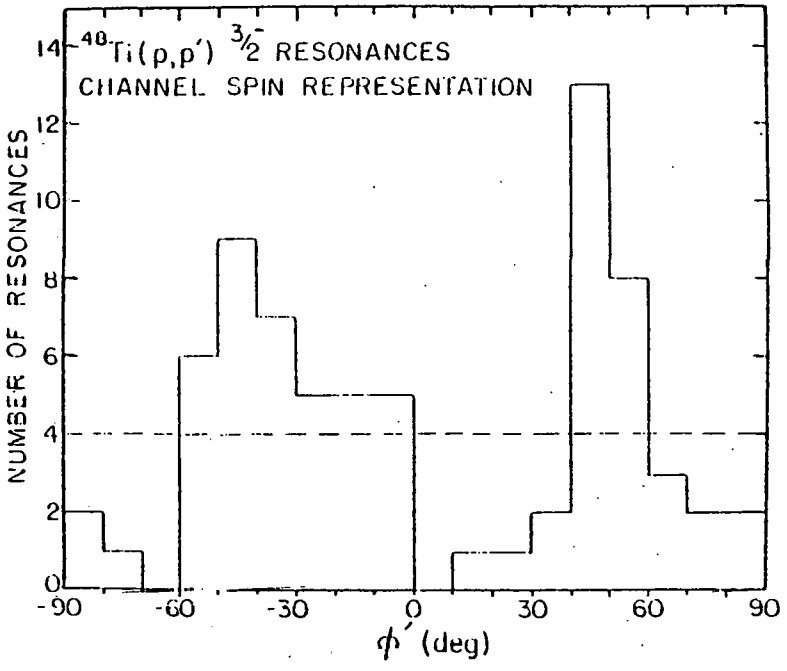

Fig. B2-3. Distribution of ϕ for $3/2^-$ resonances in ^{49}V. The dashed line represents the extreme statistical predictions.

that each bump is associated with a particular region of excitation energy. This is consistent with an intermediate structure interpretation. We have already published a preliminary report on this work: "Observation of Intermediate Structure in Inelastic Proton Amplitudes in ^{49}V", W. K. Wells, E. G. Bilpuch, and G. E. Mitchell, Physics Letters 86B, 18 (1979). A more detailed report will be prepared in the near future.

f. ^{48}Ti - $5/2^+$ Resonances

Known $\ell = 2$ resonances in $^{48}Ti(p,p)$ have been examined up to $E_p = 3.1$ MeV. The allowed angular distributions for $5/2^+$ resonances are shown in Fig. B2-4. Since the $\ell' = 0$ term dominates, the γ-ray distributions have large a_4 values for $5/2^+$ resonances. Since a_4 is necessarily zero for $3/2^+$ resonances, in practice it is usually easy to determine the J value of the resonance. For nearly 50 $5/2^+$ resonances mixing ratios were determined. Preliminary analysis indicates very reliable extraction of results when the $\ell' = 2$ admixture is about 10% or greater. For smaller admixtures, the errors are larger.

Preliminary results are shown in Fig. B2-5. (There are only two independent ratios; for simplicity all three values are included here.) Although these results are quite preliminary, and additional analysis and corrections will probably smooth the data somewhat, the behavior of the mixing parameters is quite striking. Strong non-statistical behavior is evident. Continued analysis of these data is in progress.

g. ^{54}Fe - $\ell = 3$ Resonances

Angular distributions have been measured for 10 $\ell = 3$ resonances in the $^{54}Fe(p,p'\gamma)$ reaction. The formalism was generalized to conveniently include mixed ℓ'-values and up to four inelastic amplitudes, and analysis programs were written. All 10 resonances were found to have $J^\pi = 5/2^-$. Values of the $p_{1/2}$ and $p_{3/2}$ amplitudes and the summed $f_{5/2} + f_{7/2}$ amplitudes $\ell' = 3$ admixture were determined for all resonances. Usually the $\ell' = 3$ admixture was too small to permit separate determination of $f_{5/2}$ and $f_{7/2}$ amplitudes. Five of the resonances were fragments of the $5/2^-$ analogue state near $E_p = 3.8$ MeV. Spectroscopic properties were extracted for the analogue state, including a value of 3% for the $\ell' = 3$ admixture.

A paper on this work has been prepared and is being submitted to Zeitschrift für Physik.

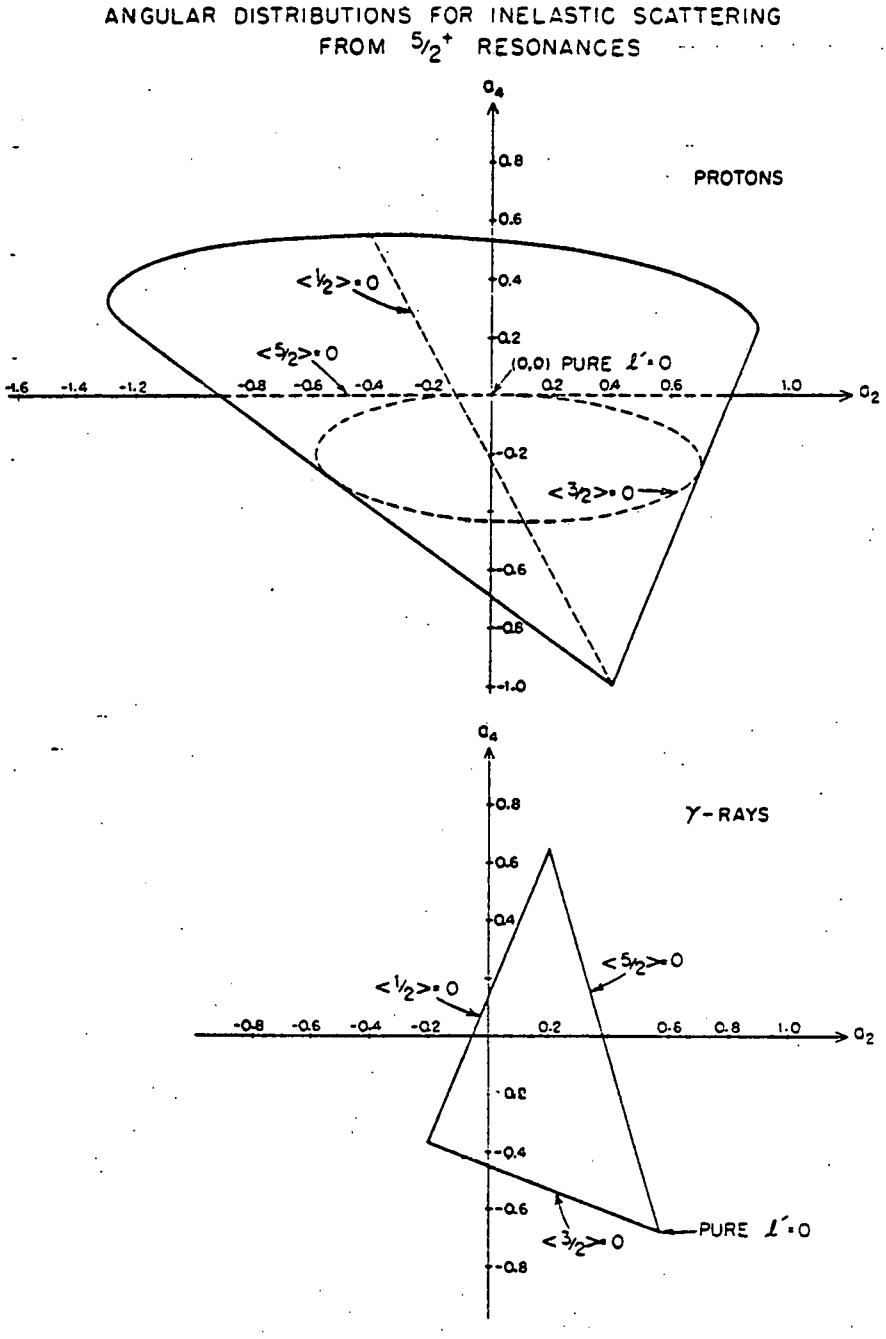
ANGULAR DISTRIBUTIONS FOR INELASTIC SCATTERING
FROM 5/2+ RESONANCES
a4
PROTONS
<1/2>=0
<5/2>=0
(0,0) PURE l'=0
<3/2>=0
a2
γ-RAYS
<5/2>=0
<1/2>=0
<3/2>=0
PURE l'=0

Fig. B2-4.

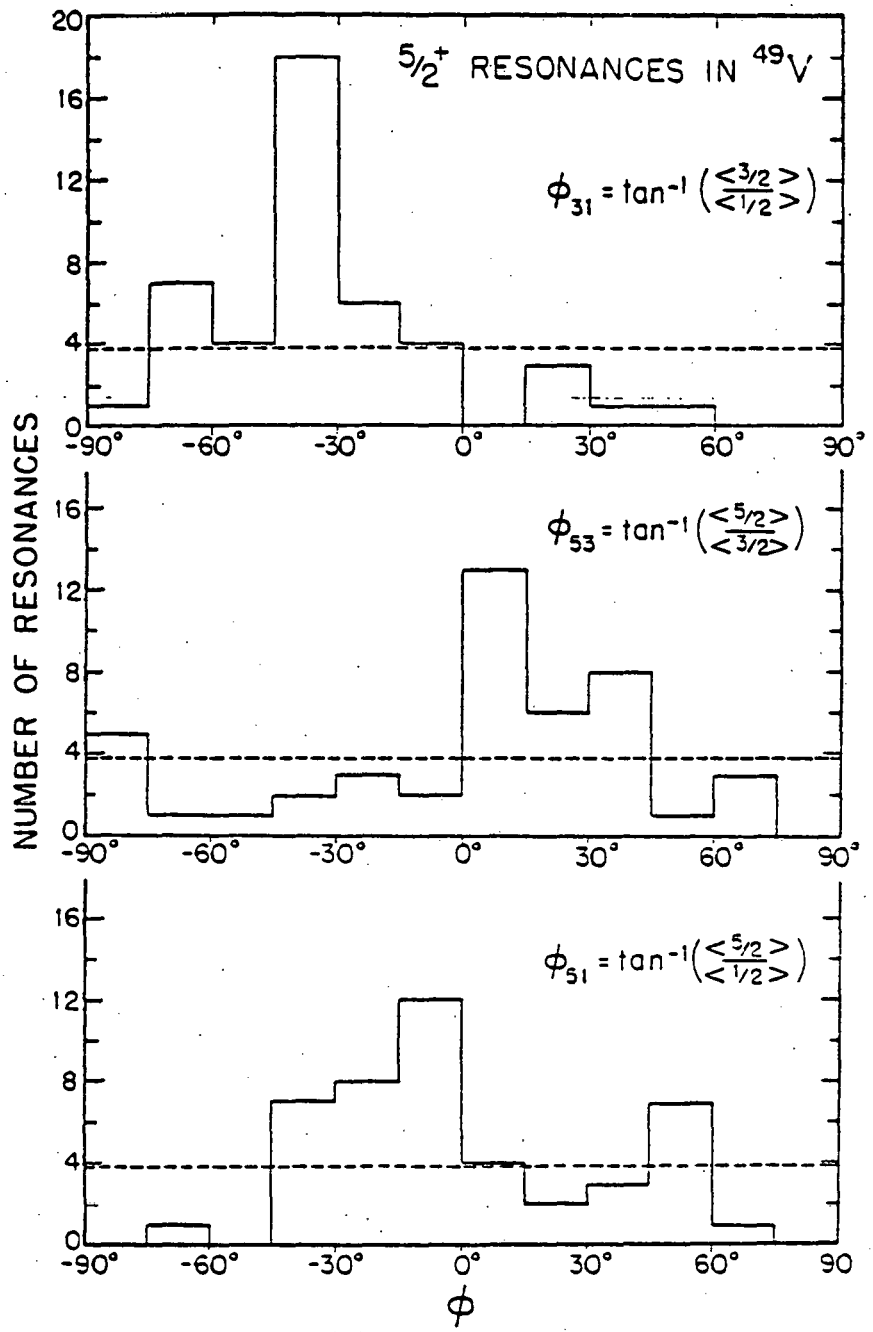

Fig. B2-5. Distributions of ϕ for $5/2^+$ resonances in ^{49}V. These are three ϕ's corresponding to the three ratios of amplitudes. These results are preliminary.

C. RADIATIVE CAPTURE REACTIONS

1. The Capture Program - General Status (N. R. Roberson, H. R. Weller, S. A. Wender, D. R. Tilley, M. Jensen, S. Manglos, L. Ward, M. Wright, C. Fitzpatrick, S. King, G. Mitev)

Work in the capture program has continued along two major lines:

(1) Proton Capture using the Cyclo-Graaff beams (18-31 MeV protons), and

(2) Polarized neutron capture using the recently added pulsed polarized beam.

The major emphasis of our Cyclo-Graaff effort has been directed towards confirming the anomalous effect observed in the $T(p,\gamma)^4He$ reaction which suggested the existence of a narrow ($\Gamma \sim 3$ MeV) 2^+ resonance near 40 MeV in ^4He. These measurements have been completed and, together with the $^4He(e,p)T$ measurements done at the Linear Accelerator Laboratory (Saskatchewan), provide convincing evidence for the existence of this effect.

We have also utilized the Cyclo-Graaff beam to study capture reactions leading to highly excited bound and unbound final states. Several reactions ($^{13}C+p$, $^{16}O+p$, ^7Li+p) have been observed. We have found that with protons of 22-30 MeV our system performs well enough in these cases to be able to observe capture to states as high as 20-25 MeV in the final nucleus. Studies of this type aimed at understanding the reaction mechanism of the capture process as well as searching for giant resonances built on these excited states will receive more attention in the future. The performance of the Cyclo-Graaff has been quite satisfactory, so that future work in this area can now be vigorously pursued.

Polarized neutron capture measurements have continued on ^{40}Ca, ^{13}C and ^3He targets. The addition of the two stage bunching system now allows us to run with a pulsed polarized neutron beam so that time-of-flight criteria can be employed to clean up the spectra. This, plus system improvements (e.g., a new deuterium gas cell) has increased the quantity and quality of our polarized neutron capture data.

Our experiment on ^{40}Ca has indicated that direct E2 radiation in itself is not adequate for describing the non-E1 effects seen in nucleon capture data. If we attribute the observed non-E1 effects to non-direct E2 strength, we find that this E2 strength is almost completely coherent. This result suggests that the GQR is decaying in a non-statistical manner, at least in the neutron channel which we are observing.

The data which we are obtaining on $^{13}C+n$ represent the first measurements of the giant resonance region of ^{14}C. In this case we are also finding that

large non-E1 effects other than direct E2 are present since we are observing significant non-zero b_1 coefficients.

One long range goal of our polarized neutron capture studies is to see if relative phases obtained between T-matrix elements in the more abundant polarized proton capture experiment can be used to predict the corresponding phases for neutrons. If so, many (γ,n) experiments could be more fully analyzed. Our study of $^{13}C(\vec{n},\gamma)$ gives relative phases which differ from those observed in $^{13}C(\vec{p},\gamma)$ by an amount almost equal to that predicted by a schematic direct-semidirect model calculation. This is an encouraging result which we hope to explore more fully in the near future.

We have also begun to study the $^3He(n,\gamma)^4He$ reaction. We have made preliminary measurements of unpolarized cross sections using a high pressure gas target. The polarized $(\vec{n},\gamma)$ measurements should be interesting, especially in comparison with the $T(\vec{p},\gamma)^4He$ results, since the b_2 coefficient is almost a direct measure of the S = 1 capture amplitude and has been shown to be sensitive to the spin orbit nucleon-nucleus force parameter.[1] While the rate at which we have been able to accumulate high quality polarized neutron capture data has been a bit disappointing, the data we have obtained have been quite revealing. Efforts to increase our rate of data collection are underway. The possibilities of increasing the polarized beam intensity, and adding additional detector(s) are both being investigated.

2. Improved Beam Dump for Cyclo-Graaff Experiments

In charged particle radiative capture experiments, a major source of background neutrons and gamma rays is the Faraday cup in which the beam is stopped downstream from the target chamber. In our (p,γ) experiments at Cyclo-Graaff energies it is especially important that the Faraday cup be located as far as possible from the detector and be very well shielded. Because of space restrictions in our target area, the heavily shielded beam dump which we employed until recently had limited the space available for moving the detector to forward angles.

We have recently improved this situation by drilling through the concrete and steel wall of the target room and locating the electrically insulated Faraday cup within a large steel pipe (12" in diameter and 6' in length) extending into the earth beyond the target room wall as shown in Fig. C2-1. This has proved to be a very satisfactory arrangement and has essentially eliminated the background radiation from the beam dump.

3. A Study of The $^3H(p,\gamma)^4He$ Reaction (S. Manglos, D. McBroom, H. R. Weller, N. R. Roberson, S. A. Wender, D. R. Tilley)

With the cyclotron once again in operation, we have reactivated our study of ^4He with the $T(p,\gamma_0)$ reaction. Specifically, we have repeated the fore-aft asymmetry (a_S) measurement described in TUNL XV, December 1976, where

$$a_S = \frac{\sigma(55°)-\sigma(125°)}{P_1(\cos 55°)\sigma(55°)+\sigma(125°)}$$

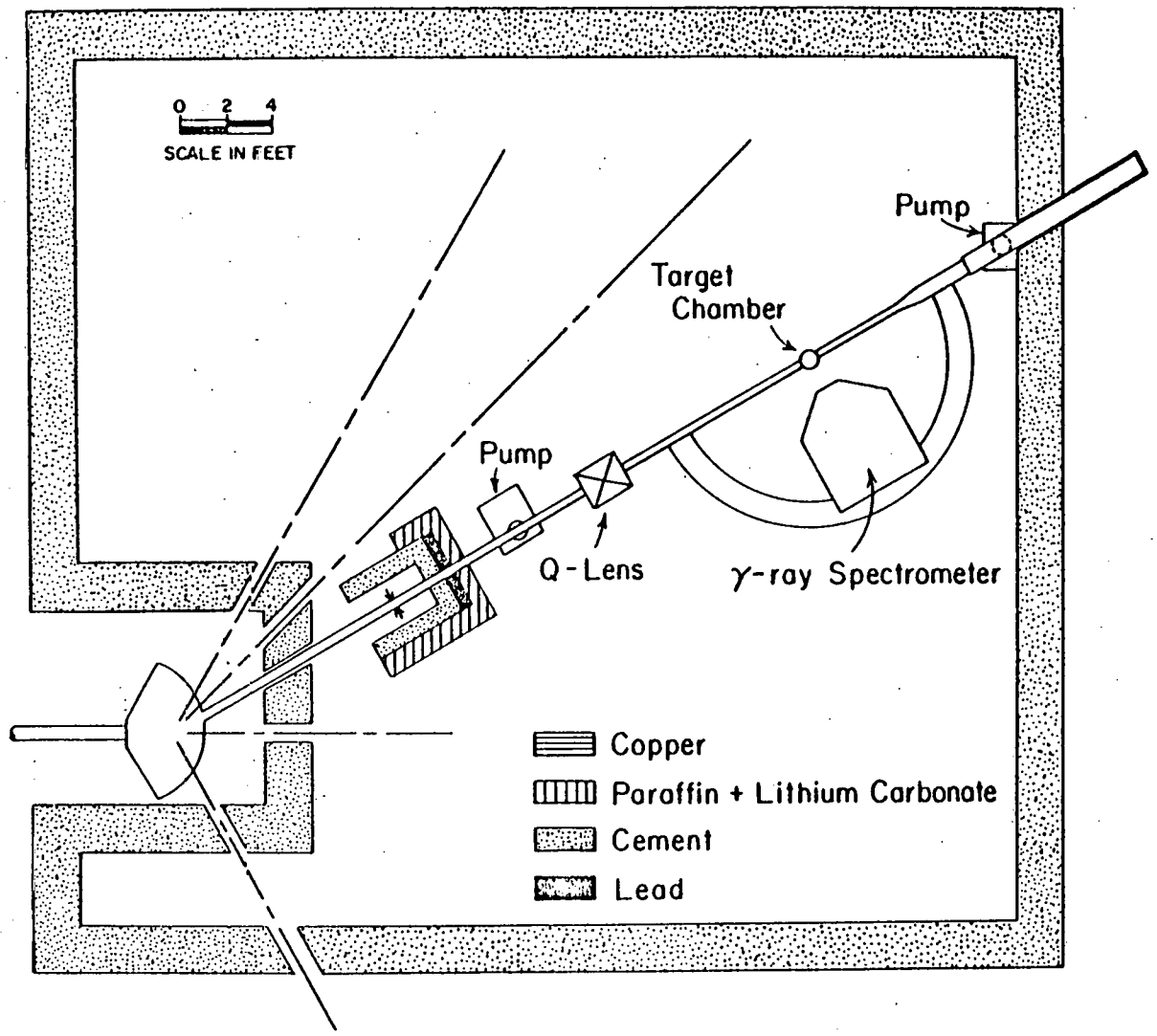

Fig. C2-1. Target rcom layout for capture experiments showing the improved beam dump.

Our latest results are shown in Fig. C3-1. The TUNL data are the averaged results

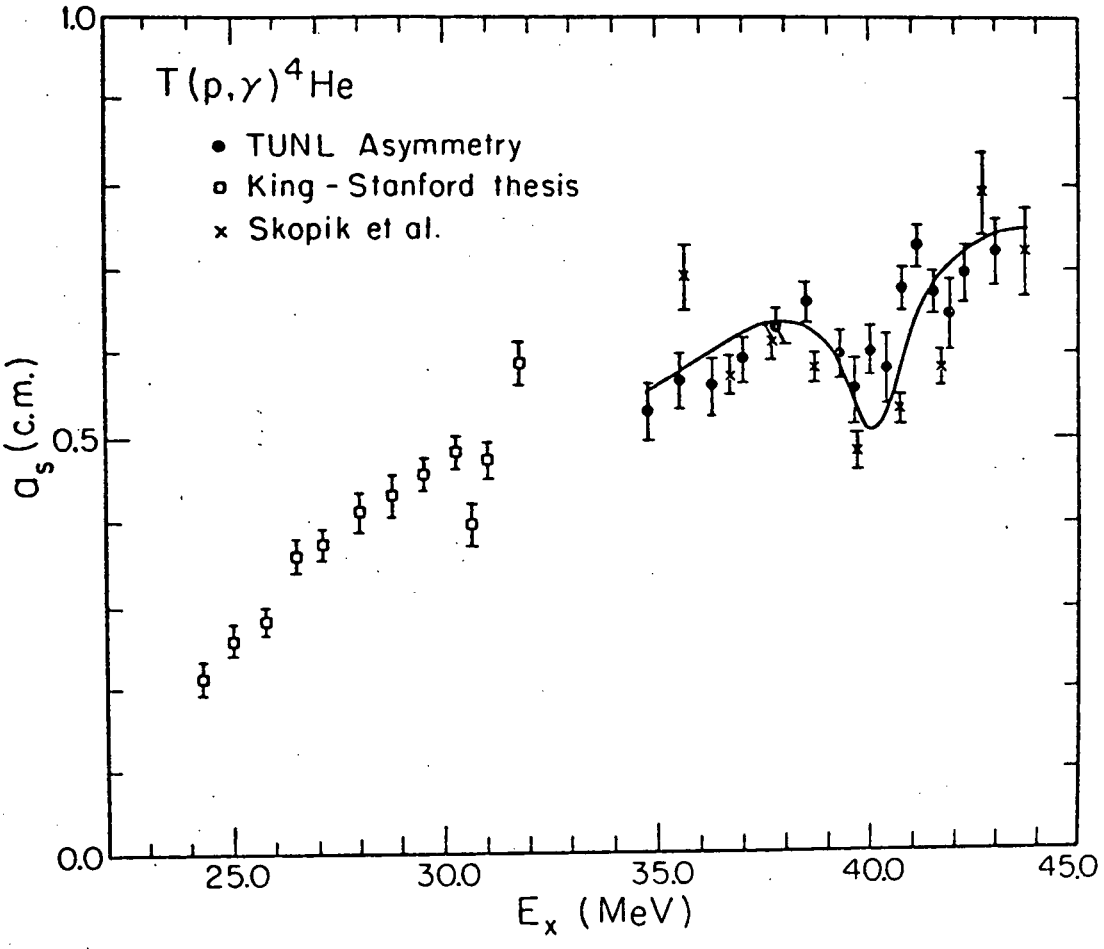

Fig. C3-1. Fore-aft asymmetry results for $^3H(p,\gamma)^4He$.

of two separate measurements. Also shown for comparison are the T(p,γ) data of King[1] and the results of Skopik et al.[2] who have studied the inverse reaction, $^4He(\gamma,p_0)T$. We are still in the process of measuring asymmetries for the excitation region of 32.5 - 34.5 MeV. Error bars shown are statistical only. The new data confirm the interesting effect observed earlier at $E_x \simeq 40$ MeV, where E_x is the excitation energy in the compound nucleus ^4He. This effect was previously attributed to a 2^+ resonance in ^4He.

We are in the process of fitting the new measurements with a model. In this model, the asymmetry arises from interference between E1 and E2 matrix elements. The E1 matrix element is obtained as a function of energy from the experimental 90° T(p,γ) cross section, and the E2 matrix element is the sum of a direct

[1] George King III, Stanford Ph.D. thesis
[2] D. Skopik, private communication

term plus a Breit-Wigner resonance term. The direct E2 term gives rise to the slowly varying "background" asymmetry, while the resonance term is to account for the narrow effect at $E_x \approx 40$ MeV.

The target used in these measurements was a tritiated titanium foil obtained from Oak Ridge. A sample γ-ray spectrum for E_p = 29.0 MeV is shown in Fig. C3-2. Also shown in the figure are the energies of possible contami-

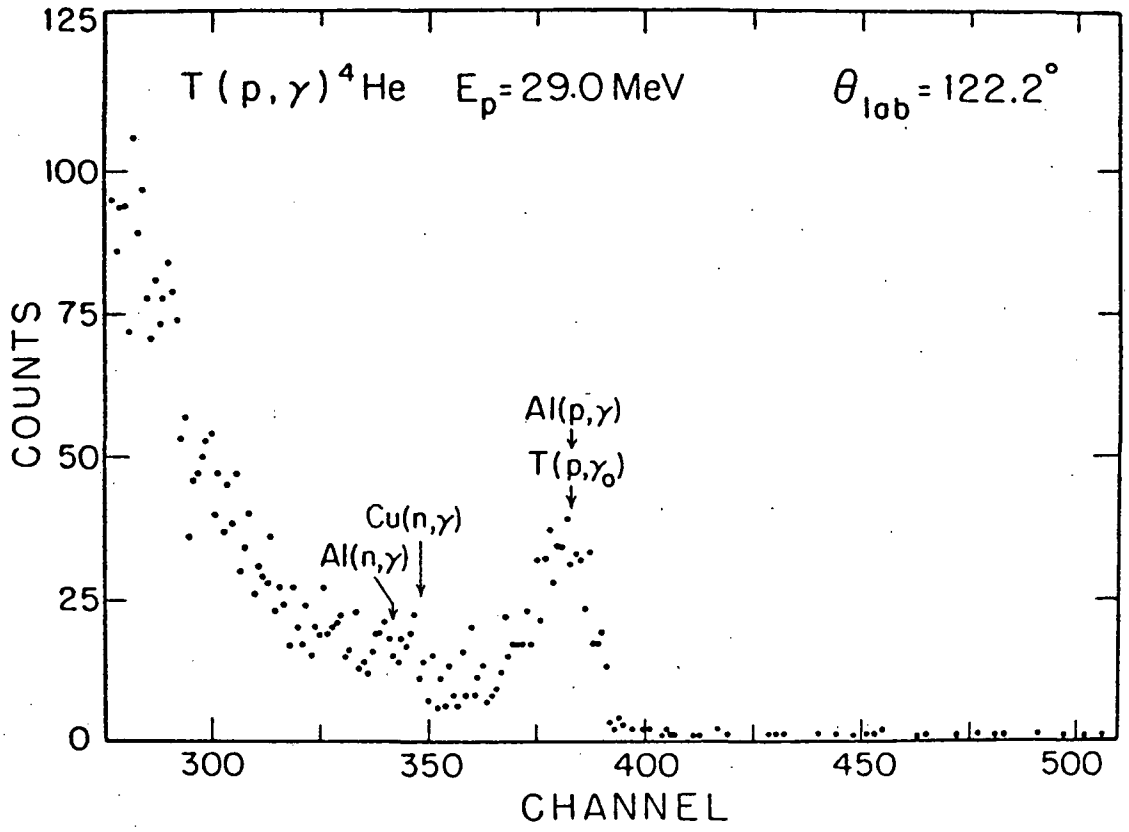

Fig. C3-2. Sample spectrum for $^3H(p,\gamma)^4He$.

nation γ-rays from other capture reactions. Neutrons are produced by the reaction $T(p,n)^3He$ and could capture in the brass target chamber or the aluminum beam pipe. As seen in the figure, kinematics calculations show that neutron capture is not important. However, γ-rays from the Al(p,γ) reaction due to scattered protons from the target could affect our results. To investigate this effect, we recorded a γ ray energy spectrum at every energy using a deuterated titanium foil of the same thickness and geometry as our tritiated target. These measurements were taken immediately after each asymmetry measurement without changing the beam conditions. No γ-rays of sufficient energy to affect the T(p,γ) results were observed.

Since the tritium target was considerably "wrinkled", due to heating during production, we worried that small movements, from run to run, in the position of the beam spot on the target could cause significant changes in the effective thickness of the target. These changes were monitored by the use of two solid state proton counters placed in the target chamber at ±160° with respect to the beam direction. The effective target thickness, as monitored by these counters, changed by less than 3% for different runs at the same beam energy. The data were corrected for these small changes. Also, to increase the stability of the proton counter yields, a smaller beam collimator (I.D. 7/64") was used, giving a smaller beam spot on target.

In the analysis of the data, spectra were fitted and summed using a standard line shape. Several variations of the fitting technique were used, but all gave asymmetry values within the statistical errors, with a few minor exceptions.

We intend to continue our analysis, adding a fit to the asymmetry data and obtaining resonance parameters for the effect at $E_x \simeq 40$ MeV.

4. Proton Capture to Highly-Excited States of ^{9}Be and ^{14}N
(S. L. Blatt, H. R. Weller, N. R. Roberson, D. R. Tilley, S. Manglos and S. A. Wender)

Recent measurements at intermediate energies have shown that γ-ray spectra from radiative proton capture reactions leading to closed-subshell and closed-subshell-plus-one proton nuclei are dominated by transitions to high lying 1p-1h and single particle states, respectively.[1] We have investigated two cases in which the final nuclei have more complex shell-model configurations. The reaction $^{13}C(p,\gamma)^{14}N$, measured at a proton energy of 25 MeV, shows strong transitions to two compact groups of final states centered near excitation energies of 5.8 and 8.9 MeV. A similar spectrum was previously published by Paul et al.[2] These appear to correspond to the $1p_{1/2} \otimes (1d_{5/2}$ or $2s_{1/2})$ T = 0 and T = 1 multiplets, as pointed out by Paul et al.[2] $^{7}Li(p,\gamma)^{8}Be$, on the other hand, exhibits transitions to many final states, up to excitation energies of at least 21 MeV. A spectrum obtained at E_p = 22 MeV is shown in Fig. C4-1. The transitions leading to the isospin mixed 2^+ states at 16.63 and 16.92 MeV are indicated. Spectra were obtained for protons of 22 to 31 MeV. These preliminary data do not show any apparent resonance like behavior in this energy range.

---

[1] M. A. Kovash et al., Phys. Rev. Lett. 42 (1979) 700
[2] P. Paul et al., Nucl. Phys. A254 (1975) 1

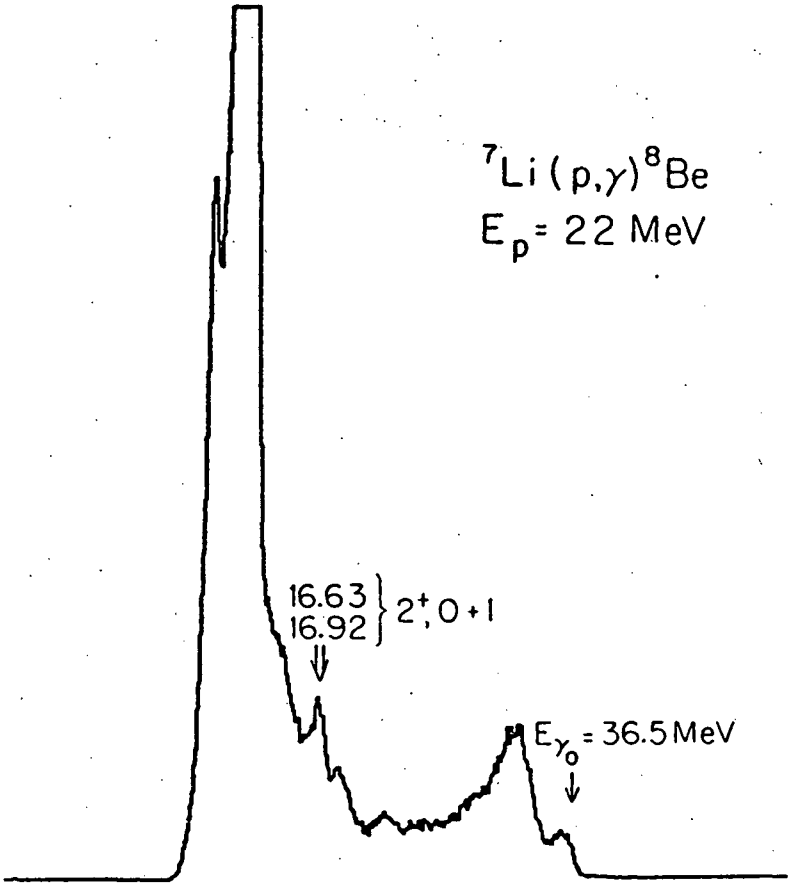

Fig. C4-1. Pulse height spectrum for ^{7}Li(p,γ)^{8}Be at E_p = 22 MeV.

5. Direct Capture Calculations for Unbound Final States (G. Mitev, H. R. Weller, S. R. Cotanch, J. M. Lafferty)

Direct capture calculations normally involve the evaluation of the radial integral $\langle \phi_{n\ell j} \; r^2 \; \phi^{(+)} \rangle$, where $\phi^{(+)}$ is an optical model wave function which describes the incoming nucleon and $\phi_{n\ell j}$ is obtained by using a Wood-Saxon potential which describes the bound single particle final state.

Recently, measurements have been reported for the ^{11}B(p,γ)^{12}C* reaction where the final state is around 19.2 MeV in ^{12}C. This state (or group of states) may be the 4$^-$ stretched configuration $(d_{5/2}\, p_{3/2}^{-1})^{4-}$. It was suggested by Kovash et al.[1] that the data may indicate a giant E1 resonance built on this state. In order to investigate the role of direct capture in the process, a calculation was performed in which the final state was treated as a barely bound $d_{5/2}$ single particle state. The optical model parameters were obtained from Perey and Perey.[2] The results of this preliminary E1 direct capture calculation as a function of proton energy are shown in Fig. C5-1. The experimental cross sections reported[1] are also shown.

[1] M. A. Kovash, S. L. Blatt, R. N. Boyd, T. R. Donoghue and H. J. Hausman, Phys. Rev. Lett. 42 (1979) 700

[2] C. M. Perey and F. G. Perey, At. and Nuc. Data Tables 17 (1976) 1

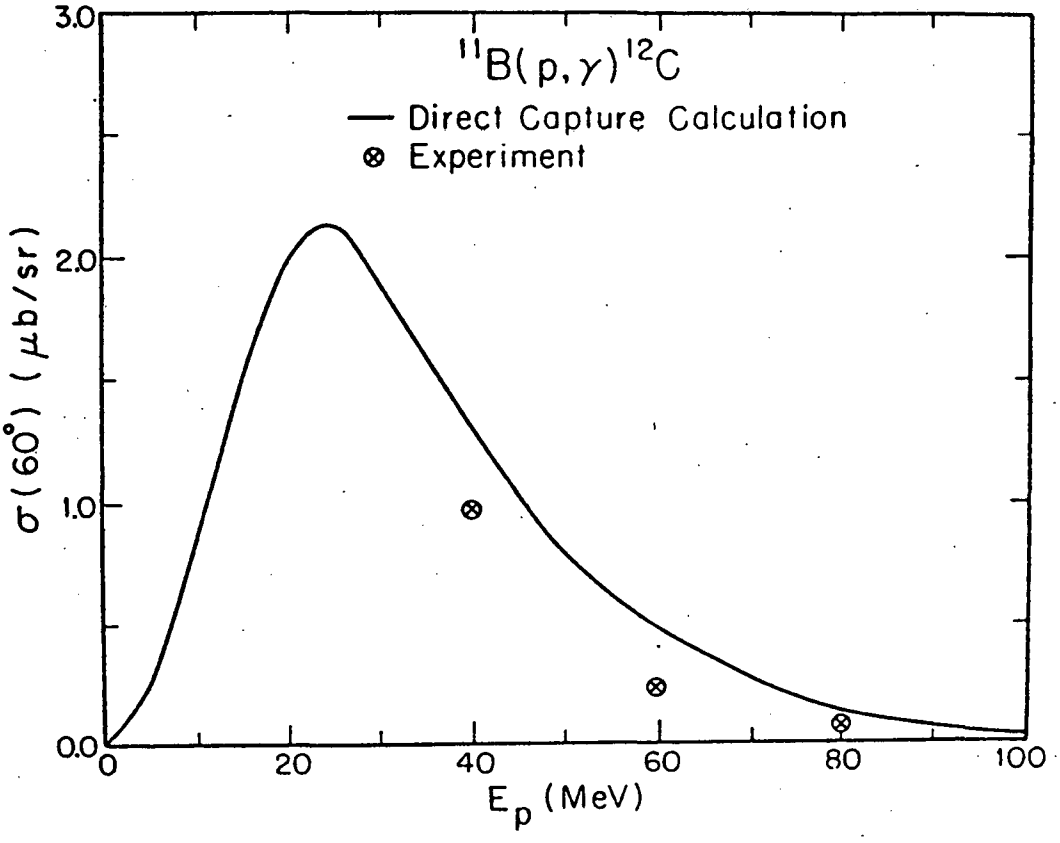

Fig. C5-1. Direct capture calculation and experimental cross section for capture to the 19.2 MeV state in ^{12}C.

Since the calculation suggested that direct capture may be important here and could, by virtue of momentum matching, produce a resonance-like shape in the cross section, it was decided that a direct capture calculation in which the continuum nature of the final state is taken into account should be undertaken. In order to accomplish this, the FORTRAN code RADCAP has been modified by replacing the bound state wavefunction $\phi_{n\ell j}$ by an optical model wavefunction χ. In addition the operator r^2 was replaced by the more precise form $j_\ell(kr) - krj_{\ell+1}(kr)$. This code will be used to calculate (p,γ) cross sections to unbound final states as a function of energy and angle. Several other cases which can be experimentally studied in our laboratory will be investigated with this code.

6. The $^{13}C(\vec{p},\gamma_{0,1})^{14}N$ Reaction (J. D. Turner,* N. R. Roberson, S. A. Wender, H. R. Weller, D. R. Tilley)

A paper entitled "Polarized Proton Capture on ^{13}C" has been accepted for publication. The abstract appears below:

---

* Now at Dept. of Physics, Furman University, Greenville, S. C.

"The 90° yield curves for the $^{13}C(\vec{p},\gamma_0)^{14}N$ and $^{13}C(\vec{p},\gamma_1)^{14}N$ reactions have been measured in 200 keV steps for E_p = 6.25 to 13.6 MeV and in 100 keV steps for E_p = 13.6 to 17.0 MeV. In addition, 50 keV step data were obtained for E_p of 12.6 to 14.55 MeV. Angular distributions of both the cross section and the analyzing power were also obtained for these two reactions at twelve energies which span the giant dipole energy region. The cross section was measured at 9 angles between 30° and 154° while the analyzing power was measured at seven angles between 42° and 142°. These data were used to obtain the complex E1 and E2 transition matrix elements in the case of $^{13}C(\vec{p},\gamma_1)^{14}N$. The results are compared to a direct-semidirect calculation. It is found that there is little justification in introducing E2 amplitudes other than a pure direct E2 term."

7. Polarized Proton Capture in ^{30}Si (C. P. Cameron,* R. L. Ledford,** M. Potokar,*** D. G. Rickel,+ N. R. Roberson, H. R. Weller, D. R. Tilley)

This work has been completed and a paper has been submitted to Physical Review C. The abstract follows:

"The 90° yield curves for the $^{30}Si(p,\gamma_0)^{31}P$ and $^{30}Si(p,\gamma_1)^{31}P$ reactions have been measured for E_p = 5.0 to 28.0 MeV. Angular distributions of cross section and analyzing power were obtained at twelve energies between E_p = 6.36 MeV and 14.45 MeV. The cross sections were measured at nine angles between 30° and 154°; the analyzing power at seven angles between 42° and 142°. For the case of $(\vec{p},\gamma_0)$ the complex T-matrix elements were extracted, assuming that the angular distributions are governed by coherent E1 and E2 processes. Two σ(E2) yield curves are obtained - one of which exhausts 9-12% of the $\Delta T = 0$ E2 energy weighted sum rule while the other exhausts 21-31%. The results are compared to direct-semidirect model calculations which suggest that the larger E2 cross sections are the physical solutions."

---

* Now at Sandia Laboratories, Albuquerque, New Mexico
** Now at Bell Laboratories, Holmdel, New Jersey
*** Fulbright Scholar, on leave from Inst. J. Stefan, U. of Ljubljana, 1978
\+ Now at E. G. and G., Los Alamos, New Mexico

This paper describes the results of an analysis, which assumes only coherent E1 and E2 radiation, of the angular distributions of cross section and analyzing power to determine the relative amplitudes and phases of the T-matrix elements contributing to the reaction. For the case of $^{30}Si(p,\gamma_0)^{31}P$, we can write these complex transition matrix elements in terms of a real amplitude and a phase as:

$$p_{1/2}(E1)e^{i\phi(p_{1/2})}\ ,\ p_{3/2}(E1)e^{i\phi(p_{3/2})}\ ,\ d_{3/2}(E2)e^{i\phi(d_{3/2})}\ ,\ d_{5/2}(E2)e^{i\phi(d_{5/2})}\ .$$

While M1 radiation could be present, the M1 giant resonance is expected to lie below the excitation region studied and to exhaust a large fraction of the M1 sum rule.[1]

To find the possible solutions for the amplitudes and relative phases a procedure was used in which these quantities were fit directly to the experimental cross sections and analyzing powers by minimizing χ^2. A detailed discussion of this procedure is given in TUNL Annual Report XVII, 1978, Section F 3. The solutions show three cases--two which are predominantly $p_{3/2}$ proton capture and one which is predominantly $p_{1/2}$ proton capture. Earlier calculations based on a simple direct-semidirect capture model[2] were shown to provide a procedure for choosing the physical solution. For the case under study here, these calculations give $\sigma(p_{3/2})/\sigma(E1)\approx 0.6$. In fact the equation for the a_0 coefficient (with the normalization $a_0 = 1 = p_{1/2}^2 + 2p_{3/2}^2 + 2d_{3/2}^2 + 3d_{5/2}^2$) indicates that if spin-orbit effects are neglected, the $p_{3/2}$ term will account for 2/3 of the E1 cross sections. Extended DSD model calculations[3] yield a similar result.

The two solutions with $\sigma(p_{3/2})$ dominant, i.e., solution set I and II, are shown in Fig. C7-1 and C7-2. The total E2 cross section can be deduced from the experimentally determined T-matrix elements and is shown in Fig. E7-3 where the solid dots correspond to solution I and the crosses to solution II. These (p,γ_0) E2 cross sections can be compared with the energy-weighted sum rule after being converted by the method of detailed balance to $\sigma_{E2}(\gamma,p_0)$. The present experiment indicates that the (γ,p_0) channel exhausts from 9 to 13% or from 21 to 31% of the $\Delta T = 0$ E2-EWSR for solution Sets I and II, respectively.

The results of calculations based on an extended direct-semidirect (DSD) capture model[3] which include electric quadrupole processes are shown as solid lines in Fig. C7-1. The same curves are also given in Fig. C7-2 for the experimental solutions Set II. The dashed lines in Fig. C7-1 and C7-2 are the results of a pure direct model calculation for the relative amplitudes. These latter results are the same as would be obtained from the simple DSD model[2] using the schematic model (form factor r^L). On the basis of a comparison of the magnitude of the relative E1

---

[1] S. S. Hanna, in Proceedings of the International Conference on Nuclear Structure and Spectroscopy, Vol. 2, ed. H. P. Blok and A. E. L. Dieperink, p. 249 and reference therein.

[2] H. R. Weller, N. R. Roberson, and S. R. Cotanch, Phys. Rev. 18C (1976) 457, and references therein.

[3] M. Potokar, Phys. Lett. 46B (1973) 346 and M. Potokar, Stanford Progress Report, 1977, p. 99 and to be published.

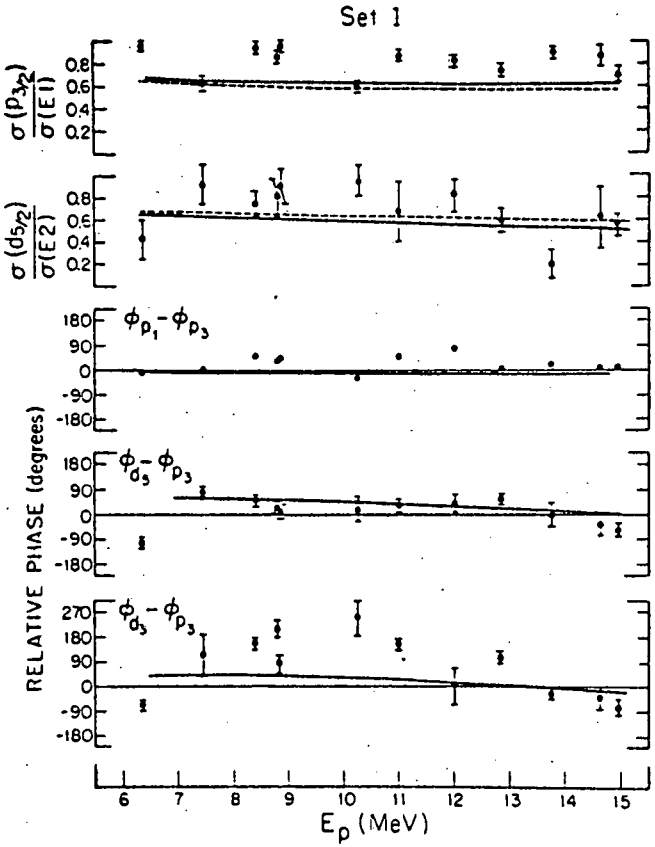

Fig. C7-1. Solution set I obtained in the analysis of $^{30}Si(p,\gamma_0)^{31}P$ data (see text).

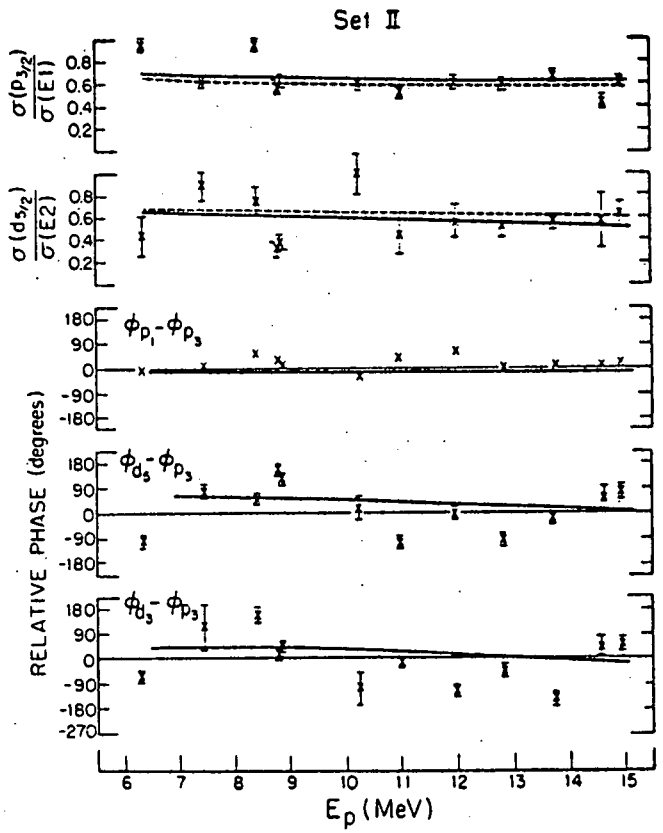

Fig. C7-2. Solution set II.

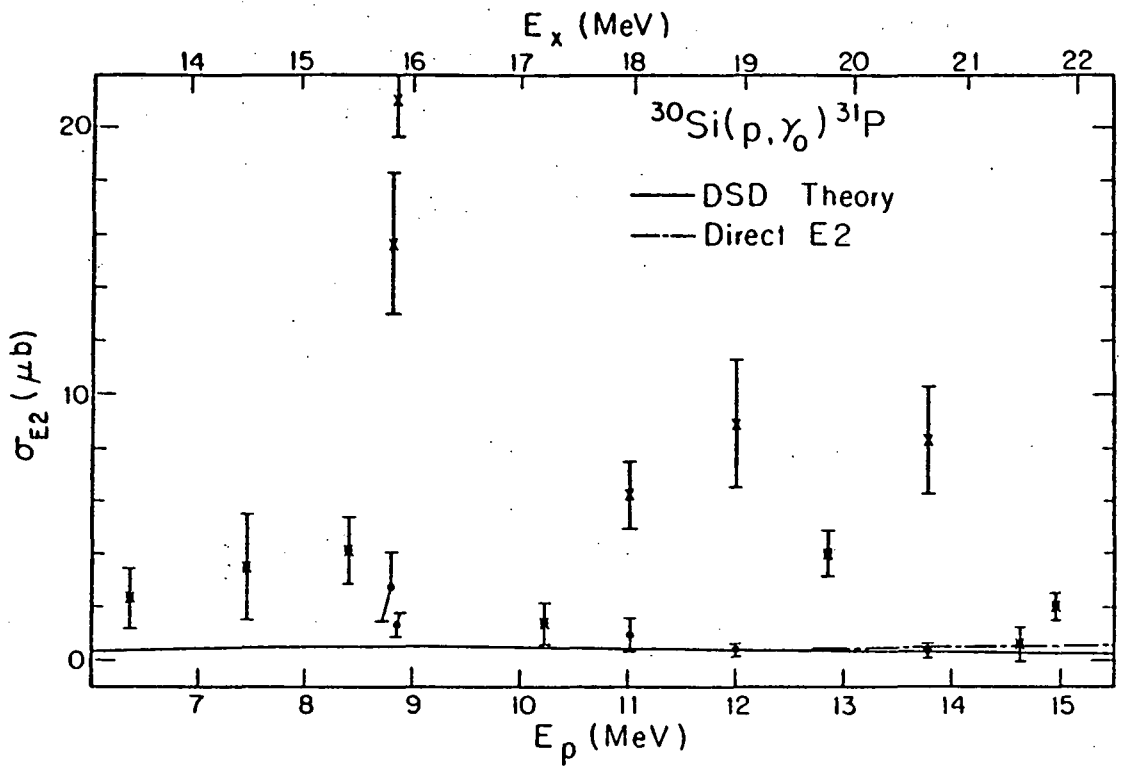

Fig. C7-3. The angle integrated E2 cross section for $^{30}Si(p,\gamma_0)$ (see text).

amplitudes with these DSD calculations, solution Set II appears to be the physical solution. This result implies that the larger E2 solutions (the x's of Fig. C7-3) are to be preferred, but it should be emphasized that solution Set I cannot be absolutely ruled out. The solid curve in Fig. C7-3 is the result of the extended DSD calculations which exhaust 2.3% or the E2 EWSR. The dot-dashed curve is the DSD results with the collective isoscalar quadrupole term ignored.

We conclude from this work that the most probable solutions imply an E2 cross section that accounts for 21 to 31% of the $\Delta T=0$ E2 EWSR ($E_x = 12.9$ to 21.9 MeV). The E2 strength appears to lie somewhat lower than the expected excitation energy of the GQR ($E_x \approx 20$ MeV), but there is no evidence that the E2 strength observed in the (γ, p_0) channel should coincide with the isoscalar GQR. This is especially true in view of the fact that the E2 cross section can be a mixture of isoscalar and isovector strengths.

8. Inelastic α-Cross Sections in The Region of The Giant Quadrupole Resonance for Nuclei Near Mass 60 (H.R. Weller, S. Manglos, S. A. Wender, N.R. Roberson, D.R. Tilley, M. Potokar)

This work has been published in Phys. Rev. C20 (1979) 1589. The abstract follows:

> "Cross sections have been measured for the (α,α') reaction leading to the first excited (2^+) state for targets of ^{52}Cr, ^{54}Fe, ^{58}Fe, and ^{60}Ni. Data were obtained at several angles as a function of E_α in the region of 8 to 18 MeV. These energies cover the region of the isoscalar giant quadrupole resonance of the composite nuclei--^{56}Fe, ^{58}Ni, ^{60}Ni, and ^{64}Zn. It has recently been reported that the giant quadrupole resonance of ^{58}Ni, ^{60}Ni, and ^{62}Ni decays primarily by α emission. Although the present data exhibit a giant resonancelike energy dependence, a coupledchannels calculation indicates that several J^π values can be expected to contribute to a resonancelike envelope in this reaction at the energies of the giant quadrupole resonance in these nuclei."

One of the principal reasons for associating the present data with the GQR was the result of Wolynec et al.[1] which reported that essentially all of the E2 strength in the GQR of ^{58}Ni could be located in the α-decay channel. This result appeared to be consistent with our data if we assumed that we were seeing a single 2^+ resonance--i.e., the GQR.

[1] E. Wolynec, W. R. Dodge, and E. Hayward, Phys. Rev. Lett. 42 (1979) 27

In attempting to understand our data, however, we found that the Coulomb Barrier and the opening of other channels played a most important role. Coupled channels calculations performed with the code Jupitor (T. Tamura) indicated that the resonance shaped envelope was probably the result of the α_1 channel opening, letting the cross section rise, and then other channels opening, taking flux away and dropping the cross section at higher energies. Similar but more refined calculations were carried out by Stanley and Halderson.[1] Their results are shown along with our data for the case of $^{54}Fe(\alpha,\alpha_1)^{54}Fe^*$ in Fig. C8-1. In the meantime the results of the $^{58}Ni(e,\alpha)$ experiments have been reanalyzed taking into account some previously neglected multiple scattering effects.[2] The result of this is a substantial reduction in the E2 strength seen in the α channel. The presently quoted value is 15 ± 3% if the Isoscalar E2-EWSR (down from 56 ± 4%). This value is still somewhat larger than the 6 ± 2% observed in the $^{58}Ni(\alpha,\alpha'\alpha)$ coincidence experiment.[3]

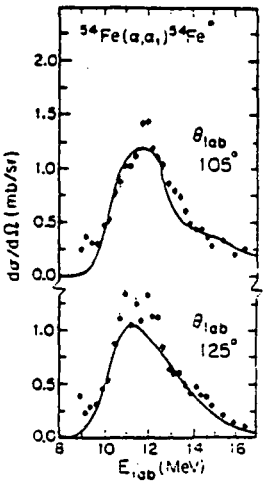

Fig. C8-1.

It is interesting to further test the coupled channels calculation by comparing its prediction for the capture cross section with experiment. In ^{58}Ni about 3.9% of the IS-EWSR have been reportedly seen in the $^{54}Fe(\alpha,\gamma)^{58}Ni$ experiment[4] (the $(\alpha,\alpha'\alpha)$ experiment reports ~1%).[3] If the ground state of ^{58}Ni is represented as an α-particle coupled to the 0^+ or 2^+ states of ^{54}Fe, the coupled channels calculation can be extended to the case of α capture. It is found that the E2 cross section is nonresonant so that the α-cluster capture process appears to contribute only to the "background" as a direct capture process.[1]

The conclusion of this study is that, insofar as our α-scattering measurements are concerned, the coupled-channels calculations indicate that there does not appear to be any selective excitation of 2^+ strength (2^+ strength accounts for ~17% of the total peak cross section). In addition, this 2^+ component in the GQR region does not carry any appreciable E2 strength.

---

[1] D. P. Stanley and Dean Halderson, to be published in Phys. Rev. C

[2] Evans Hayward, private communication

[3] M. T. Collins, C. C. Chang, S. L. Tabor, G. J. Wagner, and J. R. Wu, Phys. Rev. Lett. 42 (1979) 1440

[4] L. Meyer-Schützmeister et al., Phys. Rev. C17 (1978) 56

9. The $^{3}He(n,\gamma)^{4}He$ Reaction (L. Ward, D. R. Tilley, N. R. Roberson, S. A. Wender, D. Skopik, H. R. Weller)

A program to measure the absolute cross section and analyzing power for the reaction $^{3}He(\vec{n},\gamma)$ has been started. Due to the controversy[1] in the magnitude and shape of the photoneutron cross section of ^{4}He, the initial effort has been to measure the capture cross section of ^{3}He with unpolarized neutrons.

The $D(d,n)^{3}He$ reaction was used to produce the fast neutrons; the spread in neutron energy, resulting from energy losses by the deuterons in the deuterium cell ranged from 760 keV(E_n = 6.0 MeV) to 210 keV (E_n = 14.5 MeV). A gaseous ^{3}He target was used. The pressure vessel was a 1-1/2" long by 1-3/8" I.D. cylindrical stainless steel container with a hemispherical end. Except for a 1/4" flange on one end of the cell, the wall thickness was 1/16". The cell was filled to a pressure of 115 ATM. Its axis of symmetry was perpendicular to the beam axis and along the axis of rotation of the NaI spectrometer.

A $\theta_{lab} = 90°$ yield curve has been measured over the energy range of E_n = 6.0 MeV to 14.5 MeV. A typical spectrum is shown below (Fig. C9-1). The spectrum is relatively clean since the Q-value for the $^{3}He(n,\gamma)$ reaction is 20.6 MeV.

Fig. C9-2 gives a comparison of our preliminary data to other measurements. Our data have been converted to $^{4}He(\gamma,n)$ cross sections. The most noteworthy features are the magnitude and shape of the cross section as a function of energy. The absolute cross section values have been obtained by normalizing to the $^{40}Ca(n,\gamma)$ cross section and by assuming a $\sin^{2}\theta$ angular distribution. Corrections for multiple scattering and attenuation remain to be made.

It is emphasized that these results are preliminary. One area of uncertainty is the number of ^{3}He atoms in the target; a sample of the gas will be analyzed using a mass spectrograph to check the purity. An attempt is being made to weigh the gas or other gasses to calibrate the pressure gauge. Other corrections will

---

[1] Phillips, Berman, Faul, Calarco, and Hall, Physical Review C19 (1979) 2091 and references therein.

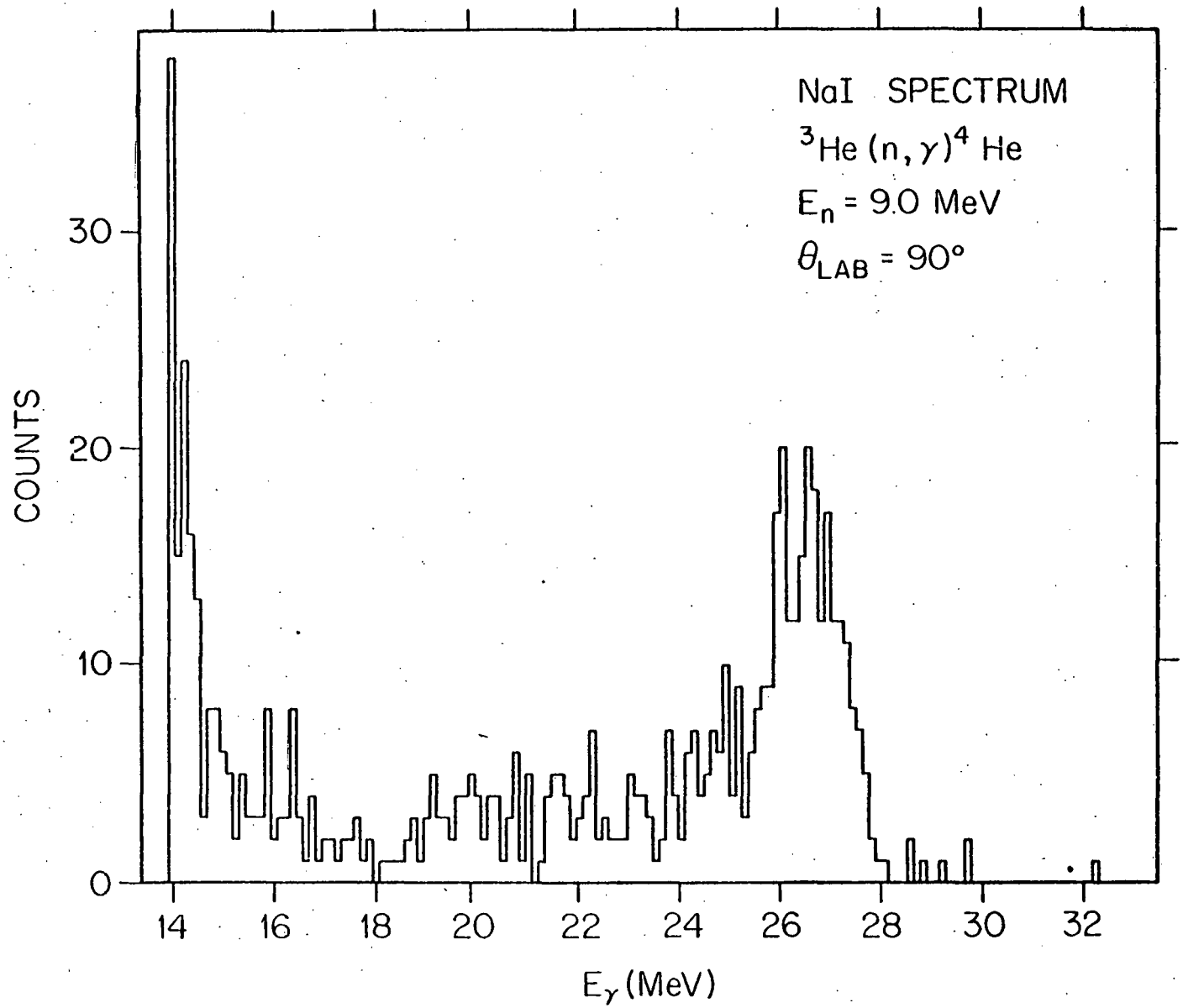

Fig. C9-1. Pulse height spectrum for $^3He(n,\gamma_0)^4He$.

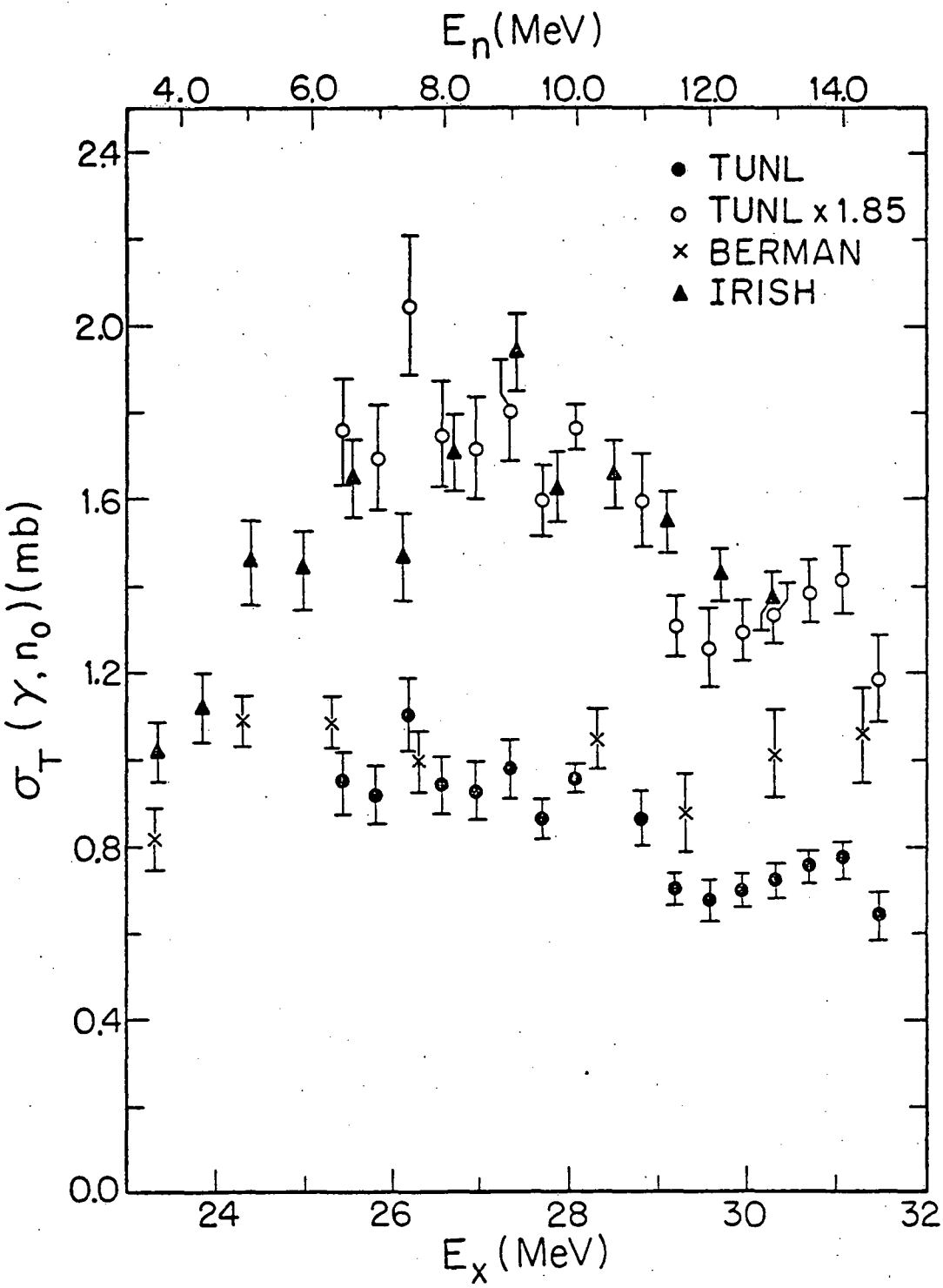

Fig. C9-2. Preliminary data for $^{3}He(n,\gamma_0)^{4}He$ cross section and comparison with other results.

also affect the cross section measurement. One important correction is neutron multiple scattering in both the gas and in the steel jacket around the gas. The steel flange can scatter neutrons into the gas and the wall can attenuate both the neutron flux and the γ-ray flux. Corrections are needed for the finite geometry and the angular dependence of the D(d,n) differential cross section $\sigma(\theta)$.

An angular distribution measurement has been partially completed at $E_n = 9.0$ MeV, and a measurement of the analyzing power will be attempted in the near future.

10. The $^{13}C(\vec{n},\gamma_0)^{14}C$ Reaction (M. J. Jensen, L. W. Ward, D. R. Tilley, S. A. Wender, N. R. Roberson, H. R. Weller, T. B. Clegg)

We have begun a study of neutron capture on ^{13}C with both polarized and unpolarized neutrons. The neutron source reaction $^2H(d,n)^3He$ with a pulsed deuteron beam incident upon a deuterium gas cell was used in this experiment. The pressure in the 1 inch long deuterium cell was 3 atm absolute when measuring the 90° excitation function, and was 6 atm absolute when measuring angular distributions of analyzing power. The ^{13}C target was 96% isotopically pure carbon powder pressed into a 38 x 38 mm lucite cylinder. Time-of-flight techniques were used with both the unpolarized and polarized beams. The use of the new double drift bunching system and the ramping of the polarized ion source (see Section J) allowed us to produce pulsed polarized deuteron beams with enough intensity for use in this experiment.

The 90° excitation function (Fig. C10-1) was measured for inci-

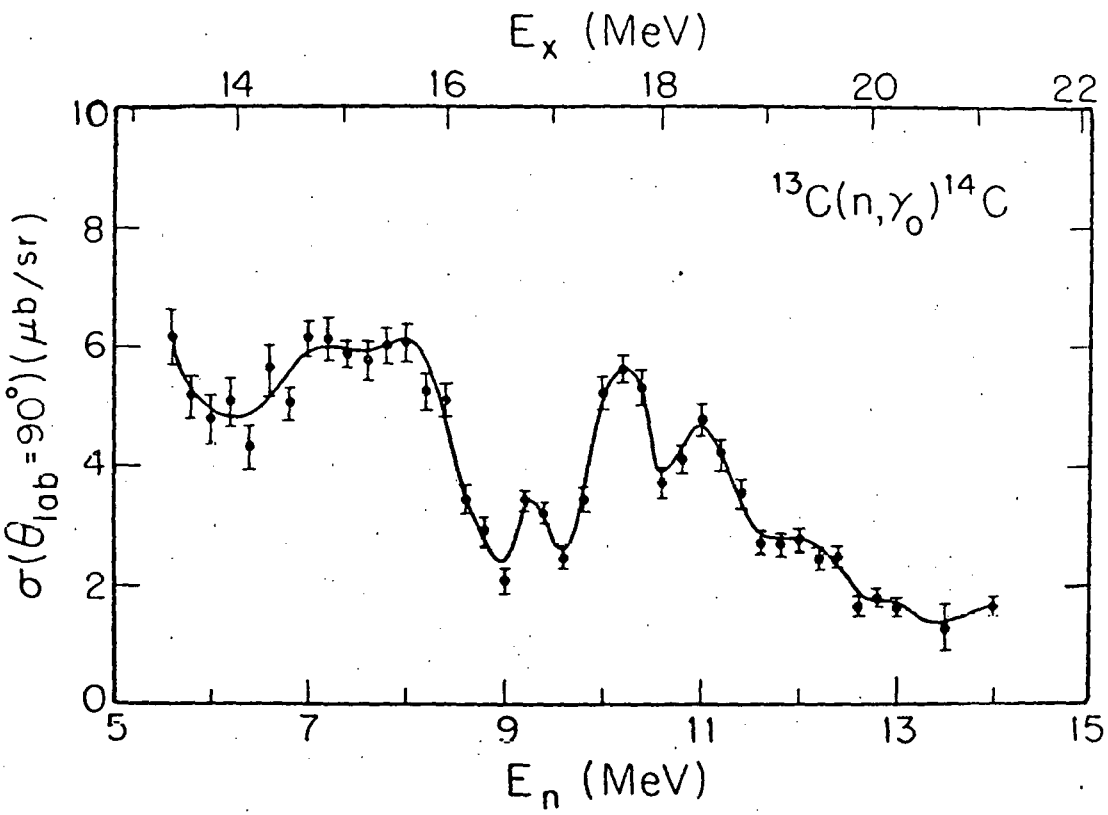

Fig. C10-1.

dent neutron energies of 5.6 to 14.0 MeV corresponding to ^{14}C excitation energies 13.4 to 21.2 MeV. Using the value of a_2 that we measured with a preliminary unpolarized beam at 10 MeV, and detail balancing, the integrated cross section exhausts 18% of the classical dipole sum. Integrating the same region in the $^{13}C(p,\gamma_1)^{14}N^*(0^+, T=1)$ reaction (radiative capture to the isobaric analogue state of ^{14}C) yields 9% of the dipole sum. The ratio of the two yields should equal the ratio of the square of their isospin coupling coefficients. The inverse reaction of photo emission of a proton from $^{14}N^*(T=1, T_z=0)$, gives $^{13}C(T=1/2, T_z=1/2)$ and a proton $(T=1/2, T_z=-1/2)$. The T=0 part of the GDR is excited so the coupling coefficient is $(1/2\ 1/2,\ 1/2 - 1/2;\ 0\ 0)^2 = 1/2$. The photoemission of a neutron from $^{14}C(T=1, T_z=1)$ gives ^{13}C and a neutron $(T=1/2, T_z=1/2)$. The $T=1$, $T_z=1$ part of the GDR is excited in this reaction so the coupling coefficient is $(1/2\ 1/2,\ 1/2\ 1/2;\ 1\ 1)^2=1$. This ratio is in good agreement with observation.

Angular distributions of cross section and analyzing powers were measured at E_n = 7.75, 10.2 and 11.0 MeV, each with seven angles ranging from 45° to 142° in the lab. The 7.75 and 10.2 MeV data were fit with Legendre and Associated Legendre polynomials ($P_\ell^{(\theta)}$ and $P_\ell{}'^{(\theta)}$) through $\ell=2$ (see Fig. C10-2).

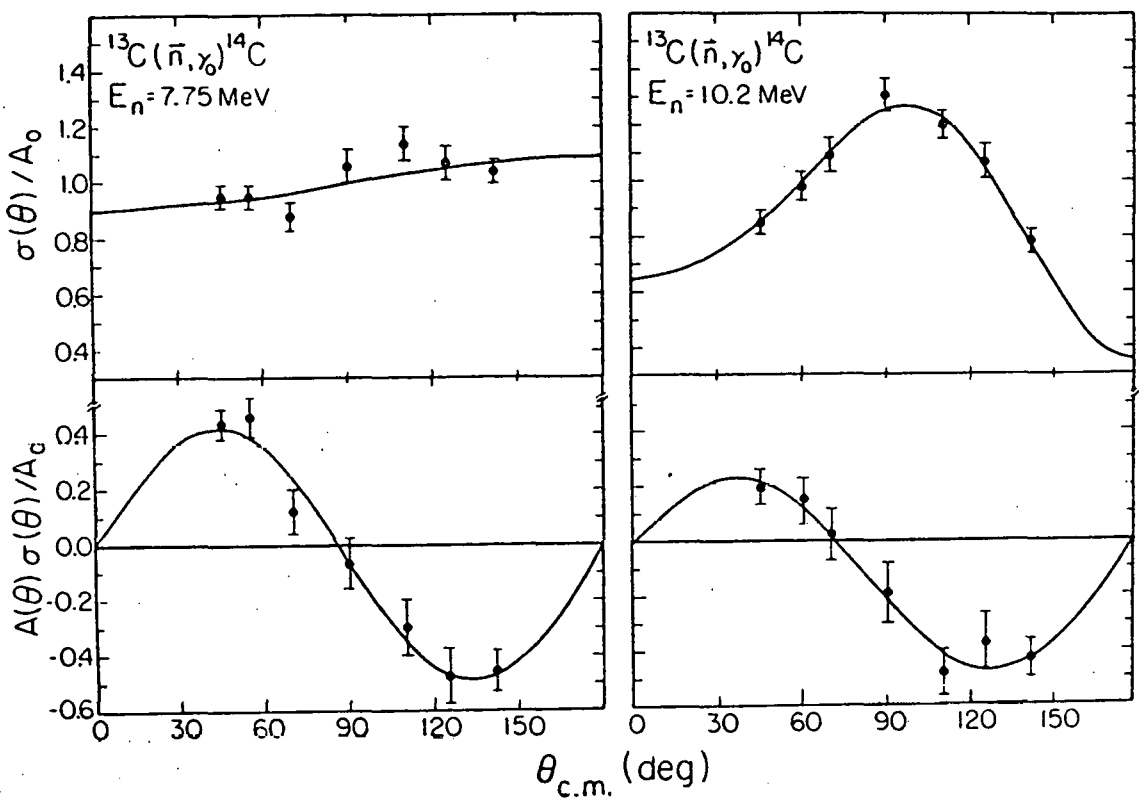

Fig. C10-2. Angular distributions of cross sections and analyzing power for $^{13}C(n,\gamma_0)^{14}$.

Crannell et al.,[1] have observed M1 states in ^{14}C at an $E_x = 11.3$ MeV. Furthermore, Snover, et al.,[2] have observed M1 states in this region of excitation energy in ^{16}O using the $(\vec{p},\gamma)$ reaction. Therefore, we have begun both an E1 - E2 and an E1 - M1 analysis. If only E1 and E2 radiation are considered, there are four T-matrix elements involved in the reaction. Using j-j coupling they may be labeled by the incoming partial waves as $s_{1/2}$ and $d_{3/2}$ for E1 radiation and $p_{3/2}$ and $f_{5/2}$ for E2 radiation. Using a direct-semidirect (DSD) calculation to select the dominant E1 matrix element as $d_{3/2}$, the four matrix-element amplitudes and phases were fit to the 10.2 MeV data. The preliminary result is $\sim(3.0 \pm 1.2)\%$ E2 radiation. However when the data are analyzed with E1 and M1 matrix elements $s_{1/2}$, $d_{3/2}$, $p_{1/2}$, and $p_{3/2}$, the 10.2 MeV data may also be described with a $(1.2 \pm 0.5)\%$ M1 contribution. Work continues on the problem of selecting the proper solution and on angular distributions at other energies.

11. Study of The Giant Dipole Resonance in ^{15}N with Fast Neutron Capture (S. A. Wender, M. Jensen, M. Potokar, N. R. Roberson, D. R. Tilley, H. R. Weller)

As discussed in our previous progress report (TUNL XVII) the $^{14}N(n,\gamma)$ reaction is of particular interest in that the neutron data complements the large amount of existing data on the A = 15 system. We have obtained the excitation function for the $^{14}N(n,\gamma_0)$ reaction for neutron energies between 6 and 13 MeV, which span the giant dipole resonance region in ^{15}N. We have also measured 8 angular distributions in this energy region.

The analysis of these data is complicated by the fact that ^{14}N, with a spin of 1^+, permits a large number of T matrix elements. However using the spectator model (as previously discussed, see E-8) we can describe the E1 radiation with only two matrix elements and a relative phase.

A comparison of the $^{14}N(n,\gamma)^{15}N$ data with the $^{14}N(p,\gamma)^{15}O$ data shows that the magnitude of the cross sections are comparable. Also, the shapes of the yield curves are similar if the $^{14}N(n,\gamma)$ data are shifted down approximately 400 keV. If this shift is attributed to a Coulomb energy difference, it would correspond to a change in the average radius of approximately 0.2 F m.

The final analysis of these data is being completed and a paper is being prepared for publication.

---

[1] Crannel, et al., Nucl. Phys. A278 (1977)
[2] K. A. Snover, P. G. Ikossi, and T. A. Trainor, Phys. Rev. Lett. 43 (1979) 117

12. A Study of The $^{40}Ca(\vec{n},\gamma_0)$ Reaction (M. J. Jensen, D. R. Tilley, H. R. Weller, N. R. Roberson, S. A. Wender, T. B. Clegg)

A paper on this work has been published in Physical Review Letters 43 (1979) 9, 609. The following is the abstract of the paper.

"The capture of fast polarized neutrons incident on ^{40}Ca has been measured at an incident neutron energy of 10.0 MeV. The results indicate a significant non-E1 contribution in the giant-dipole-energy region of ^{41}Ca. When the data at E_n = 10 MeV are analyzed with the use of a model, they are found to be consistent with an E2 strength which is (3.2 ± 2.7)% of the total capture cross section. Some of the implications of this result are discussed."

In addition to our work at E_n = 10.0 MeV, we have measured analyzing powers at E_n = 8, 9 and 11 MeV. At these energies the data were of a quality sufficient for an E1 analysis. The cross section and analyzing power were expanded in Legendre and Associated Legendre series. The equations for the coefficients A_0, a_2, and b_2 were then solved in terms of $g_{9/2}$ and $d_{5/2}$ amplitudes and their relative phase. There are two solutions, one with $g_{9/2}$ dominating and one with $d_{5/2}$ dominating. In Fig. C12-1 we show both solutions in terms of the $g_{9/2}$ value. The solid lines

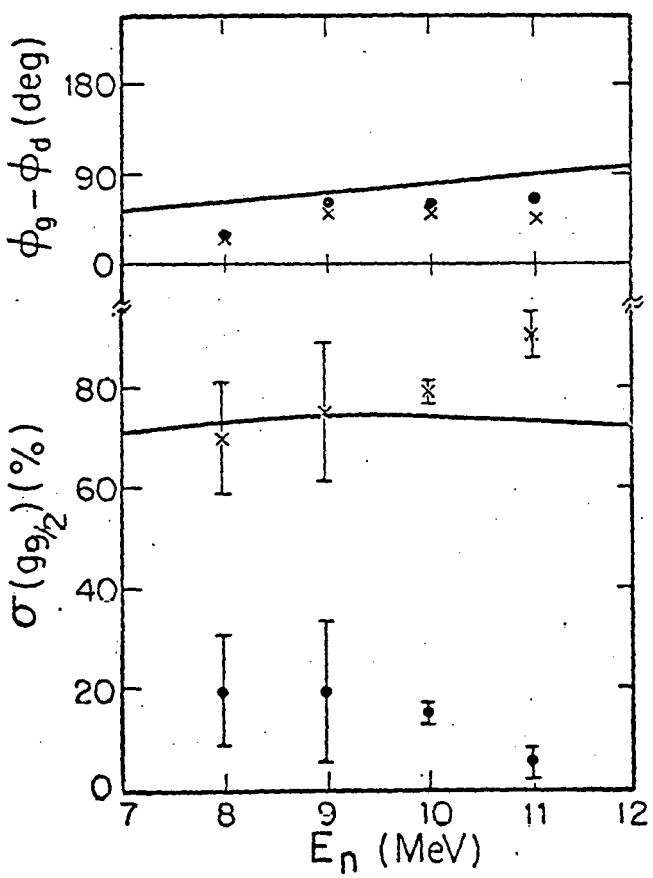

Fig. C12-1. Solutions obtained for the $g_{9/2}$ relative amplitude and $\phi_g - \phi_d$ phase from analysis of $^{40}Ca(n,\gamma_0)$ data shown with the results of DSD calculations (solid lines).

are the DSD calculation of the $g_{9/2}$ relative amplitude and the $\phi_g - \phi_d$ phase. From this we choose the $g_{9/2}$ dominant solution as being the physical one.

Our best data set was obtained at E_n = 10 MeV. The results are shown in Fig. C12-2. The cross section data shown here include our previous unpolarized

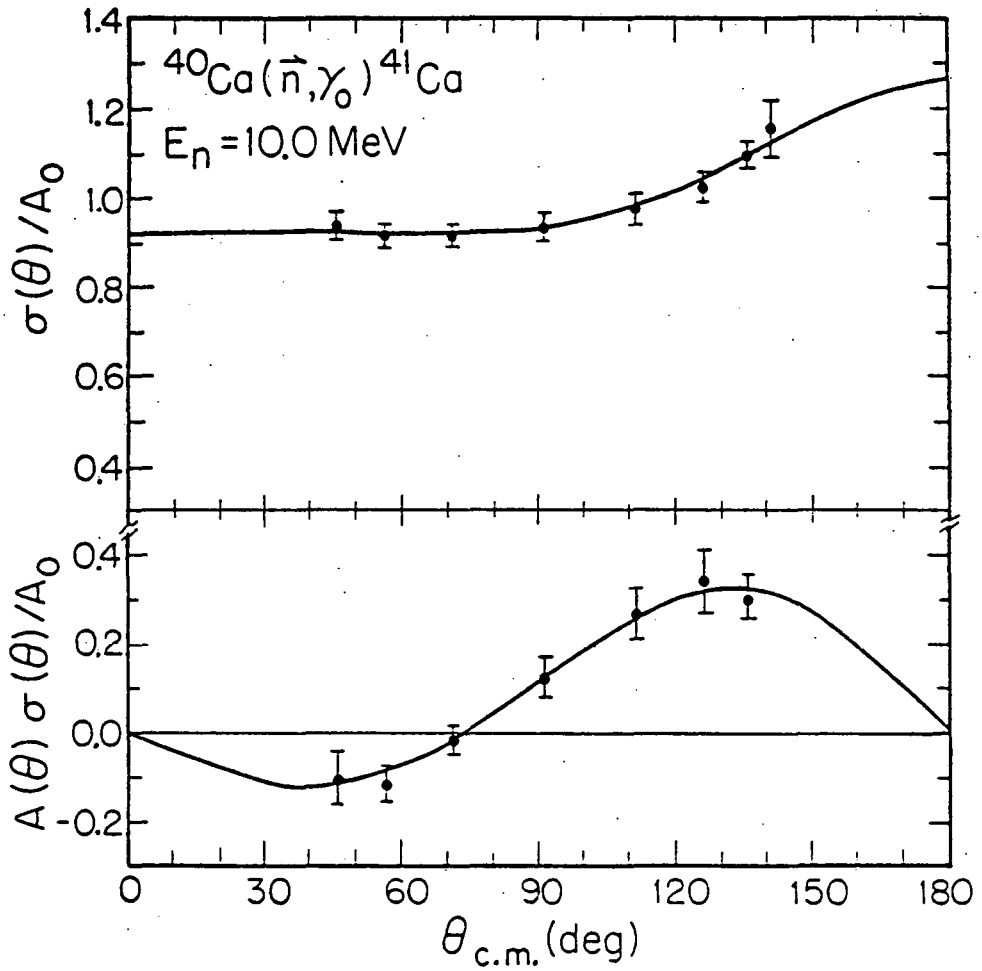

Fig. C12-2. Angular distributions of cross section and analyzing power for $^{40}Ca(n,\gamma_0)$.

measurements.[1] Significant non-E1 radiation is indicated by the fore-aft asymmetry in $\sigma(\theta)$ and by the lack of a pure sin 2θ pattern in $\sigma(\theta)\,A(\theta)$.

Due to the large number of T-matrix elements present in this problem, simplifying assumptions are necessary to extract T-matrix amplitudes and phases from the data. If we label the T-matrix elements by the incoming neutron quantum numbers

[1] S. A. Wender, et al., Phys. Rev. Lett. 41 (1978) 1217

in j-j coupling we have, for E1 radiation, three possibilities: $g_{9/2}$, $g_{7/2}$, and $d_{5/2}$. For E2 radiation there are five possibilities: $p_{3/2}$, $f_{5/2}$, $f_{7/2}$, $h_{9/2}$ and $h_{11/2}$. A direct-semidirect (DSD) calculation suggests that two E1 and two E2 matrix elements will dominate: $g_{9/2}$ and $d_{5/2}$ for E1 and $f_{7/2}$ and $h_{11/2}$ for E2.

The cross section and analyzing power data were fit directly to the four amplitudes and three relative phases. The solid lines on Fig. E14-2 correspond to the fit with the $g_{9/2}$ matrix element dominating the E1 capture. This solution has (75 ± 4)% $g_{9/2}$ (E1) which is in excellent agreement with the DSD prediction of 74%. (See Fig. E14-1.) Then $d_{5/2}$ accounts for (21 ± 4)% of the cross section. The E1 phase difference $(\theta_g - \theta_d)$ is 47° ± 4°. The E2 solutions are (2.1 ± 2.7)% $f_{7/2}$ and (1.2 ± 0.4)% $h_{11/2}$, for a total of (3.2 ± 2.7)% of the total cross section.

Using Youngblood's[1] (α,α') measurement of the E2 isoscalar resonance position and width we can estimate that the (γ,n_0) channel exhausts ~3% of the isoscalar energy weighted sum. Note that this estimate is made from a measurement at only a single energy.

The E2 solutions obtained above indicate a large uncertainty in the $f_{7/2}$ strength, almost overlapping zero. This is apparently a result of the non-linear nature of the relevant equations more than the statistical errors in the data. The DSD calculation indicates that the $h_{11/2}$ E2 term will account for ~85% of the E2 cross section. If the E_n = 10 MeV data are fitted with only the $h_{11/2}$ E2 T-matrix element and the two E1 terms previously discussed, an acceptable fit (χ^2) is obtained. This result indicates that the $h_{11/2}$ E2 term accounts for 1.3 ± 0.4% of the total cross section.

Under this situation the b_1 expression contains only one term:

$$b_1 = -6.65\, g_{9/2}\, h_{11/2} \sin(\phi_h - \phi_g) \quad .$$

The solution indicates that $\sin(\phi_h - \phi_g) = 0.96$. Since the phase factor is ~1.0, we cannot obtain the experimental value of b_1 with a smaller E2 strength (supposing part of it was incoherent and therefore not contributing to b_1) and a compensating variation in the phase difference. So we see that almost all of the $h_{11/2}$ strength must be coherent. Of course it is important to remember that although the DSD calculation supports the interpretation of the non-E1 strength as E2-strength, the observations alone do not rule out the possibility of M1 strength, which has been ignored here.

---

[1] D. H. Youngblood, et al., Phys. Rev. C13 (1976) 994

The conclusions which we draw from this experiment are listed below:

1. The E1 cross section for the $^{40}Ca(n,\gamma_0)^{41}Ca$ reaction is dominated (70-85%) by $g_{9/2}$ neutron capture in the region of the GDR.

2. There is non-E1 radiation present in the fast neutron capture reaction on ^{40}Ca.

3. If this radiation is assumed to be E2, the data can be fitted if the E2 strength is 1 to 3% of the total.

4. If we apply the isoscalar GQR parameters for ^{40}Ca from the (α,α') experiments to the present case, the E2 strength seen here would correspond to about 1-3% of the IS-E2-EWSR in the n_0 channel for ^{41}Ca.

5. The E2 strength appears to be almost entirely coherent with respect to the E1 strength and is therefore "semi-direct".

13. Study of The $^{208}Pb(n,\gamma)^{207}Pb$ Reaction (L. Ward, M. Jensen, M. Potokar, D. R. Tilley, H. R. Weller, S. A. Wender, N. R. Roberson, S. Raman,* S. King)

No new experimental data on $^{208}Pb(n,\gamma)$ have been obtained since the last report. However, from earlier experimental runs, there remains a considerable body of data awaiting analysis. We have measured the 90° yield in the region between 7 and 13 MeV, the fore aft asymmetry at 10.5, 11.0 and 11.5 MeV, and an angular distribution at 10 MeV. None of these data have been satisfactorily analyzed as yet since (because of the low Q value and closely spaced final states) the spectra require a better multiple peak fitting routine than we have available at present. We are now developing a more adequate code for this purpose.

Although the analysis is crude, we have presented in Fig. C13-1

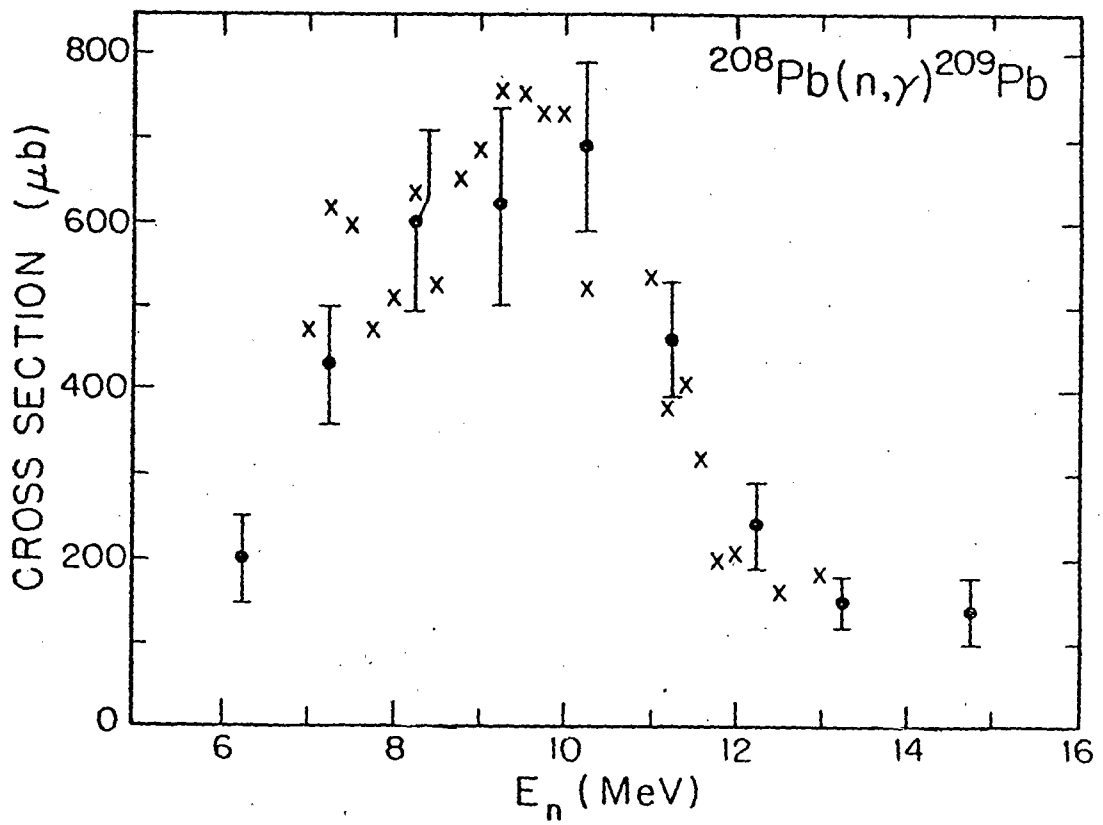

Fig. C13-1. Preliminary $^{208}Pb(n,\gamma_0)$ cross section data (crosses) shown along with data from Ref. 1.

our preliminary 90° yield curve data arbitrarily normalized to the total cross section data of Bergqvist, Drake, and McDaniels.[1] In spite of the considerable point scatter (which we attribute to the inadequate spectral analysis) it is apparent that the two sets of data are in agreement as to the general shape of the giant dipole resonance.

---

* Oak Ridge National Laboratory

[1] I. Bergqvist, D. M. Drake, and D. K. McDaniels, Nuclear Physics A191 (1972) 641

D. ATOMIC PHYSICS

1. General Status of The Program (M. Clark, J. Swenson, S. M. Shafroth, E. N. Strait,* J. Willis, J. A. Tanis,** R. Mowat,++ A. Waltner, S. L. Varghese+)

The major accomplishment in instrumentation for the Atomic Physics Program this year has been to install and make operational a sputter ion source (General Ionex, Hi conex 836). In addition we have constructed a parallel plate electron spectrometer and built a new beam line. Work has continued on target thickness effects, and Resonant Raman effects. We have started x-ray angular distribution measurements. Work on x-rays and gamma rays following nuclear fusion reactions has been extended using F^{q+} beams and C^{q+} beams from the sputter ion source.

2. Target Thickness Effects in Heavy Ion Collisions (S. M. Shafroth, J. A. Tanis, J. Willis, J. R. Mowat)

During 1979 we have extended our target thickness work to include target thickness effects on projectile K x rays and REC for Cl^{q+} on C.

This work was reported on at Kyoto, Japan by Professor Mowat ICPEAC XI, August 1979. It was entitled, "Target Thickness Analysis of Projectile K X-Rays and REC for 40-80 Mev Cl on C", J. A. Tanis, S. M. Shafroth and J. R. Mowat.

We found that Cl K vacancy production in C targets was about half that observed for Cu targets depending on the incident Cl^{q+} energy. The REC cross sections in C are 2 - 3 times smaller than for Cu which is consistent with Bethe-Salpeter theory if it is assumed that each weekly bound electron contributes equally to the REC process.

Further work on target thickness effects in Radiative Electron capture has been done, and a comment has been prepared for submission to Phys. Rev. A. It is entitled "Radiative Electron Capture by Cl Ions Incident on C and Cu Foils" by J. A. Tanis and S. M. Shafroth, J. W. Willis, and J. R. Mowat. The abstract follows:

> "Radiative electron capture (REC) cross sections for 40-80 MeV Cl ions incident on thin C Foils are reported and compared with previous results using Cu targets. Good agreement is obtained with the free-electron theory of Bethe and Salpeter by assuming that each of the "free" target electrons contributes equally to REC."

---

* On leave from McCalister College, St. Paul, Minn.
** Now at Lawrence Berkeley Laboratory
\+ East Carolina University
++ North Carolina State University

Fig. D2-1 illustrates the REC results and shows the relationship between C and Cu targets.

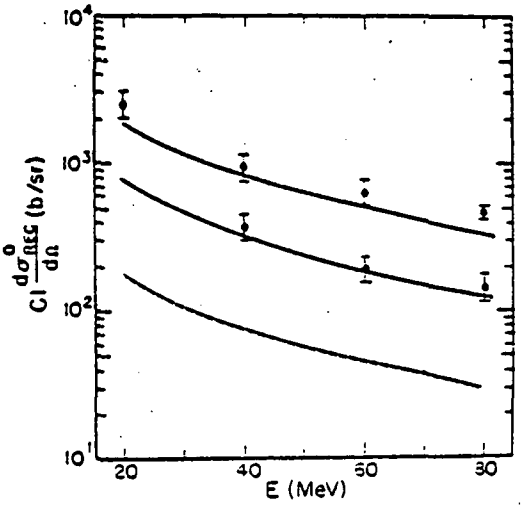

Fig. D2-1.

A paper is being presented at the DEAP (Division of Electron and Atomic Physics) Houston, Texas in December 1979 entitled "Variations in Hypersatellite K x-ray Intensities with Target Thickness", by J. A. Tanis, S. M. Shafroth, J. W. Willis and J. R. Mowat. It is also being submitted for publication. The abstract follows:

> "Hypersatellite K x-ray intensities for 2.3 MeV/amu Cl ions incident on thin C foils have been measured as a function of target thickness. The double-to-single K vacancy x-ray intensity ratio increases by a factor of about 3.5 over the range of energies investigated, reaching values as high as 30%. A quantitative explanation of the observed results is obtained using the three-component model of Gardner et al."

A typical x-ray spectrum for 80 MeV Cl^{10+} incident at 90° on 141 $\mu g/cm^2$ C taken with a Si(Li) detector is shown in Fig. D2-2. The bulges on the high

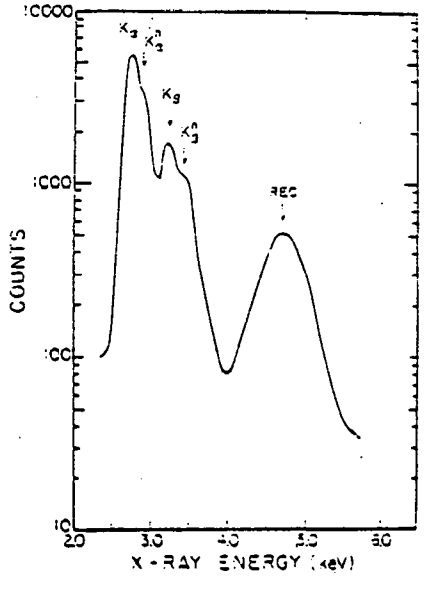

Fig. D2-2.

energy sides of the K_α and K_β peaks are due to hypersatellites. Fig. D2-3 shows a

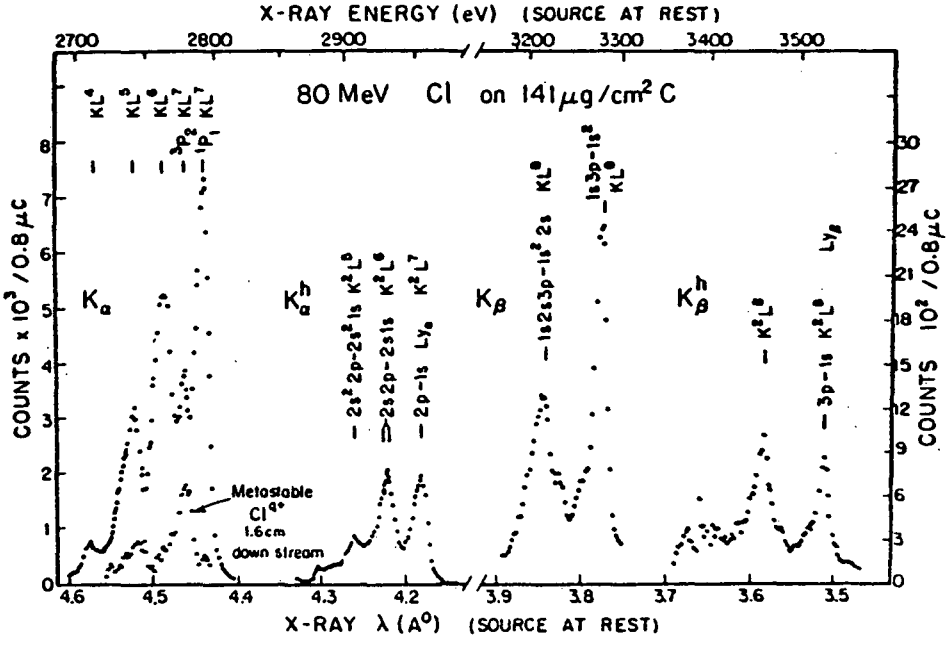

Fig. D2-3.

high-resolution spectrum taken under similar conditions but with a curved crystal Bragg spectrometer. The satellites and hypersatellites of Cl K_α and K_β are labelled. Fig. D2-4 shows the cross sections for single and double K vacancy production in the

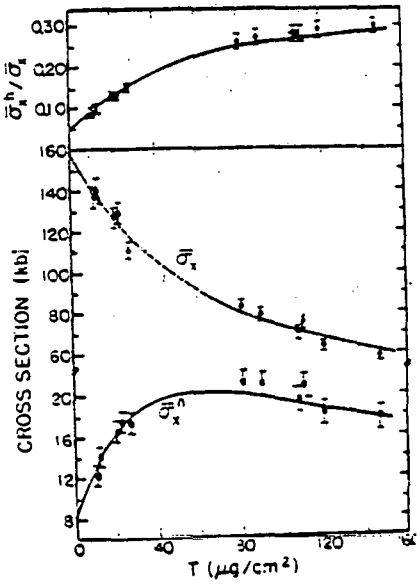

Fig. D2-4.

Cl projectile as well as the ratio of these two vs target thickness. The solid curves are theoretical, based on a three component model.

A full length paper on target thickness effects has been submitted to Phys. Rev. A. It is entitled, "Systematics of Target and Projectile K x-ray Production and REC for 20-80 Cl q^+ Ions Incident on 25-200 $\mu g/cm^2$ Cu Targets" by J. A.

Tanis, W. W. Jacobs and S. M. Shafroth. The abstract follows:

> "A systematic investigation of K x-ray production for 20-80 MeV Cl ions in collision with thin self-supporting Cu targets has been conducted. Target and projectile characteristic x rays and radiative electron capture (REC) have been measured as a function of target thickness for incident charge states $q \leq Z_1 - 2$. At 80 MeV data were also obtained for $q = Z_1 - 1$. Large enhancements in both characteristic x-ray production and REC were observed for $q = Z_1 - 1$. Measured x-ray cross sections were parametrized vs. target thickness using the model of Betz et al. and least squares fits to the data were performed. Target K x-ray production for $q \leq Z_1 - 2$ is described adequately by direct Coulomb excitation. For $q = Z_1 - 1$ it is found that the enhancement is predicted quite well by the method of Gray et al. The mean fluorescence yield for the highly stripped Cl ions is determined and found to increase by a factor of about six over the range 20-80 MeV, having a value (~0.1) nearly equal to the single K-vacancy value at 20 MeV. The radiative lifetime for the projectile ions is found to be $\sim 3 \times 10^{-14}$ sec which is about three times larger than the single K-vacancy radiative lifetime calculated by Scofield. Parametrization of the REC cross sections vs. target thickness is used to normalize the measured REC intensity to the fraction of ions with K vacancies. Resulting REC cross sections are compared with the free-electron theory of Bethe and Salpeter and good agreement is obtained if it is assumed that each of the "loosely" bound electrons in Cu contributes equally to the REC process. By combining the results obtained for the characteristic x rays and REC, the fluorescence yield for K-shell capture events may be estimated and is found to have values in the range $(2\text{-}4) \times 10^{-3}$ for the beam energies studied."

3. X-ray Angular Distribution Experiments (J. E. Willis, S. Hurst, M. Clark, S. M. Shafroth, S. L. Varghese, J. R. Mowat)

a. REC

We have studied the angular distribution of REC radiation for the case of 40 to 60 MeV Cl^{8+} on Cu. A computer program called X-SOFT was written in order to correct the observed REC x-ray spectrum channel by channel for differential absorption at the various angles of observation. This is essential because the REC spectrum is appreciably Doppler shifted. A report on this work will be given at Houston, Texas (DEAP) December 10-12, 1979.

b. Pb L x-rays

During the summer of 1979 we took data which should permit us to obtain the angular distribution of Pb L x-rays induced by bombardment of thin (220 $\mu g/cm^2$) targets by 3 MeV protons. Data were normalized to Rutherford scattered protons or to charge collected in a suppressed Faraday cup. A second run was done using a target emission consisting of a 100 $\mu g/cm^2$ layer of lead on to which was evaporated a 200 $\mu g/cm^2$ layer of silver. The idea was to use the silver K x rays as an isotropic source and take ratios of Pb $L\ell$, $L\alpha$, $L\beta$, $L\gamma$ to Ag $K\alpha$. However we encountered an unanticipated effect. Namely, the silver diffused to some extent through the lead and this affected the corrections at the few percent level. Thus more work is required before definite results at the 1% level are obtained. If we assume that the target was layered we find a small ~3% increase in Pb $L\alpha$ radiation at 25°.

Small effects of this order may arise according to theory since the substate populations of ejected L electrons are impact-parameter dependent as shown in Merzbacher and Wu. This experiment is integral over all impact parameters. Should we find an effect we will attempt an impact parameter dependent measurement. Such an experiment should be possible with a new intrinsic germanium x-ray detector which is being paid for by UNC. The new detector will have 100 mm^2 sensitive area, 10 mm depth, 175 eV resolution at 5.9 keV and be capable of operating at high count rates and adaptable for coincidence timing.

Fig. D3-1 shows a schematic drawing of the target chamber which has been designed for this work.

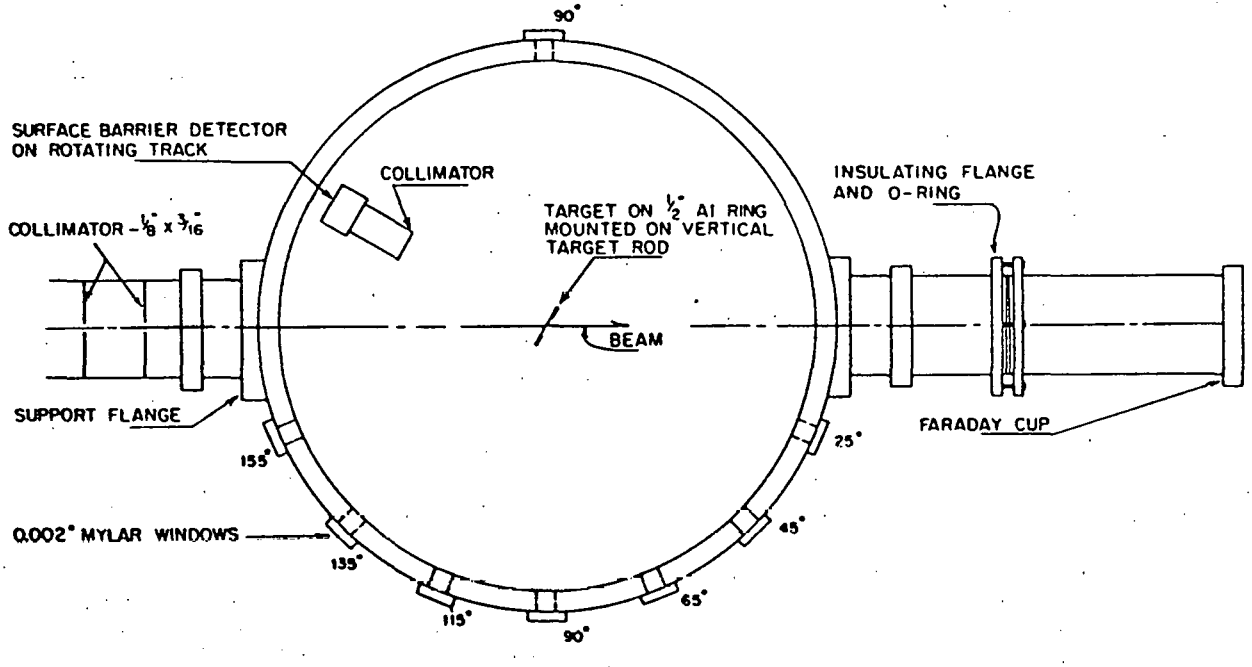

X-RAY ANGULAR DISTRIBUTION CHAMBER

Fig. D3-1.

4. Electron Spectroscopy (J. K. Swenson, M. Clark, J. Willis, S. M. Shafroth, R. Mowat)

a. Resonant Raman Scattered Auger Electrons

Having demonstrated that Resonant Raman X-Ray scattering takes place when a target element is exposed to below-threshold radiation, a search was made to examine this effect when the initial vacancy is filled via a radiationless transition (Auger Effect).

Using a Ni anode X-Ray tube (E_K = 7.48 keV) and a critical absorber of Co (t = 30 $\mu g/cm^2$) to filter out above-threshold K X-Rays, targets of Co (Kabs. = 7.71 keV) and Tb (L_3abs. = 7.52 keV) were examined. A theoretical shift of 230 eV in the K Auger electrons in Co and a shift of 40 eV in the L_3 Auger electrons should be seen.

Experiments were performed with a 30° parallel plate electrostatic analyzer. Since the resolution of this instrument was so low (2.5%) transitions corresponding to individual initial and final states were not observed. What was sought was a shift in the centroid of the KLL Auger group in Co and the $L_3M_{4,5}M_{4,5}$ group in Tb. The results of these two experiments look promising however they are inconclusive as intensities in "shifted" structures were of the same order as the simultaneously occuring unshifted transitions which took place due to the small amounts of fluorescing radiation that inevitably get through the absorber. The cross-section for the Resonant Raman induced transitions is very small compared to that for transitions induced via above threshold radiation. Therefore essentially all fluorescing radiation must be eliminated from the spectrum of X-Ray energies that reach the target. This can be achieved by using an X-Ray monochromater.

Recently we have purchased a high reflectivity pyrolitic graphite crystal which we have incorporated into the experimental set up as a monochromater. Previous attempts at using a LiF monochromater failed due to the large loss of intensity upon reflection of the X-Rays from the crystal and the large distance between the X-Ray tube and the crystal. (An XR-D5 Goniometer was used to define the Bragg angle for Ni K radiation.) The high reflectivity graphite crystal was found to give five times the reflected intensity for Ni K radiation (compared to LiF) and was found to improve the electron count rates to the point of making this a practical method for inducing vacancies in the target. Spectra were taken using fluorescing radiation and Auger count rates were of the same order as those obtained when using the critical absorber method. This rate, however, is still too low for use with below-threshold radiation. To improve the count rate even further a tube-mounted crystal holder is being built so that the losses in intensity due to the $1/R^2$ property of the X-Ray source can be minimized. This latest improvement should increase the counting rates by another factor of eight. Hopefully this will improve the results we have thus far obtained for Co and Tb and let us make some definite conclusions.

A new spectrometer was recently built. The design was identical to that of the previous one (courtesy of R. Mowat) except for the added feature of adjustable entrance and exit slits. The adjustment of these slits does not affect the spectro-

meter constant as the slit jaws move symmetrically about the central ray position. A further improvement was the addition of three more guard plates (for a total of four). These serve to further reduce electric-field fringing effects which tend to degrade the performance of the spectrometer.

Tests are being performed comparing experimental results with the corresponding theoretical parameters. A "Hot Wire" electron source is being installed to test the theoretical resolution, transmission, and focussing properties of the spectrometer.

b. Ion Beam Electron Spectroscopy

Recent work has been done at TUNL using the adjustable slit 30° spectrometer in conjunction with the newly installed Sputter Ion Source.

The spectrometer was mounted in an existing target chamber and a highly ionized S beam was observed with the spectrometer after passing the beam through a 10 $\mu g/cm^2$ C foil. The Auger electrons from the S beam were studied (after some difficulty) and some metastable states for Li-like S were observed. More work is planned along this line once improvements in the target chamber and refinements in the geometry of the experiment are made.

We are presently engaged in redesigning the target chamber so that a study of metastable state lifetimes and energies may be made. With the availability of heavy ion beams from the sputter source studies of highly ionized ions not yet explored can be done.

Fig. D4-1 shows a schematic drawing of this spectrometer.

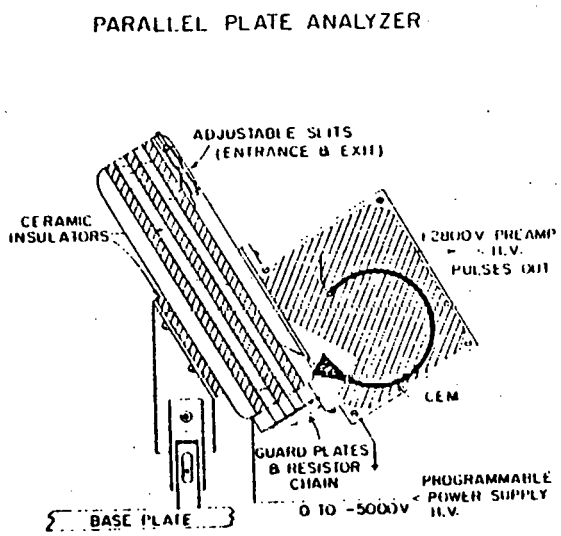

Fig. D4-1. Adjustable slit electron spectrometer.

E. OTHER EXPERIMENTS

1. X-rays and γ-rays Arising from Fusion Reaction Products Implanted in Al and Co Foils Following O^{9+}, F^{9+} and C^{9+} Bombardment

(S. L. Varghese,* A. W. Waltner, J. Willis, S. M. Shafroth, E. N. Strait**)

These experiments were planned so as to study nuclear fusion reactions using O^{9+}, F^{9+}, and (since the sputter source became available) C^{9+} projectiles on thin Co foils. The method of stacked foils was used so that typically three projectile energies could be studied with one irradiation. In this case the stack would consist of three ^{59}Co targets separated by Al catchers sufficiently thick to stop the recoiling nuclei. After irradiation the stack was separated and x ray and γ-ray activity of the individual foils was observed with Si (Li), intrinsic Ge or Ge (Li) detectors as a function of time so that half-life information could be obtained.

Typical X ray and intrinsic Ge detector spectra are shown in Figs. E1-1 and E1-2. Most of the activities arose from evaporation of several nucleons following

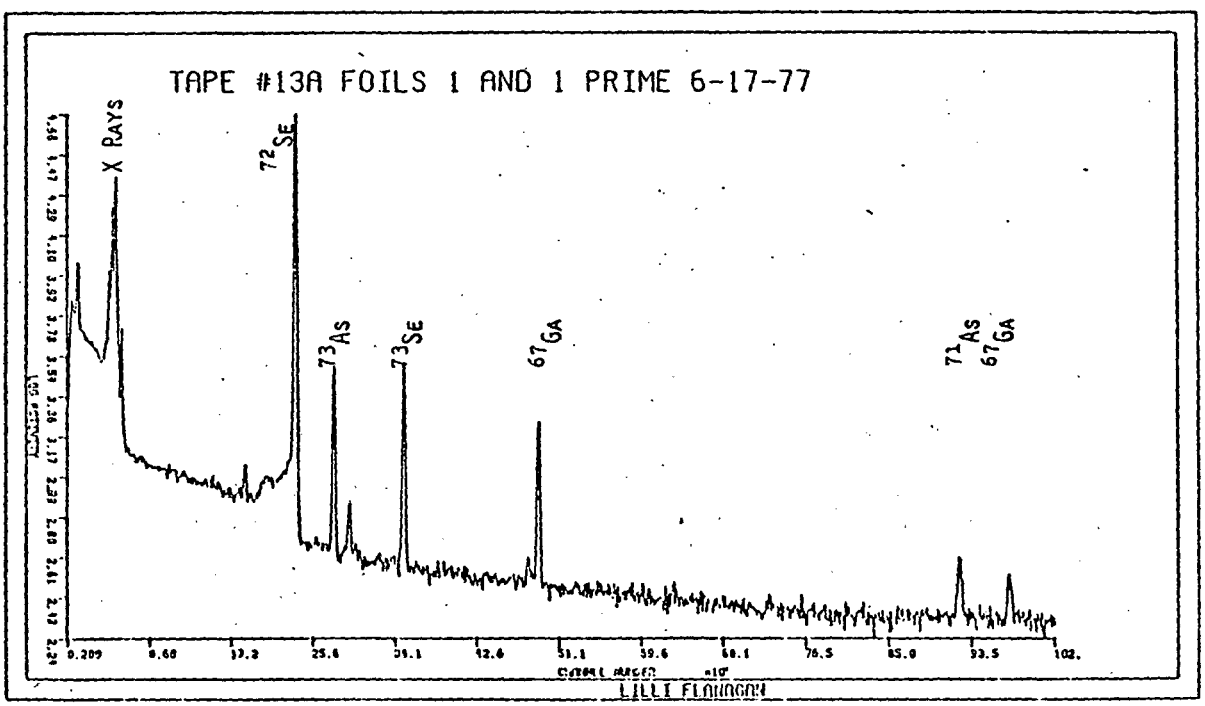

Fig. E1-1. Typical x-ray spectra arising from ^{16}O on ^{59}Co and ^{19}F on ^{59}Co.

---

* East Carolina University

** Visiting from Macalister College

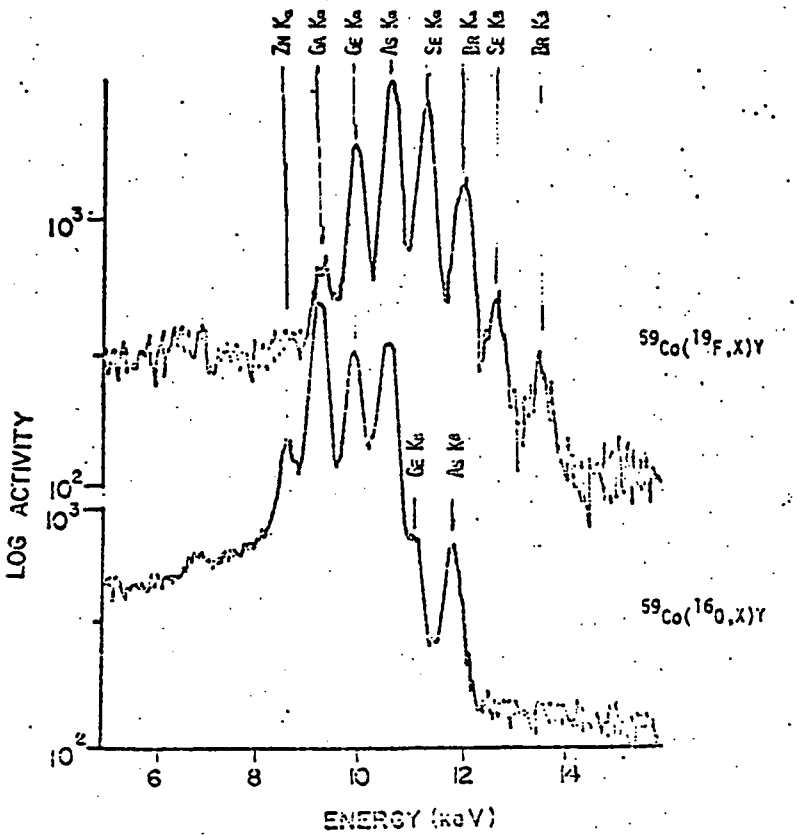

Fig. E1-2. Typical γ-ray spectrum arising from ^{16}O on ^{59}Co.

fusion so the cross sections for these processes could be extracted and compared with theory. Also ranges and straggling parameters for residual nuclei were obtained. Fig. E1-3 shows a probability plot for a typical case. Range and straggling results

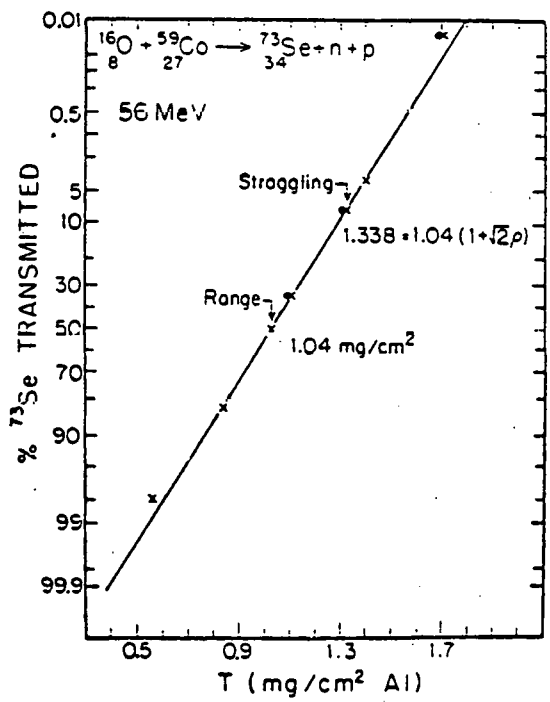

Fig. E1-3. Probability plot of ^{73}Se activity vs thickness of aluminum foil.

are summarized in Table E1-1. A paper describing some of this work has been

TABLE E1-1

Ranges and Straggling Parameters in Al for Evaporation Products Following 56 MeV ^{16}O Bombardment of ^{59}Co

	R_0 (mg/cm^2)	ρ
^{73}Se	1.04	.203
^{72}Se	0.99	.221
^{72}As	1.025	.211
^{71}As	0.95	.254
^{69}Ge	1.01	.308
^{67}Ga	1.065	.368

presented at the 8th International Conference on Atomic Collisions in Solids, Hamilton, Ontario, Canada, August 13-17, 1979. It has been accepted for publication in Nuclear Instruments and Methods. The title is: "X-Ray Identification of Fusion Reaction Products Implanted in Al Foils Following O and F Bombardment of Co Foils". S. L. Varghese, A. W. Waltner, J. E. Willis, S. M. Shafroth. The abstract follows:

> "64 MeV O^{+7} and 52.5 MeV F^{+6} ions were incident on stacked foils of Co and Al. Compound nuclei of ^{75}Br and ^{78}Kr, which decayed by evaporation of one or more nucleons, were formed. Implanted reaction products consisting of Ga through As and Ge through Kr, in the O and F experiments respectively, were identified in the Al foil. Atomic numbers of these products were determined from k-x-ray spectra and the mass numbers from γ-ray spectra[1] and half life measurements. These results and others related to straggling and range of the residual particles in the foils will be presented."

As a by product of this work we found nuclear fusion reactions arising from bombardment of the Al catcher foils with Fq^+ and Cq^+. In the former case 2.44d ^{44}Sc and 3.93h ^{44}Sc were produced. In the latter case ^{32m} ^{34m}Cl was produced. An APS talk has been given concerning the Sc activity.

[1] A. W. Waltner, D. M. Peterson, S. M. Shafroth and J. E. Willis, Bull. Am. Phys. Soc., 24 (1979) 695

F. WORK DONE ELSEWHERE BY TUNL PERSONNEL

1. Neutron Emission in Heavy Ion Reactions

a. Neutron Multiplicities in Inelastic Collisions of ^{132}Xe Ions with ^{197}Au (C. R. Gould,* R. Bass, J. Czamecki, V. Hartmann, K. Stelzer, Y. Eyal, Institut für Kernphysik, Frankfurt and GSI, Darmstadt)

This work, discussed in TUNL XVII, has now been completed and has been submitted for publication in Zeitschrift für Physik. The abstract is given below.

> "Neutrons have been detected in coincidence with charged reaction products in inelastic scattering of 7.5 MeV/u ^{132}Xe ions from ^{197}Au. The deduced neutron multiplicities associated with the heavy and light fragment, respectively, are roughly proportional to the total kinetic energy loss, and their ratios are close to the Au-Xe mass ratio for all Q-values. These results and the measured neutron energy spectra are consistent with the assumptions of thermal equilibrium between the fragments at scission, and of neutron emission from fully accelerated fragments. For deep inelastic events, the measured absolute multiplicities are smaller than expected from statistical model calculations, but an effect due to pre-equilibrium emission of particles - as suggested by an earlier analysis of the present data - cannot be definitely established."

Fig. F1-1 shows a comparison of the measured center-of-mass neutron energy spectra with the predictions of the statistical model code JULIAN, written by Y. Eyal and M. Hillman. The calculated spectra are arbitrarily normalized but show good agreement in shape with the measured neutron spectra. The spectra correspond to excitation energies of ~50 and ~75 MeV respectively for the outgoing Xe-like and Au-like ions. Initial spin values of ~35h and 50h were used in the calculation for the Xe and Au ions.

* On leave from N. C. State University, work supported by Humboldt Foundation, West Germany

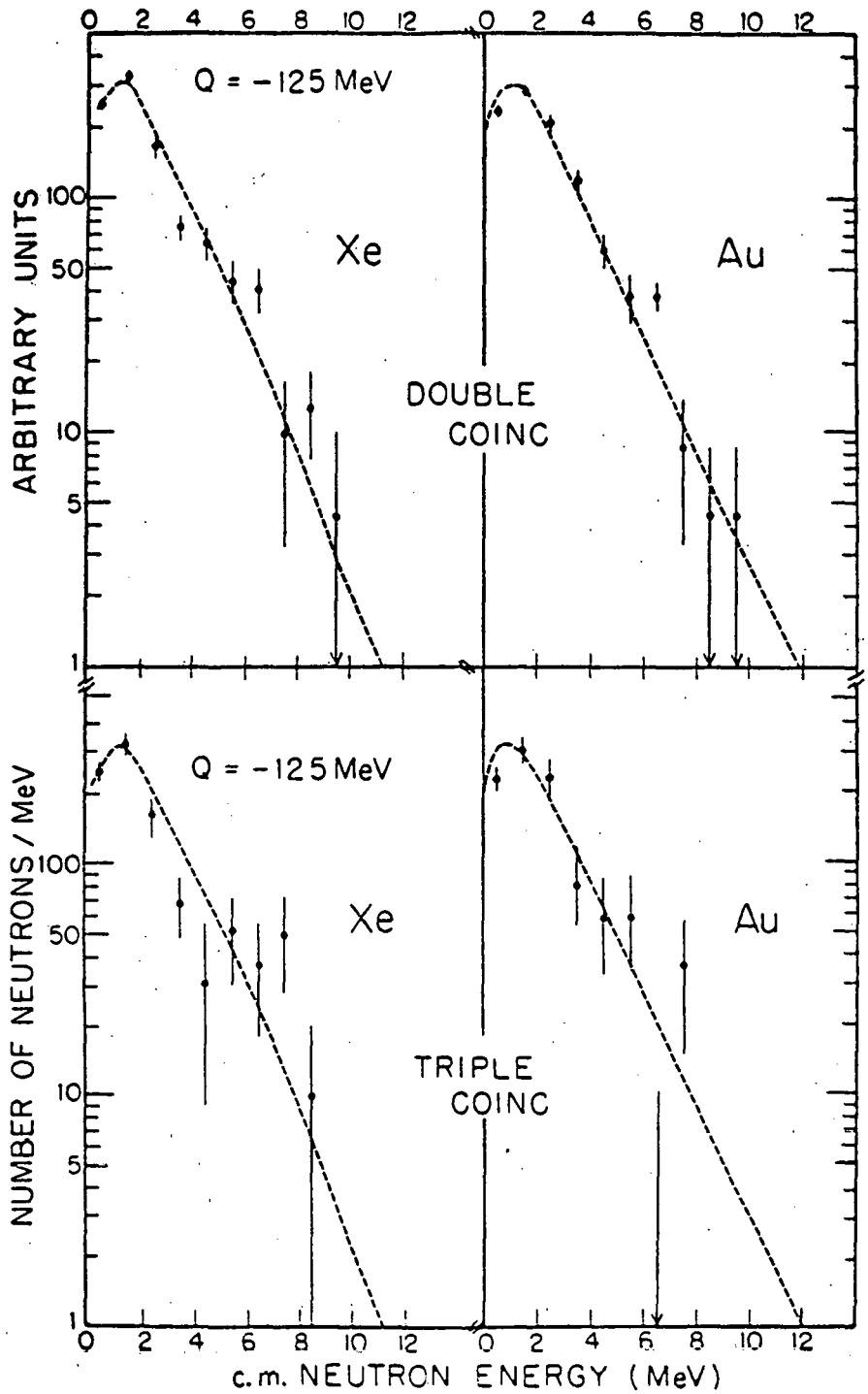

Fig. F1-1. Measured center-of-mass neutron energy spectra and comparison with statistical model predictions (see text).

b. Neutron Emission in Deep Inelastic Collisions Induced by ^{86}Kr on ^{166}Er at 5.7, 7.0 and 7.9 MeV/Nucleon (Y. Eyal, A. Gavron, I. Tserruya, Z. Fraenkel, Y. Eisen, S. Wald ((Weizmann Institute, Rehovot)), R. Bass, C. R. Gould, G. Kreyling, R. Renfordt, K. Stelzer, R. Zitzmann ((IKF, Frankfurt)), A. Gobbi, U. Lynen, H. Stelzer, I. Rode and R. Bock ((GSI, Darmstadt)))

This was the first experiment to measure neutron yields in deep inelastic scattering events as a function of total kinetic energy loss, fragment mass, and fragment and neutron emission angles. The results of the 7.0 MeV/nucleon data were published in Phys. Rev. Letters 41, 625 (1978). A more complete analysis of the final data set has now been submitted to Physical Review. The abstract appears below:

> "Neutron emission associated with deep inelastic collisions of 496-, 602-, and 675-MeV ^{86}Kr with ^{166}Er has been studied as a function of kinetic energy loss, fragment mass and neutron scattering angles. The major de-excitation process is neutron evaporation from fully accelerated fragments. The excitation energy is shared between the fragments in proportion to their mass, indicating energy equilibration in the intermediate dinuclear composite system for the completely damped as for the quasielastic components. Within limits imposed by the systematic uncertainties, the angular and velocity distributions of the neutrons in the laboratory frame are consistent with isotropic emission of neutrons in the c.m. frame of the fragments. We find no evidence for pre-equilibrium effects. The observed multiplicities and energy spectra of the neutrons are consistent with predictions of statistical-model calculations."

c. Neutron Emission in Fusion Reactions Between Heavy Ions (U. Arlt, R. Bass, C. R. Gould, V. Hartmann, R. Renfordt, K. Sapotta, K. Stelzer, G. Kreyling ((IKF, Frankfurt)))

Feasibility studies have been carried out at GSI, Darmstadt to investigate neutron and gamma ray emission in fusion reactions between 4.2 MeV/nucleon ^{86}Kr ions and ^{12}C and ^{64}Ni targets. Four NE213 liquid scintillators were used to measure 2-, 3- and 4-fold coincidences between outgoing neutrons and also between neutrons and gamma rays detected in a Ge(Li) detector. Preliminary results indicate that the neutron energy spectra are consistent with evaporation and that the angular distributions of the neutrons exhibit marked anisotropies, possibly reflecting angular momentum effects. Further experimental studies are planned. A preliminary report on this work was presented at Gent, (Verhandlung DPG (VI) 14 (79) 758).

G. ACCELERATOR DEVELOPMENT AND INSTRUMENTATION

1. 3 MeV Lab Development (C. R. Westerfeldt, R. O. Nelson, K. B. Sales, G. E. Mitchell, E. G. Bilpuch)

A great deal of work has been performed this past year in improving the facilities of the 3 MeV laboratory. Last spring the laboratory was shut down for several weeks for the replacement of the tube pumping station, installation of a new water system, and overhaul of both the compressed air and water cooling systems. The original HVEC mercury diffusion pumping station was replaced by one with a CVC 7" oil diffusion pump and a refrigerated baffle. This new pump has a pumping speed several times that of the mercury pump, requires no chilled water for cooling, no dry ice traps, and routinely develops vacuums five times lower than previously possible. An additional benefit derived from this changeover is the reduction of the tendency of the accelerator tube to spark at high terminal potentials. In fact we are now able to routinely perform experiments above 3 MeV, and have gone as high as 3.35 MeV with no adverse effects.

A terminal stabilizer system has been designed for the 3 MeV accelerator. Its purpose is to stabilize the beam energy inside the accelerator, in order to reduce the need for corrections to the target rod potential by the homogenizer circuitry. This would also reduce the motion of the beam spot on the target, and the consequent problems of detector collimation. If this technique is successful, we should also be able to obtain a high resolution alpha particle beam in our scattering chamber. At present we should have to run the alphas through the electrostatic analyzer, and apply the correction signal on the target rod. A prototype of the terminal amplifier has been constructed and bench tested. We expect to construct the terminal amplifier shortly and install it for testing next year.

A third development project is aimed at determining the effect of Doppler broadening on our total resolution function. We have constructed a special liquid nitrogen cooled target rod for elastic scattering experiments. No data have yet been taken with this device, but it should be tested shortly.

---

[1]Overly et al., Nucl. Instr. and Meth. 68 (1969) 61

H. COMPUTER RELATED DEVELOPMENT

1. The Prime Computer System (B. H. Chou, B. H. Dubendorff, R. O. Nelson, K. B. Sales, J. F. Shriner, C. R. Westerfeldt, S. E. Edwards, N. R. Roberson)

Improvements to the Prime computer system have been made in several areas this past year. We have purchased the Prime Computer Revision 15.5 operating system, ordered a 9 track magnetic tape unit, upgraded our CAMAC interface hardware and software, and converted all of our DDP-224 analysis programs to run on the Prime.

We are now using the Rev. 15.5 operating system on a limited basis while we determine whether it will support all of our present in-house programming. The major difficulty is that the supervisor program has been enlarged from 6200 locations to 20,000 locations, or one third of available memory. While this is a large increase we are still able to load and execute our largest existing programs with only minor modifications. The Revision 15.5 operating system will be the last revision to support the Prime 300 computer.

We have ordered a Pertec nine track magnetic tape unit which will give us compatability with the new computer system for the tandem laboratory. The purchase of a 9 track magnetic tape unit was the only major purchase for the Prime computer this year. It was necessitated by the very limited support given to 7 track magnetic tapes at Prime Computer Co., and the almost universal usage of 9 track MTU's by all computer facilities with which we interact. The new computer system for the tandem laboratory will have 9 track MTU's exclusively, and so to transfer data, programs, etc., between these computers, will require us to have a compatible 9 track MTU. The 9 track MTU will allow us easy access to software at Prime Computer Co. and elsewhere.

Hardware improvements have been made in the Camac interface. The Camac interface has been upgraded so that we are now able to take coincidence data. In addition a Borer model 1302 ADC buffer has been purchased, and an interface between it and our ADC-router system has been designed. This buffer has 2 - 256 word memories, which will allow data collection at the maximum rate determined by the ADC dead time. The data accumulating program will now be interrupted only once for each 256 data points, at which time a DMT operation will transfer all 256 points to the data matrix in memory. In the past the program was interrupted for each data point. We hope that this data buffer will alleviate problems associated with high counting rates and high ADC dead time.

The Camac supporting software has been increased with the addition of a special package of routines to support the interactive analysis routines. Another program under development will support the new ADC buffer. Several Camac oriented subroutines have also been written or modified to support the newly installed analysis programs.

This past year has also seen the removal of all of our analysis programs from the old DDP-224, and their installation on the Prime. This has been of great benefit to the users of the Prime System. We are now able to take data online, strip the data from magnetic tape and do preliminary or final analysis of the data, all on the same computer. The only analysis not done in-house is the final analysis of elastic scattering data done at TUCC with the program MULTI. The Prime's small interactive version of MULTI has proven capable of giving nearly final fits to even the most complicated single channel data. This has saved us considerable analysis time at TUCC.

2. New Computing Facilities (C. R. Gould, N. R. Roberson, S. E. Edwards, M. Jensen, S. A. Wender)

The current computing facilities at TUNL have been in operation for about 14 years. The design of a new computer system to be installed and put in operation during 1980 has been completed. A DEC VAX 11/780 will be delivered early in February.

In our early planning for a new system, we believed that the best arrangement was that of a central computer for off-line users linked with a network of satellite computers, each dedicated to data acquisition for a single user. Cost consideration suggested that the facility be built around 16 bit machines. For fast direct storage of large data arrays it was also proposed that some bulk memory would be necessary for at least one of the satellite computers.

In considering the implementation of this system, we became aware of several drawbacks:

i) Peripherals are unnecessarily duplicated on the satellite machines
ii) General network hardware and software is expensive
iii) The satellite machines are capable of only limited data reduction. More sophisticated monitoring of the experiment requires transfer of data blocks back to the main CPU.
iv) The bulk memory is wasted for anything but data acquisition.
v) The limitations of 16-bit addressing are inconvenient and restrictive. Programs are generally partitioned in 128 Kbyte segments and double word storage is necessary as counts per channel frequently overflow 65,000.

The system thus appeared somewhat complicated to operate, required very reliable network software to exploit its capabilities fully and was still somewhat wasteful of resources. We then began to consider the centralized facility concept as it applied to the new generation of large memory, 32-bit minicomputers.

We now feel that these large minicomputers, which were just beginning to appear on the market at the time we were formulating our ideas, do in fact provide the best solution to the data acquisition and analysis needs of a medium size nuclear physics facility such as TUNL.

Our present view of the proposed computer facility is shown in Fig. H2-1.

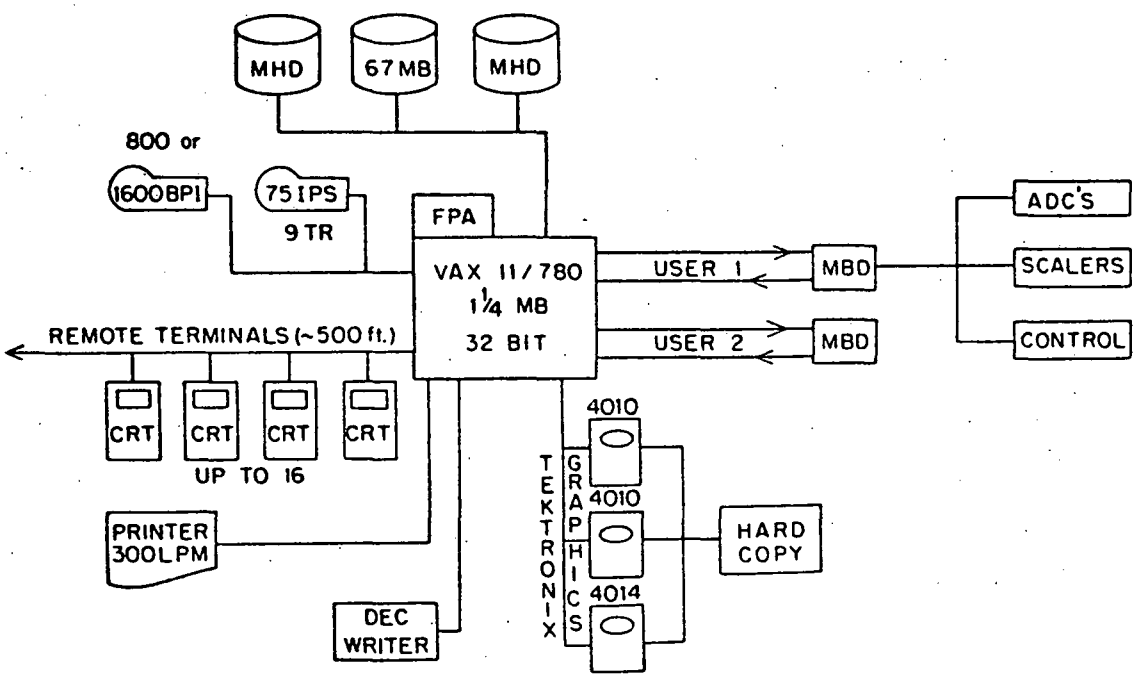

Fig. H2-1. Block diagram of the proposed computing facility. The blocks labelled MBD are intelligent branch drivers (LAMPF design) for Camac systems.

THIS PAGE

WAS INTENTIONALLY

LEFT BLANK

10 x 10 push button panel, any arrangement of the available ADC's into single or multiparameter groups, 2) provides one word of pre-buffering by transferring the ADC data into input data registers with subsequent resetting of the ADC's, and 3) provides fast transfer of the data register contents to memory via DMA channels. The first two goals have already been met with a design which is currently in operation at the TUNL Prime-300 facility.

All our present computing is done in Fortran and we envisage that this will continue to be the case with the new system. This includes the data acquisition programs where special purpose subroutines will be written to handle non standard peripherals. We anticipate 4-5 users engaged in off-line computation, most of whom will be doing text editing, program development and background utility work. One main user will be doing interactive graphics computing, for example data tape read back, peak fitting, searching on optical model parameters etc. Finally we envisage one user engaged in lengthy calculation not requiring any interactive capability, for example Monte Carlo calculations of neutron multiple scattering corrections. These kinds of job could be left running for many hours in one partition of a time shared computer without affecting the flow of interactive or background computing.

I. NUCLEAR THEORY AND PHENOMENOLOGY

Introduction

The progress in nuclear theory and phenomenology described here is primarily related to the experimental program at TUNL. For example, the theory of the optical potential is applied to elastic and quasi-elastic scattering and to polarization effects in deuteron scattering, while the calculations of radiative-capture reactions and of atomic effects in nuclear resonances have analyzed data taken at TUNL.

1. Many-Body Theory of Nuclear Reactions (S. R. Cotanch)

Progress continues in the development of practical techniques for the proper many-body description of nuclear reactions. The recent unitary estimate for multistep processes[1] provides an effective sum-rule for higher-order effects as well as establishing physical guidelines for deciding which class of corrections to include in model calculations. Current investigations are directed towards obtaining an improved treatment of rearrangement reactions by deriving a correction term series which can be perturbatively ordered. Heretofore, this has not been achieved since in rearrangement no unique residual interaction characterizes the system. The present work introduces the concept of an averaged partition interaction and an averaged intermediate Green's function. The resulting integral equations accommodate all important channels and boundary conditions. Studies of approximation schemes to further reduce these equations are underway.

2. Theoretical Determination of the Optical Potential (S. R. Cotanch)

The Feshbach expression for the optical potential has been extended. In particular the imaginary part which accounts for absorption has been mathematically separated into components which correspond to quasi-direct and compound mechanisms. Each component can be manipulated into a non-local interaction which is separable, but of rank higher than zero. The resulting non-local Schrodinger equation is thus transformed into a local, inhomogeneous equation. The inhomogeneity plays the role of a source/sink term and is amenable to simplifying approximations. Besides providing a theoretical basis for determining the optical potential, the results provide additional physical insight into the absorption process. More importantly, the treatment suggests a consistent way for applying an optical-model analysis at low energies for both light and heavy nuclei.

3. The Lane Model for (p,n)(p,p) and (n,n) Reactions (R. C. Byrd, S. R. Cotanch, R. L. Walter)

a. $^{9}Be(p,n_0)^{9}B$

Results of previous analyses of the ^{9}Be + nucleon system were presented as invited papers at the Telluride Conference on the (p,n) Reaction and the

[1] S. R. Cotanch, Phys. Rev. C19 (1979) 693

Nucleon-Nucleon Force, and at the 1979 Nuclear Division meeting.[1] The basic analysis has also been published in Physical Review Letters. The Lane potentials obtained in this study were successful in simultaneously describing all available cross-section and polarization data for the (p,p), (p,n), and (n,n) reactions. A summary of results is shown in Fig. M3-1. The predictions made by these potentials have also been compared very recently to the $^{9}Be(\vec{n},n)^{9}Be$ analyzing powers which we measured. (See Section B.) As shown in Fig. M3-1, the predictions describe the data quite reasonably. With the availability of these new data, further parameter variations will be investigated. It may be found that simultaneous descriptions of the analyzing powers for the (p,p), (p,n), and (n,n) processes will, for the first time, unambiguously require the addition of a spin-orbit symmetry potential to the Lane optical model.

b. $^{13}C(p,n_0)^{13}N$ and $^{15}N(p,n_0)^{15}O$

Because of the pronounced resonance structure in the $^{13}C(p,n_0)^{13}N$ and $^{15}N(p,n_0)^{15}O$ reactions, application of a direct reaction model first required energy-averaging of the different observables. For the (p,p) and (n,n) channels, results were either averaged or generated from smoothly-varying phase-shift parameters.[2,3] Cross sections for the (p,n) channel were obtained from averaged Legendre polynomial coefficients which we generated. The most conspicuous feature of the Lane model potentials obtained in fitting the data was the strong energy dependence in the real symmetry strengths. Although analyses are not yet complete, results from a parameter set which varies only linearly with energy are shown in Fig. I3-1 for the $^{15}N(p,n)^{15}O$ reaction at 11.5 MeV.

4. A Computer Code for Radiative Capture Reactions (J.M. Lafferty, Jr., S. R. Cotanch)

The code RADCAP, which computes direct radiative capture processes, has been expanded to compute the differential cross-section for projectiles with spins 0 or 1/2. This generalized program, referred to as PARCAP, is available to all TUNL personnel. In the near future the code will be further generalized for projectiles (or clusters) with spins 1, 3/2, and 2. In addition the code will be extended to calculate magnetic transitions and phenomenological semi-direct transitions.

5. Cluster-Model Calculations for Alpha Capture (J. M. Lafferty, Jr., S. R. Cotanch)

In a series of recent articles,[1] a specific cluster model of light nuclei has been developed. It has been successful in accounting for a large number of static nuclear properties (e.g., energies, moments, electromagnetic transition rates, etc.). We have applied this model above the alpha-emission threshold and have performed calculations of direct E2 radiative capture in the energy region spanning the isoscalar quadrupole giant resonance for the reaction $^{28}Si(\alpha,\gamma)^{32}S$. Comparison with data showed that the calculations did not reproduce the low energy (< 10 MeV) resonances, implying that the reaction goes via a compound mechanism. For energies above the GQR, direct E2 calculations account for only ~20% of the experimental total cross-section, but if the model is extended to include core excitations the entire total cross-section can be reproduced.

Preliminary portions of this work have been presented at the 1979

[1] B. Buck and A. A. Pitt, Nucl. Phys. A295 (1978) 1; A280 (1977) 133

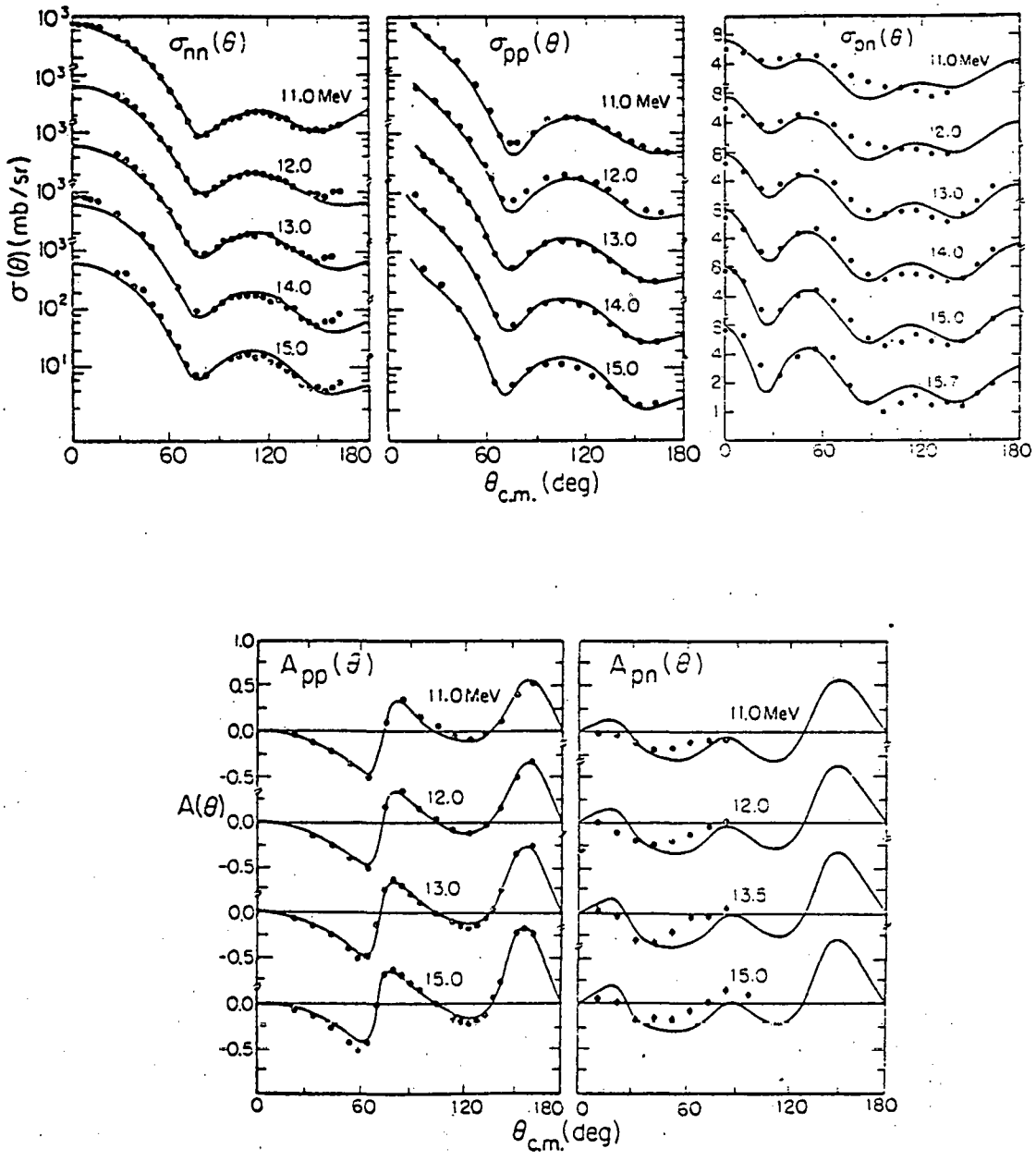

Fig. I3-1. Experimental data (dots) for the reactions $^{9}Be(n,n)^{9}Be$, $^{9}Be(p,p)^{9}Be$ and $^{9}Be(p,n)^{9}B$ compared to Lane model calculations using a single optical potential to represent the ^{9}Be + nucleon interaction.

American Physical Society meeting of the Nuclear Division.[1]

[1] J. M. Lafferty and S. R. Cotanch, BAPS 24 (1979) 845

APPENDIX I

A. PUBLISHED JOURNAL ARTICLES January 1979 - December 1979

1. Study of Inelastic Proton Amplitudes for a Fragmented Analogue State in ^{45}Sc, G.E. Mitchell, T.R. Dittrich, and E.G. Bilpuch, Zeitschrift für Physik A289 (1979) 211.

2. Phase Relation for a Common Doorway State in ^{47}V, J.R. Chandler, G.E. Mitchell, and E.G. Bilpuch, Phys. Rev. C20 (1979) 52.

3. Observation of Intermediate Structure in Inelastic Proton Amplitudes in ^{49}V, W.K. Wells, E.G. Bilpuch, and G.E. Mitchell, Phys. Letters 86B (1979) 18.

4. Reactions $^{15}N(\gamma,d_0)^{13}C$ and $^{13}C(d,\gamma_0)^{15}N$ in The Giant Resonance Region, D.M. Skopik, J.J. Murphy II, H.R. Weller, R.A. Blue, N.R. Roberson, S.A. Wender and D.R. Tilley, Phys. Rev. C20 (1979) 409.

5. Polarized Neutron Capture in The Giant Resonance Region of ^{41}Ca, M. Jensen, D.R. Tilley, H.R. Weller, N.R. Roberson, S.A. Wender, T.B. Clegg, Phys. Rev. Lett. 43 (1979) 609.

6. Inelastic α-Cross Sections in The Region of The GQR for Nuclei Near Mass 60, H.R. Weller, S. Manglos, S.A. Wender, N.R. Roberson, M. Potokar and D.R. Tilley, Phys. Rev. C20 (1979) 1589.

7. Elastic and Inelastic Scattering of 7 to 14 MeV Neutrons from Lithium-6 and Lithium-7, H. Hogue, P.L. von Behren, D.W. Glasgow, S.G. Glendinning, P.W. Lisowski, C.E. Nelson, F.O. Purser, W. Tornow, C.R. Gould, L.W. Seagondollar, Nucl. Sci. and Eng. 69 (1979) 22.

8. Simple Unitary Estimate for Multistep Processes, S.R. Cotanch, Phys. Rev. C19 (1979) 693.

9. Detailed Study of The Lane Potential: Multichannel and Polarization Constraints, R.C. Byrd, R.L. Walter and S.R. Cotanch, Phys. Rev. Lett. 43 (1979) 260.

APPENDIX I (Continued)

B. JOURNAL ARTICLES ACCEPTED FOR PUBLICATION

1. Polarized Proton Capture on ^{13}C, J.D. Turner, N.R. Roberson, S.A. Wender, H.R. Weller and D.R. Tilley, Phys. Rev. C. (to be published Feb. 1980).

2. Study of The Structure of Low Lying Levels of ^{29}Si via The $^{28}Si(\vec{d},p\gamma)$ Reaction and Multistep Reaction Calculations, H. Clement, R.N. Boyd, C.R. Gould and T.B. Clegg, accepted for publication in Nuclear Physics.

3. Neutron Emission in Deep Inelastic Collisions Induced by ^{86}Kr on ^{166}Er at 5.7, 7.0 and 7.9 MeV/Nucleon, Y. Eyal, A. Gavron, I. Tserruya, Z. Fraenkel, Y. Eisen, S. Wald, R. Bass, C.R. Gould, G. Kreyling, R. Renfordt, K. Stelzer, R. Zitzman, A. Gobbi, U. Lynen, H. Stelzer, I. Rode, R. Bock, accepted for publication in Phys. Rev. C.

APPENDIX I (Continued)

C. JOURNAL ARTICLES SUBMITTED FOR PUBLICATION

1. Neutron Multiplicities in Inelastic Collisions of ^{132}Xe with ^{197}Au, C.R. Gould, R. Bass, J.V. Czarnecki, V. Hartmann, K. Stelzer, R. Zitzmann, Y. Eyal, submitted to Zeitschrift für Physik.

2. Inelastic Proton Amplitudes for f-wave Resonances in ^{55}Co, W.A. Watson III, E.G. Bilpuch and G.E. Mitchell, submitted to Zeitschrift für Physik.

3. Polarized Proton Capture in ^{30}Si, C.P. Cameron, R.L. Ledford, M. Potokar, N.R. Roberson, H.R. Weller and D.R. Tilley, submitted to Phys. Rev. C.

APPENDIX II

INVITED TALKS, CONFERENCE AND TECHNICAL REPORTS AND BOOK CHAPTERS BY TUNL PERSONNEL

January 1979-December 1979

1. High Resolution Proton Scattering, G.E. Mitchell, IEEE Transactions on Nuclear Science, Vol. NS-26, p. 1207 (1979).

2. Experimental Demonstration of Phase Relation for Common Doorway States, G.E. Mitchell, T.R. Dittrich, and E.G. Bilpuch, Neutron Capture Gamma-Ray Spectroscopy, ed., R.E. Chrien and W.R. Kane (Plenum Press, New York, 1979) p. 696.

3. Statistical Properties from High Resolution Proton Resonance Reactions, G.E. Mitchell, invited talk, to be published in the Proceedings of The International Conference on Theory and Applications of Moment Methods in Many Fermion Systems (Ames, Iowa, September, 1979).

4. Fine Structure of Isobaric Analogue Resonances, G.E. Mitchell, invited talk at Adriatic Europhysics Study Conference on Statistical Properties of Nuclei (Hvar, Yugoslavia, October, 1979), published in Fizika, 11, supplement 2 (1979) 11.

5. Evidence for an E2 Resonance Observed by Radiative Capture of Fast Neutrons by ^{40}Ca, N.R. Roberson, M. Potokar, D.R. Tilley, S.A. Wender and H.R. Weller, to be published in "Proceedings of the Third International Symposium on Neutron Capture Gamma-Ray Spectroscopy and Related Topics", ed. by Robert Chrien and Walter R. Kane, Plenum Press, N. Y. (1979).

6. Polarized Neutron Capture in the Giant Resonance Region of ^{41}Ca, M. Jensen, T.B. Clegg, N.R. Roberson, D.R. Tilley, S.A. Wender and H.R. Weller, "International Conference on Nuclear Physics with Electromagnetic Interactions", June 1979, Mainz, Germany.

7. Neutron Emission in Deep Inelastic Reactions Induced by ^{86}Kr on ^{166}Er at 5.7, 7.0 and 7.9 MeV/Nucleon, Y. Eyal, A. Gavron, I. Tserruya, Z. Fraenkel, Y. Eisen, S. Wald, R. Bass, C.R. Gould, G. Kreyling, R. Renfordt, K. Stelzer, R. Zitzmann, A. Gobbi, U. Lynen, H. Stelzer, I. Rode, R. Bock, International Workshop VII on Gross Properties of Nuclei and Nuclear Excitations, Hirschegg, Kleinwalsertal, Austria (Jan. 1979).

8. Proposed Computing Facilities for Triangle Universities Nuclear Laboratory, C.R. Gould, N.R. Roberson, S.E. Edwards, M. Jensen and S.A. Wender, IEEE Transactions on Nuclear Science NS26 (1979) 4373.

9. Target Thickness Analysis of Projectile K x-rays and REC for 40-80 MeV Cl on C, J.A. Tanis, S.M. Shafroth, and R. Mowat, ICPEAC XII, Kyoto, Japan, 29 Aug. - 4 Sept. 1979.

10. X-ray Identification of Fusion Reaction Products Implanted in Al Foils, Following O and F Bombardment of Co Foils, S.L. Varghese, A.W. Waltner, J.E. Willis, and S.M. Shafroth, 8th Int. Nat. Conf. Atomic Collisions in Solids, Hamilton, Canada, Aug. 13-17 (1979).

APPENDIX II (Continued)

INVITED TALKS, CONFERENCE AND TECHNICAL REPORTS AND BOOK CHAPTERS BY TUNL PERSONNEL

January 1979-December 1979

11. Double Differential Neutron Scattering Cross Sections for Fe, Cu, Ni and Pb between 8 and 12 MeV, A. Beyerle, C. Gould, W. Seagondollar, P. Thambidurai, S. El-Kadi, G. Glendinning, C.E. Nelson, F.O. Purser and R.L. Walter, in Neutron Cross Sections for Technology, ed. C.H. Johnson (in press) and Bull. Am. Phys. Soc. 24 (1979) 866.

12. Neutron Elastic and Inelastic Scattering from ^{63}Cu, ^{65}Cu, ^{54}Fe, and ^{56}Fe between 8 and 12 MeV, S. El-Kadi, R. Pedroni, C.E. Nelson, G. Glendinning, F.O. Purser, R.L. Walter, A. Beyerle, C. Gould, and W. Seagondollar, in Neutron Cross Sections for Technology, Ed. C.H. Johnson (in press) and Bull. Am. Phys. Soc. 24 (1979) 866.

APPENDIX III

ABSTRACTS OF CONTRIBUTED PAPERS PRESENTED AT AMERICAN PHYSICAL SOCIETY AND OTHER MEETINGS

1. High Resolution Study of the $^{64}Zn(p,p)$ Reaction, K.B. Sales, G.E. Mitchell, E.G. Bilpuch and C.R. Westerfeldt, Bull. Am. Phys. Soc. 24 (1979) 107.

2. High Resolution Proton Inelastic Scattering on ^{54}Fe, W.A. Watson, III, E.G. Bilpuch, C.R. Westerfeldt, G.E. Mitchell and K.B. Sales, Bull. Am. Phys. Soc. 24 (1979) 107.

3. Fast Neutron Capture Study of the GDR of ^{15}N, S.A. Wender, M. Potokar, N.R. Roberson, H.R. Weller, M.J. Jensen and D.R. Tilley, Bull. Am. Phys. Soc. 24 (1979) 646.

4. E2 Strength in the $^{13}C(\vec{p},\gamma_1)^{14}N$ Reaction at the Giant Resonance Region, J.D. Turner, N.R. Roberson, S.A. Wender, H.R. Weller, D.R. Tilley, Bull. Am. Phys. Soc. 24 (1979) 646.

5. E2 Strength in the GDR Region Observed with Polarized Neutron Capture on ^{40}Ca, M.J. Jensen, D.R. Tilley, S.A. Wender, N.R. Roberson, H.R. Weller, T.B. Clegg, Bull. Am. Phys. Soc. 24 (1979) 646.

6. Inelastic Alpha Cross Sections in the GQR Region for Nuclei Near Mass 60, H.R. Weller, S. Manglos, M. Potokar, N.R. Roberson, S.A. Wender, D.R. Tilley, Bull. Am. Phys. Soc. 24 (1979) 646.

7. Neutronemission bei Fusionsreaktionen mit schweren Ionen, U. Arlt, R. Bass, C.R. Gould, V. Hartmann, R. Renfordt, K. Sapotta, K. Stelzer, and G. Kreyling, Verhandl. DPG VI, 14 (1979) 758.

8. Optical Model Fits to Nucleon Scattering from ^{10}B, ^{11}B, S.G. Glendinning, F.O. Purser and C.R. Gould, Bull. Am. Phys. Soc. 24 (1979) 830.

9. E2 Strength of the GDR Region Observed with Polarized Neutron Capture on ^{40}Ca, M.J. Jensen, D.R. Tilley, S.A. Wender, N.R. Roberson, H.R. Weller and T.B. Clegg, Bull. Am. Phys. Soc. 24 (1979) 646.

10. Search for Resonant Raman Scattered Electrons, J.K. Swenson, A. Kodre, S.M. Shafroth and R. Mowat, North Carolina Academy of Sciences, Univ. of N. C. Greensboro meeting, 31 March 1979.

11. Search for Shifted Auger Electrons Induced by Below Threshold X-Rays, J.V. Swendon, A. Kodre, S.M. Shafroth and R. Mowat, Bull. Am. Phys. Soc. 24 (1979) 561.

12. Reaction Mechanisms for ^{59}Co $(^{16}O,X)Y$ Reactions, A.W. Waltner, D.M. Peterson, S.M. Shafroth and J.E. Willis, Bull. Am. Phys. Soc. 24 (1979) 695.

APPENDIX III (Continued)

ABSTRACTS OF CONTRIBUTED PAPERS PRESENTED AT AMERICAN PHYSICAL SOCIETY AND OTHER MEETINGS

13. A Comparison of the Nuclear Reactions due to ^{16}O and ^{19}F on ^{59}Co, A.W. Waltner, D.M. Peterson, S.L. Varghese, S.M. Shafroth and J.E. Willis, Bull. Am. Phys. Soc. 24 (1979) 825.

14. Cl Hypersatellite Intensities vs. Target Thickness Resulting from Cl + C Collisions, J.A. Tanis, S.M. Shafroth, J.E. Willis and J.R. Mowat, Bull. Am. Phys. Soc. 24 (1979) 1172.

15. Angular Distribution of Radiative Electron Capture, J.E. Willis, M. Clark, S.M. Shafroth, S.L. Varghese and J.R. Mowat, Bull. Am. Phys. Soc. 24 (1979) 1197.

16. Cluster Model Calculations for Alpha Capture, J.M. Lafferty and S.R. Cotanch, Bull. Am. Phys. Soc. 24 (1979) 845.

17. Recent Modifications of the TUNL Fast Neutron Cross Section Facility, L.W. Seagondollar, A.G. Beyerle, C.R. Gould, F.O. Purser, S. El-Kadi, S.G. Glendinning and C.E. Nelson, Bull. Am. Phys. Soc. 24 (1979) 878.

18. Finite Geometry and Multiple Scattering Corrections for Neutron Cross Section Measurements, H.H. Hogue and A.G. Beyerle, Bull. Am. Phys. Soc. 24 (1979) 877.

19. Scattering of 8 to 14 MeV Neutrons from ^{10}B, S.G. Glendinning, S. El-Kadi, D.H. Epperson, H.H. Hogue, C.E. Nelson, F.O. Purser, A. Beyerle, L.W. Seagondollar and C.R. Gould, Bull. Am. Phys. Soc. 24 (1979) 656.

20. Improvements in the TUNL Fast Neutron Cross Section Facility, L.W. Seagondollar, A.G. Beyerle, C.R. Gould, F.O. Purser, S. El-Kadi, S.G. Glendinning, H.H. Hogue, C.E. Nelson and R.L. Walter, Bull. Am. Phys. Soc. 24 (1979) 652.

APPENDIX IV

COLLOQUIA AND SEMINAR TALKS

G.E. MITCHELL

"High Resolution Proton Resonance Reactions"

1. Presented at Institut Jožef Stefan, Yubljana, Yugoslavia, October 1979